

THE IMPROVED FRESNEL VIRTUAL IMAGE DISPLAY SYSTEM (VIDS)

BY Wiley V. Dykes



19970117 198

FINAL REPORT

DISTRIBUTION STATEMENT A

Approved for public release;
Distribution Unlimited

PREPARED FOR
U.S. ARMY PROJECT MANAGER FOR TRAINING DEVICES
BY
RESEARCH AND TECHNOLOGY DEPARTMENT, CODE N-731
NAVAL TRAINING EQUIPMENT CENTER
ORLANDO, FLORIDA 32813

FEBRUARY 1983

SECURITY CLASSIFICATION OF THIS PAGE (When Data Entered)

UNCLASSIFIED

SECURITY CLASSIFICATION OF THIS PAGE(When Data Entered)

television picture as an input visual. The eye relief (eye clearance) of both systems is 24 inches and both have a field-of-view which is 480H X 360V. The exit pupil size of each is 12 inches wide by 6 inches high. Before any fabrication effort began on the VIDS a discovery was made that changed the Fresnel element design. This "Improved VIDS" design which incorporates curved facets and undercut grooves gives several advantages over the original Fresnel design. The most significant advantages are: the expected transmission increases at the edge of the field from 24% to 75% and because the grooves appear more on edge they tend to be less noticeable to the observer. This "Improved VIDS" design is presented in Section V.

Only the achromatized (5 elements) VIDS was manufactured as part of the task. This VIDS was subjected to complete optical testing but only the test results are discussed in this report. It is important to note that with uncoated elements the transmission was measured on axis at 68%. Transmission therefore could be expected to increase to 85 or 90% with anti-reflection coatings. Distortion through the system was less than 4%. The present VIDS does have some optical imperfections. The most noticeable being excessive spherical aberration which causes a sight image movement with head motion. Optical problems of Fresnel ring visibility and light cross talk should also be analyzed and corrections in design made.

The VIDS was subjectively tested by experienced pilots. They compared the VIDS to their present helicopter simulator (Device 2B31) at Ft Rucker, AL. In their opinion over 80% considered the VIDS as brighter, gave a better picture and presented a better illusion of depth than the 2B31. This report suggests a development effort to provide design and manufacture of a Wide Angle VIDS for future training.

UNCLASSIFIED

SECURITY CLASSIFICATION OF THIS PAGE(When Data Entered)

TABLE OF CONTENTS

Section	Page
I INTRODUCTION.....	1
II BACKGROUND.....	3
GENERAL.....	3
VIDS HISTORY.....	4
III VIDS SPECIFICATIONS.....	8
IV PRELIMINARY DESIGN APPROACH.....	12
OPTICAL DESIGN	
DESIGN APPROACH.....	13
DESIGN TYPES EXAMINED.....	15
SPECIAL PURPOSE PROGRAM.....	20
FURTHER DESIGN TYPES.....	25
DESIGN CONCLUSIONS.....	27
DESIGN RESULTS (MONOCHROMATIC).....	28
ACHROMATIZATION.....	34
DESIGN RESULTS (ACHROMATIZED DESIGN).....	38
FRESNEL SHADING.....	42
ASTIGMATISM.....	48
MECHANICAL DESIGN	
MECHANICAL DESIGN PARAMETERS.....	60
ADJUSTABLE FRESNEL MOUNTS.....	60
MECHANICAL PROVISIONS.....	61
OPTO-MECHANICAL ADJUSTMENT AND ALIGN-ACHROMATIZED FRESNEL DOUBLET LEAKPROOF DESIGN.....	61
FRESNEL DOUBLET LEAKPROOF DESIGN.....	62
CONCLUSIONS.....	67
V IMPROVED VIDS DESIGN.....	68
DISCUSSION.....	68
IMPROVED VIDS DESIGN REPORT.....	68
INTRODUCTION.....	69

TABLE OF CONTENTS (Cont)

Section	Page
FRESNEL OBSCURATION.....	71
OBSCURATION VALUES.....	87
ALTERNATIVE SYSTEMS.....	89
FINITE DEPTH FRESNELS.....	90
MEETINGS.....	92
CONCLUSIONS.....	93
RECOMMENDATIONS.....	94
VI OPTICAL TESTING.....	96
GENERAL.....	96
TEST DATA.....	96
VII SUBJECTIVE EVALUATION.....	99
VIII RECOMMENDATIONS.....	103
DISTRIBUTION LIST.....	105

LIST OF ILLUSTRATIONS

Figure	Page
1. Viewing Area.....	10
2. Point Pairs in the Viewing Area.....	10
3. Object Points for Checking Ray Disparities.....	11
4. Points for Checking Chromatic Disparities.....	11
5. File No. 103.....	18
6. File No. 104.....	18
7. File No. 105.....	18
8. File No. 106.....	19
9. File No. 107.....	19
10. File No. 108.....	19
11. File No. 109.....	26
12. File No. 110.....	26
13. File No. 111.....	26
14. File No. 114.....	29

LIST OF ILLUSTRATIONS (Cont)

Section	Page
15. File No. 120.....	29
16. File No. 121.....	29
17. File No. 124.....	30
18. Non-Achromatized Fresnel Lens Design.....	31
19. Points for Checking Chromatic Disparities.....	36
20. Achromatized Fresnel Lens Design.....	40
21. Ray Refraction.....	44
22. Ray Refraction.....	44
23. Ray Refraction.....	44
24. Pupil Points for Astigmatism Calculations.....	50
25. 4.375" Axial Field Position.....	56
26. 6.25" Axial Field Position.....	57
27. 8.75" Off-Axis Field Point.....	58
28. 12.5" Off-Axis Field Point.....	59
29. Mechanical Arrangement.....	63
30. Fresnel Cells and Mount.....	64
31. Liquid-Tight Assembly.....	65
32. Fresnel and Liquid.....	66
V-1a. Standard Fresnel Surface.....	70
V-1b. New (Livermore) Fresnel Surface.....	70
V-2a. Fresnel Obscuration.....	72
V-2b. Fresnel Obscuration.....	72
V-2c. Fresnel Obscuration.....	73
V-2d. Fresnel Obscuration.....	73
V-3. Fresnel Draft Angles.....	82
V-4. Fresnel Obscuration (Full Pupil).....	83
V-5. Slope Values.....	84
V-6. Fresnel Draft Angles (6" Dia. Pupil).....	85
V-7. Fresnel Obscuration (6" Dia. Pupil).....	86

LIST OF TABLES

Table	Page
1. Vergence Angle Tolerances.....	8
2. Non-Achromatized Design.....	33
3. Color Disparity (Non-Achromatized).....	37

LIST OF TABLES (Cont)

Section	Page
4. Des. 125.019B.....	41
5. Color Disparity (Achromatized).....	43
6. Achromatized Design - Values of 0.....	45
7. Achromatized Design.....	47
8. Axial Point.....	51
9. 4.375" Off-Axis Field Point.....	52
10. 6.25" Off-Axis Field Point.....	53
11. 8.75" Off-Axis Field Point.....	54
12. 12.5" Off-Axis Field Point.....	55
V-1. Values of Intersection Points.....	76-78
V-2. Values of Intersection Points.....	79-80

SECTION I

INTRODUCTION

Military trainers are expected to present a training environment which realistically represents the real world. The basic goal of this task was to develop an economical and effective way to provide a visual system of optical elements that could convert real images into virtual images so that they realistically appear to originate at real world distances.

Many approaches are used to create virtual image displays but all, for one reason or another, have serious limitations and are not able to furnish the desired results. The most common approaches used and their most apparent problems are as follows: (1) The Glass Lens System which provides a direct view of video imagery, straight through the system. These systems offer good image quality and transmission but they are heavy, very expensive, and usually furnish a very small exit pupil. (2) Another interesting approach utilizes refractive plastic lenses (acrylics) instead of glass, the Singer-Link's old VAMP is such a system. Its major shortcomings arise from using plastic materials of only one refractive index thus making good chromatic corrections impossible. Also, since the lenses were made from plate stock, their thickness was limited and the resulting shape was not the best for image correction. (3) Probably the most common virtual imaging device in current use is the Conventional Spherical Mirror arrangement. This system employs an on axis spherical mirror and a diagonal beam splitter to introduce its visual input. But because the system's input must come from "folded axis" its "stacking" capability is limited in its use for complete wrap-around viewing. Also, in this beam splitter/spherical mirror system the light from the input device passes through the beam splitter twice, thus its intensity is greatly reduced. Theoretically the maximum transmission is 25% yet, in actual practice a 15 to 18% efficiency is more to be expected. Another related problem is that of providing a sufficiently large bright TV picture to be viewed through this system. Generally, this system is relatively expensive and presents low light levels. (4) Another very popular virtual imaging system in use today is the Farrand Company's "Pancake Window." With this system, images from a CRT are made to appear to come from infinity through a unique lightweight combination of mirrored beam splitters, polarizers and quarter wave plates. This is a direct view device and therefore, lends itself to being stacked to form wide angle displays, but its optical efficiency is less than 2%. High output color light valves are in development but, when made they will be very expensive. (5) The Fresnel and liquid lens approach, with which this report deals, offers an improved means to achieve a Virtual Image Display System (VIDS). This system offers low cost, lightweight, extremely high transmission (85% to 90%) and provides good image quality. The VIDS is a color corrected device with on axis transmission and therefore lends itself to "stacking" to form wide angle displays.

This report actually describes two different Virtual Image Display Systems

of the Fresnel type. The first is a three element system which has not been achromatized, and the second is a five element achromatized system which utilizes one liquid filled doublet, one air spaced doublet and one single element. Both systems have been designed for use with a 25" RCA CRT and both have space between the single element and the doublets to install a mirror for system folding should it become desirable. The eye relief (eye clearance) of both systems is 24 inches and both have a field-of-view which is 48 H x 36 V. The exit pupil size of both systems is 12" wide by 6" high. Only the achromatized system has been constructed and with uncoated elements the transmission was measured at 68%. Transmission is expected to be increaseable to 85 to 90% with antireflection coatings. Distortion in both systems is less than 4%.

SECTION II

BACKGROUND

General: Virtual imaging systems used in trainers for visual simulation are generally rather large, heavy and bulky devices because of their large exit pupil requirements. Those made from optical quality glass are usually exceedingly expensive. Even when ground and polished plastic lenses are used, costs may be reduced slightly but the desired image quality is not achievable because of the limited availability of refractive indices in plastics. Thus, optical design with plastics makes it extremely difficult, if not impossible, to correct for the image deficiencies.

In mid 1973, a three year in-house investigation entitled "Non-Glass Elements for Visual Simulation in Naval Vehicles Simulators" was started at the Naval Training Equipment Center (NTEC)(NAVTRAEEQIPCEN). The project sponsor was the Naval Electronics System Command and the principal investigator was Dr. G. Rosendahl. The technical objective was to "investigate ways and means to replace heavy, bulky and costly imaging systems used for visual simulation with lighter, less voluminous and less costly imaging devices without undue compromise of image quality and, where possible, to improve image quality. The study will lead to a recommendation for breadboarding a representative imaging system for visual simulation." This investigation dealt primarily with examination of methods of using liquid filled lenses in plastic envelopes. In the study Dr. Rosendahl used Scientific Calculations Inc. ACCOS-V program and the Sigma 7 computer to develop a Thin Lens Theory Program to be used for designing liquid filled lens for evaluation. During the study, a plastic (acrylic) envelope was formed from sheet material which had been heated and shaped over a male mold. The two halves were then bolted together and a liquid with a specific refractive index poured into the shell. The lens yielded only partial success because the acrylic sheet material did not form with a uniform radius of curvature, but formed with flat plates with bent edges somewhat like that of a tortoise shell. It is likely that had such a system been cast from liquid plastic material, in a mold with the proper shape, this approach would have been successful. Other work accomplished during the "Study of Non-Glass Elements" included: (1) The ACCOS-V Program for Computer Supported Lens Design was adapted to the NTEC Sigma-7 computer, and several special problems were investigated on the Sigma-7, such as, "Handling of Equidistant Surfaces" and "Calculation of Ray Disparities for Bi-Ocular Vision."(2) Bi-ocular vision

1. Research and Technical Work Unit Summary, DD-1498, Non-Glass Elements for Visual Simulation in Naval Vehicle Simulators, 12 April 1973, Dr. G. Rosendahl, Naval Training Equipment Center, Orlando, Florida

requirements were studied when it was found that reference literature did not provide sufficient data for determining tolerances for ray disparities in bi-ocular vision. (3) The design of a virtual image display, in conjunction with a computer generated CRT display was started which determined that even a 30 degree field would require a minimum of two components, one a general aspheric and one a conic surface. (4) Methods for color correcting virtual imaging systems were investigated. A large variety of refractive indices and dispersions were found in liquids, whereas only two are available in plastics. Therefore the optical designer has a much greater variety of materials from which to choose for image and color correction.²

VIDS History

By early 1975 the art of precision diamond turning of Fresnel lenses had reached a point where they might be considered more than novelties. Fresnel lenses, with their grooved surfaces, of proper shapes cut into plastic plate material, offered an excellent possibility of reducing weight and volume. But, only through a combination of Fresnel lenses and refracting liquids did Dr. Rosendahl feel the optical designer might find a sufficiently good, chromatic corrected, virtual image (infinity) system.³ Dr. Rosendahl also predicted in his January 1977 "Research and Technology Summary (DD 1498)" that "Fresnel lens virtual image window units can be cut into pentagon shapes such that multiple windows may be mosaicked together for wide angle coverage. Mosaicked Fresnel virtual image window units can be fed individually from television displays, from a computer generated imagery system, or from a combination of both."⁴

In September 1976, a Statement of Work was written at NTEC for an optical device which was to be an efficient, lightweight, compact, low cost virtual image display system needed for future flight trainers and vehicle crew trainers.⁵ This device was intended to meet tri-service requirements with specific US Army applications in synthetic flight trainers and tank driver

2. Research and Technology Work Unit Summary, DD-1498, Virtual Image Display System, 28 Jan 1977, Dr. G. Rosendahl, NAVTRAEEQUIPCEN, Orlando, FL

3. Ibid

4. Ibid

5. Statement of Work, Virtual Image Display System, 13 Jan 1976, Dr. G. Rosendahl, NAVTRAEEQUIPCEN, Orlando, Florida

simulators. Preliminary investigations during the "Non-Glass Element Study" had indicated that such a virtual image display system could be developed using Fresnel lenses. This Virtual Image Display System (VIDS) was presented to the Army Project Manager for Training Devices (PM TRADE) and was funded in January 1977.

The scope of this new project was to develop a breadboard model of a virtual image display device with which feasibility of the Fresnel lens approach could be demonstrated. The breadboard device was to be designed to provide a field-of-view, resolution, viewing volume and eye relief comparable to the system used on Device 2B31, the CH-47 Chinook Helicopter Simulator at Ft Rucker, Alabama. The procurement package and Specification for the breadboard were written at NTEC (see Section III, this report, Specification for VIDS).

An announcement was made in the 15 December 1976 issue of the Commerce Business Daily for Research and Development Sources to build the VIDS. Of the 12 firms responding to this announcement, only three were found to be acceptable. Requests for Proposal went to the qualified respondents and only Advanced Technology Systems (ATS), a Division of the Austin Co., in Roselle, NJ, responded with a proposal and bid. ATS was awarded the first phase of a Cost Plus Fixed Fee (CPFF) contract to design the Virtual Image System. Contract N61339-77-C-0113 (issued on 19 Aug 1977) provided for the Design Report for the VIDS. The Phase I cost, including Monthly Progress Reports, was 40 thousand dollars. The Design Report was delivered in March 1978 (see Section IV of this report for complete details).

The ATS Design Report described two Virtual Images systems - the first, a three element Fresnel, non-achromatized system, and, the second, an achromatized virtual image device, using five Fresnel lenses with a dispersive liquid between the elements of the first doublet. Both systems were designed for use with a 25" TV as the input image source. The five element achromatized Virtual Image Display System was selected for development and funded as Phase II of the contract. In August 1978 the contract was modified to make Phase II a Fixed Price Contract. The Government costs for manufacture and test of the VIDS was 125 thousand dollars. The contract was expected to be completed in eight months.

ATS immediately ordered seven acrylic blanks for fabrication of the five element VIDS and two spare elements, and the dispersive liquid for the doublet from Cargille Labs. ATS had planned to have Optical Sciences Group (OSG), in California use their diamond turning equipment to cut the Fresnel elements.

However, OSG's equipment had broken down and ATS was informed that it would take about 15 months before their equipment could be replaced. ATS then learned that Lawrence Livermore Laboratory (LLL) in California had similar diamond turning equipment in operation. After completing discussion with LLL on cutting the Fresnels, ATS placed orders for five diamond tipped tools and a vacuum chuck. The lead time on the tools was quoted at 20 weeks and LLL was quoting four months to turn the lenses after receipt of the tools. Thus, the contract delivery was slipped until August 1979. But, "Higher Priority" Government work kept LLL from cutting the elements. LLL reported in October 1979 that they had mounted and balanced the vacuum chuck and were proceeding to flatten the plastic blanks. LLL had also completed the programming for their numerically controlled machine but still would not commit to a delivery date on the Fresnel lenses. ATS requested and received a contract change from NAVTRAEEQIPCEN to the effect that delivery would occur six weeks after the contractor received acceptable Fresnel lenses from their subcontractor.

During early 1979 an approach that would improve the VIDS system was conceived at NTEC. A small study contract was issued to Arthur Cox Associates, Park Ridge, IL to investigate the new approach. This contract, N61339-79-M-1950, determined that a much improved VIDS could be achieved with the addition of curved facets and undercut grooves on the Fresnel lenses. The most significant advantage was the expected transmission increases at the edge of the field from 24% to 75% (the Improved Virtual Image System is discussed in Section V of this report). The advantages of this new approach were discussed with ATS by Dr. Cox of Arthur Cox Associates. In November 1979, ATS proposed that they be allowed to build the improved VIDS at no additional cost. This contract change was granted.

In January 1980, ATS reported that a major earthquake had occurred in the Livermore, California, area and caused significant damage at Livermore Labs. "After extensive investigation of the disposition of the diamond turning machine and its seismic support block, J. Bryan reports that no significant damage or misalignment occurred and the cutting of the Fresnel lenses will resume on February 14th."⁶ It was May before LLL started to cut the Fresnel grooves and by July two Fresnels had been cut. The remaining three elements were cut by Fall, but, a dispute over cost overruns developed between ATS and LLL. LLL refused to release the Fresnel lenses to ATS until ATS negotiated a new price for the LLL work. In January 1981, ATS offered to pay LLL the \$80K

6. Monthly Progress Report for January 1980, ATS, Fairlawn, NJ, 14 Feb 1980

that had been agreed to and to put \$46K in escrow pending arbitration. LLL finally agreed and shipped the lenses to ATS.

ATS assembled the VIDS in March 1981 and began optical testing. In-plant testing was completed in May and the VIDS was shipped to NTEC, Orlando. At NTEC, the VIDS underwent further testing and was found to contain an excessive amount of oblique spherical aberration which caused an undesirable image movement with head motion. ATS transported the VIDS back to their plant, but could not complete an easy fix. As consideration, ATS offered to deliver the VIDS to Fort Rucker, AL, to provide a 1025 line TV monitor, to assist with subjective evaluations, and return the VIDS to NTEC. This consideration was accepted.

In October 1981, NTEC (Code N-731) conducted a subjective evaluation of the Virtual Image Display System at Fort Rucker, AL. The prototype device was evaluated by students transitioning into CH-47 helicopters, and their instructors. First, both were asked to answer a questionnaire comparing the VIDS with the Device 2B31 Visual System (a conventional mirror beam splitter system). The second part of the questionnaire dealt with optical properties of the VIDS and its prospect as a "trainer visual." The questionnaire was completed by 25 experienced helicopter pilots having between 800 and 8000 flight hours each. After each participant had an opportunity to view both visual devices for a reasonable length of time, he was asked to complete the questionnaire. The results indicated that: 84% considered the VIDS brighter than the 2B31; 84% considered the VIDS to present better illusion of depth than the 2B31; 80% considered the VIDS to have better overall picture quality than the 2B31; 96% said the VIDS was usable for routine helicopter training; and 80% said the VIDS was usable for Nap-of-the-Earth (NOE) and poor visibility training. A Program Implementation Plan (PIP) was written to continue development of the VIDS into a wide angle system. Funding for the Wide Angle VIDS is now being provided by the Air Force Human Resource Laboratory (AFHRL) at Williams Air Force Base, AZ, for use on the Advanced Simulator for Undergraduate Pilot Training (ASUPT).

SECTION III

VIDS SPECIFICATIONS

The purpose of the Virtual Image Display System Study and the manufacture of a breadboard device was to demonstrate the feasibility of an economical and effective means to achieve an infinity visual display for training simulators. The specification for the Virtual Image Display System was intended to produce a "lightweight, compact, straight through system, of high light transmittance and designed for bi-ocular seeing,"⁷ The specified input device to the VIDS was a 25" RCA TV using cathode ray tube number RCA 1908 P22 with a faceplate size of 20" X 15", approximately 1/4 inch thick and radius of curvature of 40.7 inches.

Generally, the performance specification stipulated a refracting system utilizing Fresnel elements. The viewing area, or exit pupil size, was specified to be a truncated circle 12 inches in diameter by six inches high. This pupil area was divided into two areas: "A" the central area of best seeing conditions and "B" the good seeing area (See Figure 1). The eye relief was specified to be 25 inches and the viewing angle $36^{\circ}V \times 48^{\circ}H$. The distortion at the center of pupil was not to exceed 4%. Astigmatism was specified not to exceed .75 diopters within any light pencil of 5mm diameter. The behavior of ray pairs was specified with the following table (Values are in minutes of arc).

TABLE 1. VERGENCE ANGLE TOLERANCES

	Area A	Area B
Convergence (Max.)	30.0	40.0
Divergence (Max.)	0.0	-10.0
Dipvergence (Max.)	+15	+ 18
Chromatic Errors (CE)	+ 4	+ 6

7. Specifications for Virutal Image Display System, N-211-104(GR), NTEC Orlando, FL, 24 Jan 77

Points were defined in the pupil for checking ray disparities (see Figure 2). Object Points were defined for checking ray disparities (See Figure 3). And points in the pupil were defined for checking chromatic disparities (See Figure 4).

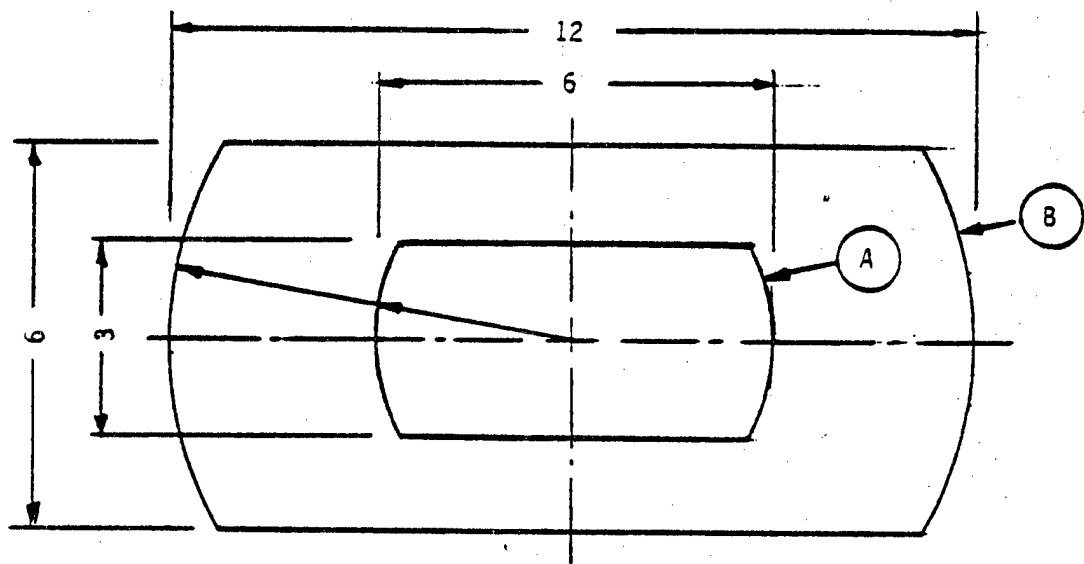


FIGURE 1. VIEWING AREA; A FOR BEST SEEING CONDITIONS,
B FOR GOOD SEEING CONDITIONS, MEASURES IN INCHES

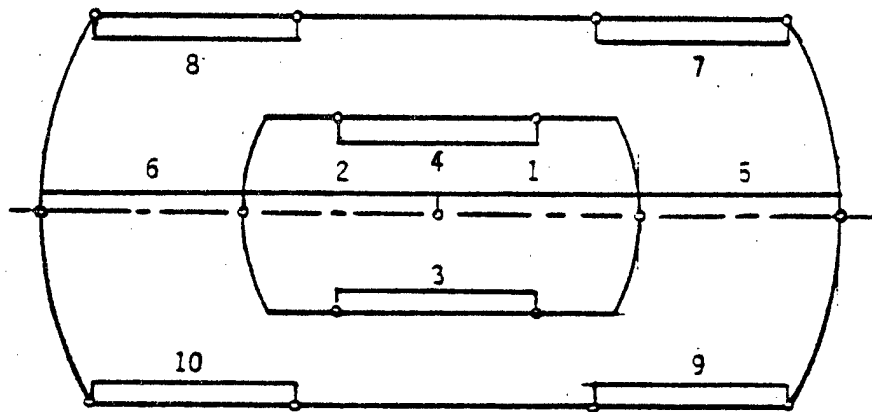


FIGURE 2. POINT PAIRS IN THE VIEWING AREA FOR
CHECKING RAY DISPARITIES

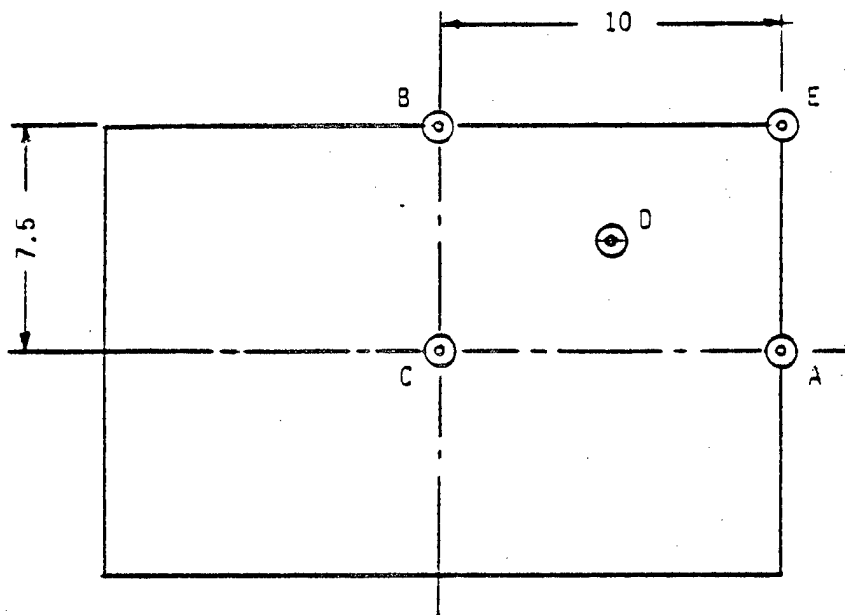


FIGURE 3. OBJECT POINTS FOR CHECKING RAY DISPARITIES
 POINT D AT THE CENTER OF QUADRANT ABCE,
 MEASURES IN INCHES

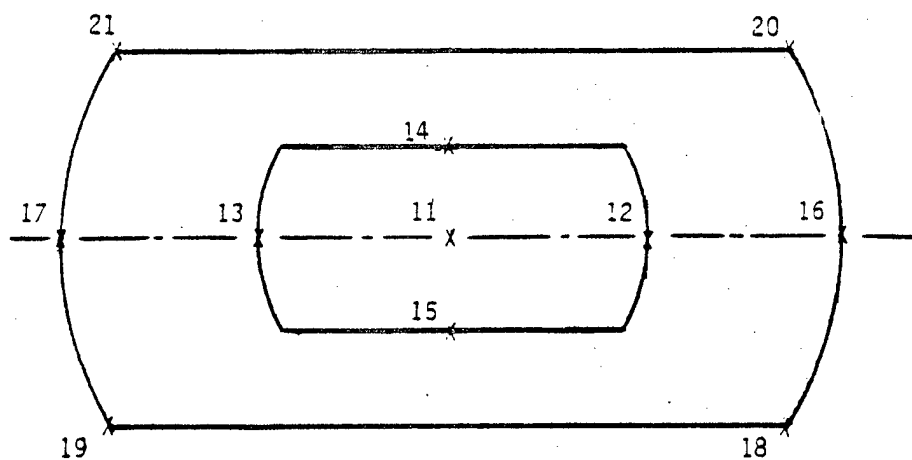


FIGURE 4. POINTS IN THE VIEWING AREA FOR CHECKING
 CHROMATIC DISPARITIES

SECTION IV

PRELIMINARY DESIGN APPROACH

Advanced Technology Systems (ATS) a Division of the Austin Company, Fairlawn, NJ was awarded a two phase contract to design and fabricate the VIDS. With Dr. Arthur Cox and Mr. Anthony Mazurkewitz as optical designers ATS prepared a Preliminary Design Report as Item A002 of the Virtual Image Display Contract, N61339-77-C-0113. The report was published by ATS in March 1978. The remainder of Section IV is taken directly from the ATS Preliminary Design Report commencing with the optical design.

DESIGN APPROACH

In the early design stages, Fresnel lenses on a curved substrate were considered. According to this, the surface has a spherical curvature ρ , but at any point where a ray meets the surface, it encounters a local region whose normal has direction cosines (L, M, N) given by the formula.

$$L = x (\rho + a + b R^2 + c R^4 + d R^6) \quad (1a)$$

$$M = y (\rho + a + b R^2 + c R^4 + d R^6) \quad (1b)$$

where $L^2 + M^2 + N^2 = 1$ and $R^2 = x^2 + y^2$

with $\rho^2 R^2 + (1 - \rho Z)^2 = 1$

NOTE: a is the spherical Fresnel term, while b, c, d are aspheric Fresnel terms.

The ray tracing process which is followed comprises a determination of the point at which a ray encounters a spherical surface with curvature ρ : from this the local direction cosines are calculated using equations (1a) and (1b): the refraction of a light ray is then evaluated using the standard formula

$$\frac{l - l^1}{L} = \frac{m - m^1}{M} = \frac{n - n^1}{N} \quad (2)$$

where (l, m, n) are the optical direction cosines of a ray after refraction, and (l^1, m^1, n^1) are the optical direction cosines before refraction.

$$l^2 + m^2 + n^2 = \mu^2; \quad l^1 + m^1 + n^1 = \mu^1 \quad (3)$$

where μ is the refractive index after refraction, and μ^1 is the refractive index before refraction.

On this basis, paraxial theory follows along standard lines using $(\rho + a)$ for the vertex curvature of the surface (including an evaluation of chromatic effects).

Means were then developed to evaluate the Seidel aberrations of a system of Fresnel lenses, using the b term in (1a) and (1b).

The basic philosophy adopted at the outset was that the reasonable correction of the Seidel aberrations was a necessary, but not a sufficient condition for the realization of a satisfactory degree of aberrational correction. Accordingly the system parameters, (ρ , a , b) for the Fresnel surfaces, and the element separations (t) were varied and adjusted in order to reduce the Seidel aberrations. Ray-tracing was then carried out, varying the Fresnel parameters (c and d) to control higher order aberrations. At this stage provision was made to use aspheric surfaces on field flattening elements.

Attention was paid mainly to the correction of mono-chromatic aberrations, tracing a standard pattern of rays through the entrance pupil at the margin of the pupil and at zonal heights corresponding to .70 and .85 of the marginal height. Rays were traced for two off-axis points corresponding to the corner of the field (field position E) and to a field point .7 of the way towards the corner point. For these off-axis points a principal ray was traced as well as 3 upper rim rays at full pupil, .85 and .70 of full pupil; and 3 lower rim rays with the same spacing together with 3 sagittal rays. The aim was to achieve a level of monochromatic performance in excess of that required by the specification, so that there would be no doubt that the requested level of performance would be achieved. Separate means would then be provided to achromatize the system. This parallels the design approach used with eyepieces employing aspheric surfaces.

In most eyepieces which use only spherical surfaces, the contact surfaces in color correcting doublets are used also to correct coma, astigmatism and distortion. A considerable literature has grown up in connection with such systems.

The alternative approach to eyepiece design which makes use of two or three generalized aspheric surfaces has not so far resulted in volume production of such systems. Their characteristics, however, have been examined over the years on a low-key basis (for example, by the Bell & Howell Company). The philosophy which emerged from this work has been

applied to the present project, namely that the monochromatic and chromatic correction functions can be separated.

Design Types Examined

In line with the above design approach, a number of design forms were evaluated. Only highlights of this effort are listed below. The file numbers given are those which have been used internally to identify specific formulae. In all cases the Fresnel elements have a thickness of .50 inches.

FILE NO. 103 (Figure 5)

The separation between elements 1 and 2 is 1.00 inches

The separation between elements 2 and 3 is 15.00 inches

The separation between elements 3 and 4 is 1.00 inches

The separation between elements 4 and 5 is 12.59 inches

The powers of elements 1 and 2 are not held equal.

The front surface of the field flattener (element 5) is a deep aspheric surface, not restricted to conic form.

The maximum distortion is +3.53% in the zone (.7 of the way to the corner) and -2.35% at the corner.

In a typical example of this type of design, the focal lengths of the elements are as follows:

Element 1 101.69 inches

Element 2 67.79 inches

Element 3 67.79 inches

Element 4 67.79 inches

Element 5 -27.12 inches

FILE NO. 104 (Figure 6)

This is derived from File No. 103 by splitting the field flattener so that it now comprises a plano-concave lens and an equi-concave lens. All field lens surfaces are spherical.

The separation between elements 1 and 2 is .50 inches

The separation between elements 2 and 3 is 12.00 inches

The separation between elements 3 and 4 is .50 inches

The separation between elements 4 and 5 is 10.00 inches
The separation between elements 5 and 6 is 3.00 inches

In a typical example of the focal lengths of the elements
are as follows:

Element 1 101.69 inches
Element 2 67.79 inches
Element 3 58.11 inches
Element 4 58.11 inches
Element 5 -81.35 inches
Element 6 -40.68 inches

FILE NO. 105 (Figure 7)

This is derived from File No. 104 by turning the first element
around so that the Fresnel surfaces faces the observer's eye and the first
surface of element 5 in the field flattener is made aspheric.

A typical example has the following data.

The separation between elements 1 and 2 is .50 inches
The separation between elements 2 and 3 is 10.0 inches
The separation between elements 3 and 4 is .50 inches
The separation between elements 5 and 6 is 3.53 inches

The focal lengths of the elements are as follows:

Element 1 135.6 inches
Element 2 67.8 inches
Element 3 67.8 inches
Element 4 67.8 inches
Element 5 -81.35 inches
Element 6 -40.68 inches

FILE NO. 106 (Figure 8)

In this form the first element has been returned to its original
configuration with a plano surface facing the observer's eye, and the
separation between elements 3 and 4 has been increased. A typical example
has the following data.

The separation between elements 1 and 2 is .50 inches
The separation between elements 2 and 3 is 8.00 inches
The separation between elements 3 and 4 is 7.50 inches
The separation between elements 4 and 5 is 4.25 inches
The separation between elements 5 and 6 is 3.00 inches

The focal lengths of the elements are as follows:

Element 1 71.36 inches
Element 2 56.49 inches
Element 3 56.49 inches
Element 4 infinity. (zero paraxial power)
Element 5 -67.79 inches
Element 6 -33.90 inches

FILE NO. 107 (Figure 9)

This belongs essentially to the same family as File No. 106 with an increased separation between the elements 5 and 6.

FILE NO. 108 (Figure 10)

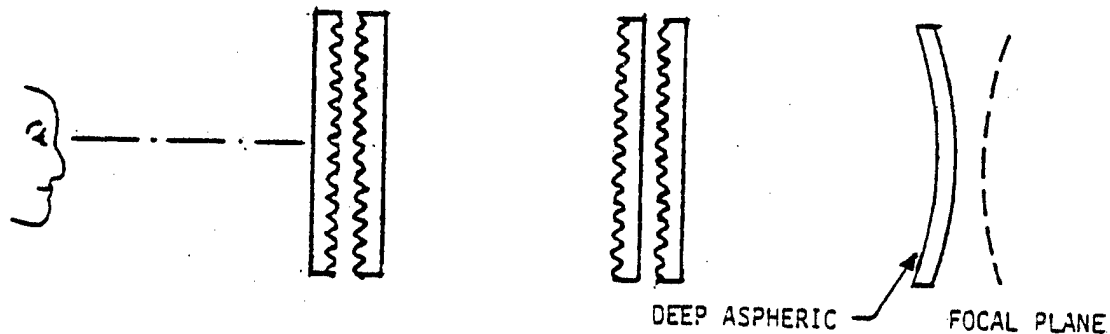
In the course of developing the system, through all the varieties up to File No. 107, it did not seem possible to achieve a very high standard of performance, one which might significantly surpass the specification requirements. In retrospect too much time was spent in attempting to realize such a high standard of performance, and the system was getting to be too complex.

There was also evidence that the higher order aspheric terms on the Fresnel surfaces were creating a backwards curving field and that the field flattening lenses might not be needed, or that if they were needed that they could have considerably less power than had been previously anticipated.

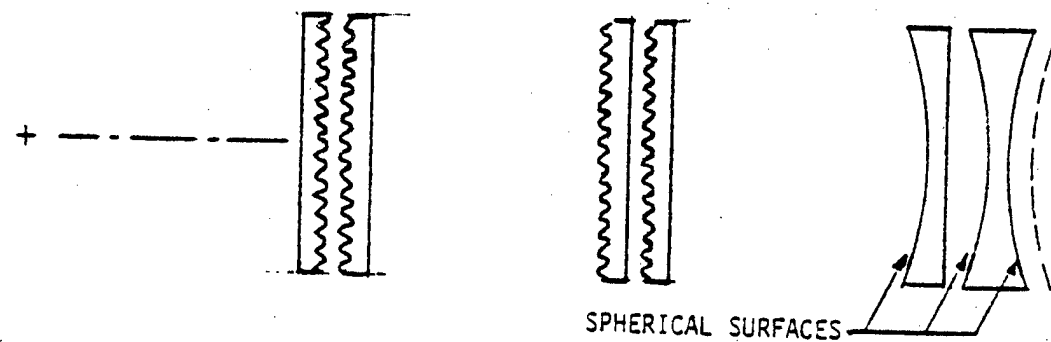
The characteristics of the form shown in the sketch were therefore examined in detail. In a typical example the following are the relevant data.

Separation between elements 1 and 2 .05 inches
Separation between elements 2 and 3 16.00 inches

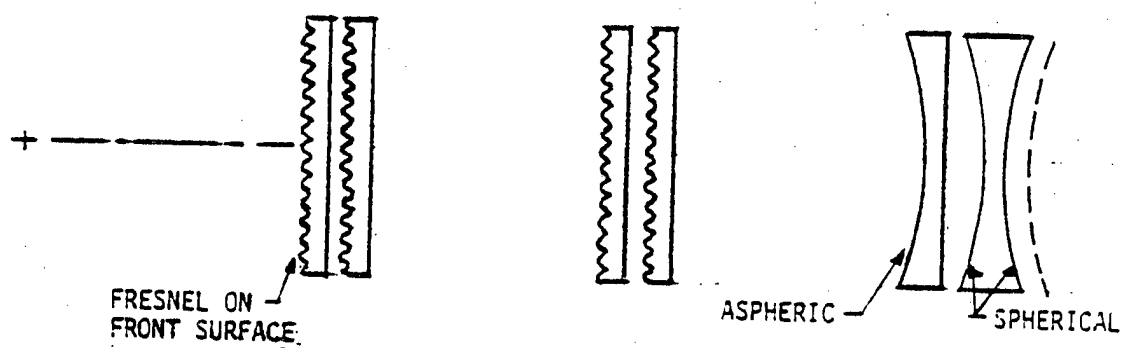
FILE NO. 103 Figure 5



FILE NO. 104 Figure 6

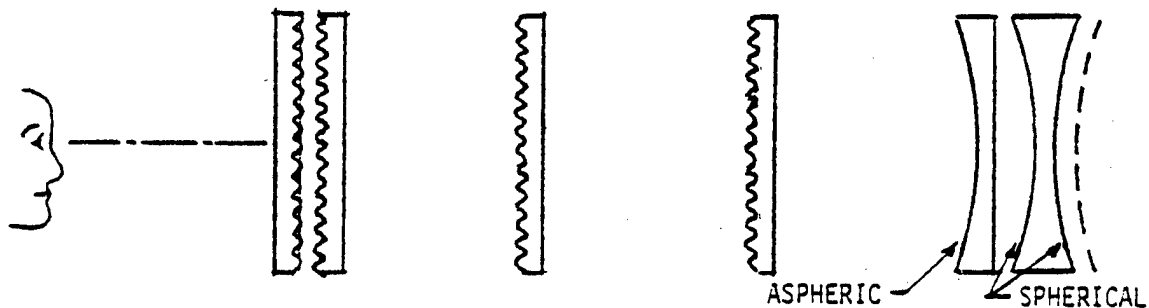


FILE NO. 105 Figure 7



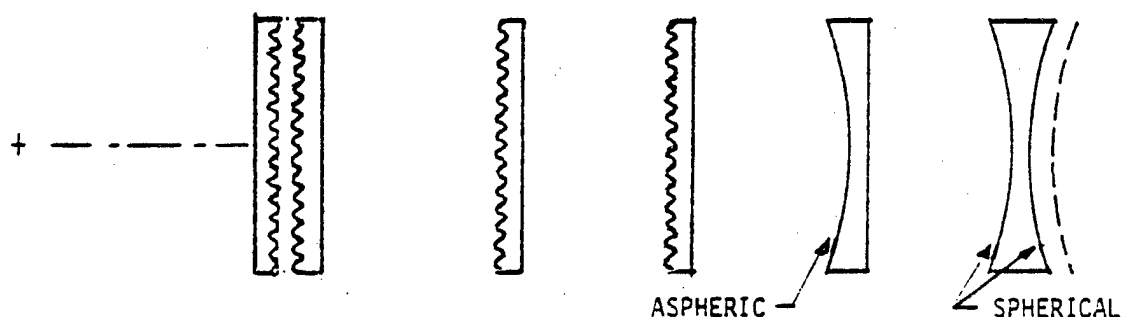
FILE NO. 106

Figure 8



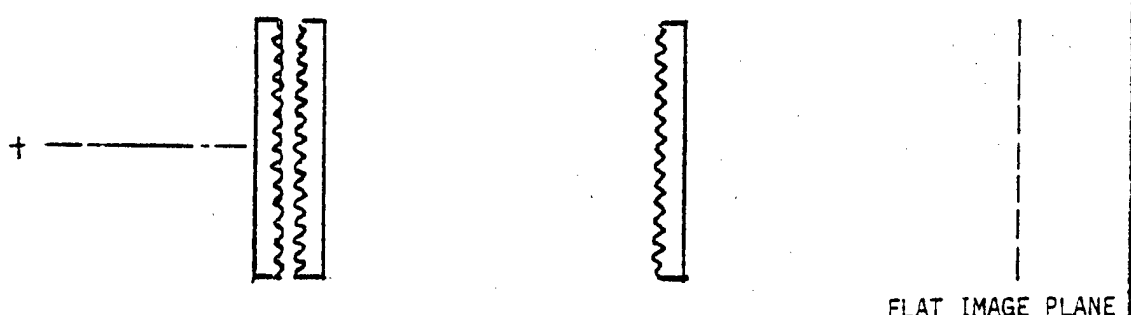
FILE NO. 107

Figure 9



FILE NO. 108

Figure 10



The focal lengths of the elements are as follows:

Element 1 50.97 inches

Element 2 45.30 inches

Element 3 0.00 (zero paraxial power)

The final member of the family (File No. 108.028A) was the first whose performance was examined in a non-classical was as described below.

Special Purpose Program

The need for a special purpose program, when designing to a reasonable compromise rather than to an ultimate level of performance, may be seen from an examination of the Seidel aberrations of a system.

In the standard form of presenting these aberrations we have parallel system of axes (ξ , η) for the pupil and (X , Y) for the image point. In these axes the image point lies at $(0, Y)$. Ray intercept errors in the image plane are denoted by $(\delta X, \delta Y)$ where

$$\delta Y = \delta \cdot \eta (\xi^2 + \eta^2) + \sigma \cdot Y \cdot (\xi^2 + \eta^2) + A_1 \eta Y^2 + D Y^3 \quad (4a)$$

$$\delta X = \delta \cdot \xi (\xi^2 + \eta^2) + 2\sigma Y \cdot \xi \eta + A_2 \xi Y^2 \quad (4b)$$

In systems of axes which are rotated through an angle θ relative to these original axis we have:

$$X^1 = X \cos \theta - Y \sin \theta ; \quad X = X^1 \cos \theta + Y^1 \sin \theta$$

$$Y^1 = Y \cos \theta + X \sin \theta ; \quad Y = Y^1 \cos \theta - X^1 \sin \theta$$

$$\xi^1 = \xi \cos \theta - \eta \sin \theta ; \quad \xi = \xi^1 \cos \theta + \eta^1 \sin \theta$$

$$\eta^1 = \eta \cos \theta + \xi \sin \theta ; \quad \eta = \eta^1 \cos \theta - \xi^1 \sin \theta$$

$$X^1^2 + Y^1^2 = X^2 + Y^2 ; \quad \xi^1^2 + \eta^1^2 = \xi^2 + \eta^2$$

On making these substitutions we obtain the general formula

$$\begin{aligned} \delta Y^1 = & \delta \eta^1 (\xi^2 + \eta^2) + \delta \cdot (Y^1 \cos \theta - X^1 \sin \theta) [\cos \theta (\xi^2 + \eta^2) - 2 \xi^1 \eta^1 \sin \theta] \\ & + (Y^1 \cos \theta - X^1 \sin \theta)^2 [\eta^1 (A_1 \cos^2 \theta + A_2 \sin^2 \theta) + \xi^1 \sin \theta \cos \theta (A_2 - A_1)] \\ & + D \cdot (Y^1 \cos \theta - X^1 \sin \theta)^3 \cos \theta \end{aligned} \quad (5a)$$

$$\begin{aligned}\delta X^1 &= \delta l^1 \left(l^1 + n^1 \right) + \sigma (Y^1 \cos \theta - X^1 \sin \theta) [2 l^1 n^1 \cos \theta - \sin \theta (n^1 + l^1)] \\ &+ (Y^1 \cos \theta - X^1 \sin \theta)^2 [\xi^1 (A_1 \sin^2 \theta + A_2 \cos^2 \theta) + n^1 \sin \theta \cos \theta (A_2 - A_1)] \\ &- D (Y^1 \cos \theta - X^1 \sin \theta)^3 \sin \theta\end{aligned}\quad (5b)$$

In these equations δ is the spherical aberration term, σ is the coma term, A_1 is the tangential astigmatism term, A_2 is the sagittal astigmatism term, and D is the distortion term.

Consider next the means of evaluating convergence or divergence and dipvergence.

If (l, m, n) are the direction cosines of a ray entering a lens of focal length F , symmetrical about the Z -axis, then the co-ordinates of the point in which the ray encounters the focal plane are given by

$$X = \frac{l}{n} X F; \quad Y = \frac{m}{n} X F \quad (6)$$

If the system possesses aberration errors so that X becomes $X + \delta X$ and Y becomes $Y + \delta Y$, then a ray with direction cosines $(l + \delta l, m + \delta m, n + \delta n)$ will reach the image point (X, Y) . For small values of $(\delta X, \delta Y)$ we have

$$\delta X = \frac{F}{n} [\delta l - l \frac{\delta n}{n}] \quad \delta Y = \frac{F}{n} [\delta m - m \frac{\delta n}{n}]$$

$$l \delta l + m \delta m + n \delta n = 0$$

Hence,

$$\delta l = \frac{n}{F} [\delta X (1 - l^2) - l m \delta Y] \quad (7a)$$

$$\delta m = \frac{n}{F} [\delta Y (1 - m^2) - l m \delta X] \quad (7b)$$

In a system of polar co-ordinates, as shown below, we have

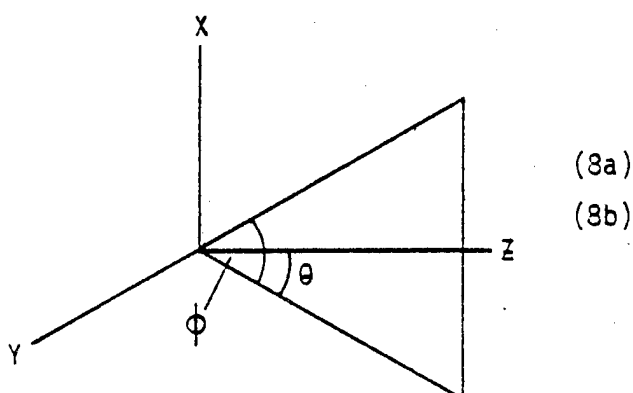
$$l = \sin \theta$$

$$m = \cos \theta \sin \phi$$

$$n = \cos \theta \cos \phi$$

$$\delta \theta = \delta l \div (1 - l^2)^{1/2}$$

$$\delta \phi = \frac{1}{n} [\delta m + \delta l \frac{l m}{1 - l^2}]$$



The difference of $\delta\theta$ values for two rays 3 inches apart in the entrance pupil has been taken as defining the dipvergence. The corresponding difference in the values of $\delta\theta$ (with proper regard to sign) has been taken as defining the convergence or divergence.

Substituting for (δl) and (δm) in terms of δX and δY we have

$$\delta\theta = \frac{n^2}{F} \frac{\delta Y}{l - l^2} \quad (9a)$$

$$\delta\theta = \frac{n}{F} \left[\delta X (l - l^2)^{1/2} - \delta Y \frac{l_m}{(l - l^2)^{1/2}} \right] \quad (9b)$$

If we now consider the behavior of two rays through pupil points (ξ^1, η^1_2) and (ξ^1, η^1_2) and apply equations (5a) and (5b)

$$\begin{aligned} \frac{\delta Y^1_1 - \delta Y^1_2}{\eta^1_1 - \eta^1_2} &= \delta [\xi^2_1 + \eta^1_1^2 + \eta^1_1 \eta^1_2 + \eta^1_2^2] \\ &+ \sigma(Y^1 \cos \theta - X^1 \sin \theta) [\delta \cos \theta (\eta^1_1 + \eta^1_2) - 2\xi^1 \sin \theta] \\ &+ (Y^1 \cos \theta - X^1 \sin \theta)^2 [A_1 \cos^2 \theta + A_2 \sin^2 \theta] \quad (10a) \end{aligned}$$

$$\begin{aligned} \frac{\delta X^1_1 - \delta X^1_2}{\eta^1_1 - \eta^1_2} &= \delta [\xi^1 (\eta^1_1 + \eta^1_2)] \\ &+ \sigma(Y^1 \cos \theta - X^1 \sin \theta) [2\xi^1 \cos \theta - \sin \theta (\eta^1_1 + \eta^1_2)] \\ &+ (Y^1 \cos \theta - X^1 \sin \theta)^2 [(A_2 - A_1) \sin \theta \cos \theta] \quad (10b) \end{aligned}$$

When $\theta = 0$

$$\begin{aligned} \frac{\delta Y^1_1 - \delta Y^1_2}{\eta^1_1 - \eta^1_2} &= \delta [l^2_1 + \eta^1_1^2 + \eta^1_1 \eta^1_2 + \eta^1_2^2] \\ &+ \sigma Y^1 + \delta (\eta^1_1 + \eta^1_2) \\ &+ Y^1 A_1 \quad (11a) \end{aligned}$$

$$\frac{\delta X^1 - \delta X^1}{n_1^1 - n_2^1} = \delta \xi^1 (n_1^1 + n_2^1) + \sigma Y^1 2\xi^1 \quad (11b)$$

When $\theta = 90$ degrees

$$\frac{\delta Y^1 - \delta Y^1}{n_1^1 - n_2^1} = \delta [\xi^1 2 + n_1^1 2 + n_2^1 2] + 2\sigma X^1 \xi^1 + A_2 X^1 2 \quad (12a)$$

$$\frac{\delta X^1 - \delta X^1}{n_1^1 - n_2^1} = \delta [\xi^1 (n_1^1 + n_2^1)] + \sigma X^1 (n_1^1 + n_2^1) \quad (12b)$$

When $\theta = 45$ degrees

$$\frac{\delta Y^1 - \delta Y^1}{n_1^1 - n_2^1} = \delta [\xi^1 2 + n_1^1 2 + n_1^1 n_2^1 + n_2^1 2] + \frac{1}{2} \sigma (Y^1 - X^1) [\xi^1 (n_1^1 + n_2^1) - 2\xi^1] + \frac{1}{4} (Y^1 - X^1)^2 [A_1 + A_2] \quad (13a)$$

$$\frac{\delta X^1 - \delta X^1}{n_1^1 - n_2^1} = \delta [\xi^1 (n_1^1 + n_2^1)] + \frac{1}{2} \sigma (Y^1 - X^1) [2\xi^1 - (n_1^1 + n_2^1)] + \frac{1}{4} (Y^1 - X^1)^2 [A_2 - A_1] \quad (14a)$$

These values are to be evaluated for the 10 pairs of points required by the specification. A point of particular importance is that for points D and E. In the field coverage, we have to take into account (approximately) a term in $A_1 + A_2$ for the convergence, and $A_1 - A_2$ for the dipvergence.

This analysis shows that when aberrations are to be balanced for a compromise solution to meet the specification requirements, the weighting factors will differ significantly from those required for a classical solution. The two methods of attack upon the problem coincide only when the classical aberrations can be reduced to very low levels. The situation is of course, much more complicated when higher order aberrations have to be taken into account.

Further Design Types

All further designs were analyzed with a special program which provided divergence or convergence and dipvergence for all 10 pairs of points and for all 5 field points.

File No. 109 (Figure 11)

This system has the same basic form as File No. 108 with the exception that the third element was made strongly negative. Results were quite unsatisfactory.

File No. 110 (Figure 12)

This is of the same form as File No. 108 with the exception that the central air-space has been increased to 18.00 inches and elements 1 and 2 have been made identical in form, each with a paraxial focal length of 54.38 inches. Element 3 has a focal length of 67.79 inches. Astigmatism could not be controlled.

File No. 111 (Figure 13)

This is derived from File No. 110 by the addition of an equi-concave field lens, each radius being equal to that of the CRT faceplate namely 40.70 inches. This was done in the hopes of establishing a better astigmatism correction than that of File No. 110 family. Results were not promising. Elements 1 and 2 were identical. Typical data are the following.

Separation between elements 1 and 2 is .05 inches

Separation between elements 2 and 3 is 18.00 inches

Separation between elements 3 and 4 is 7.00 inches

In a typical case the elements have the following focal lengths.

Element 1 54.38 inches

Element 2 54.38 inches

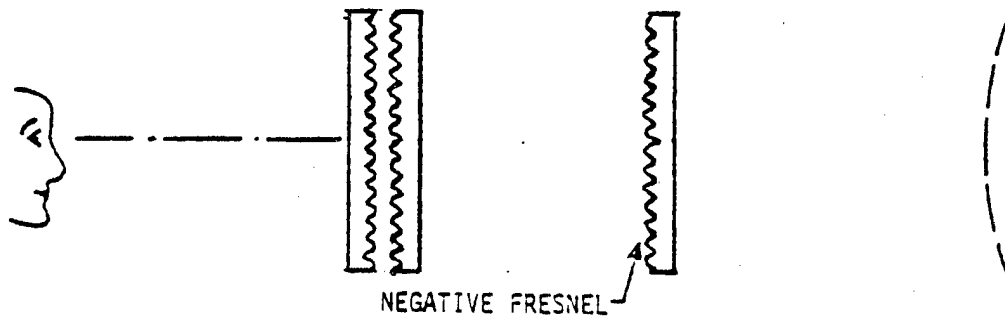
Element 3 67.79 inches

Element 4 41.39 inches

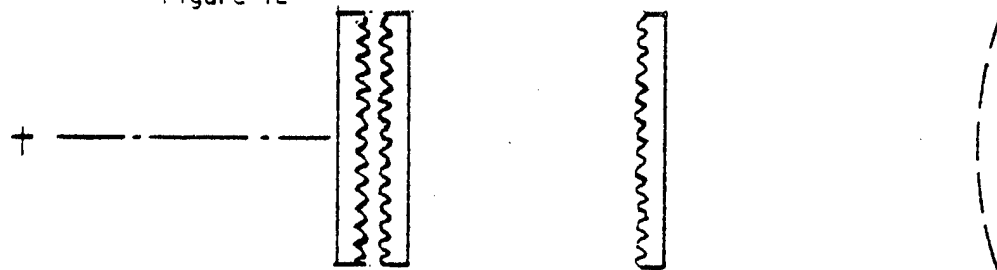
File No. 112

This is essentially the same form as File No. 111, with the spherical aberration made more under-correct. Results are not good.

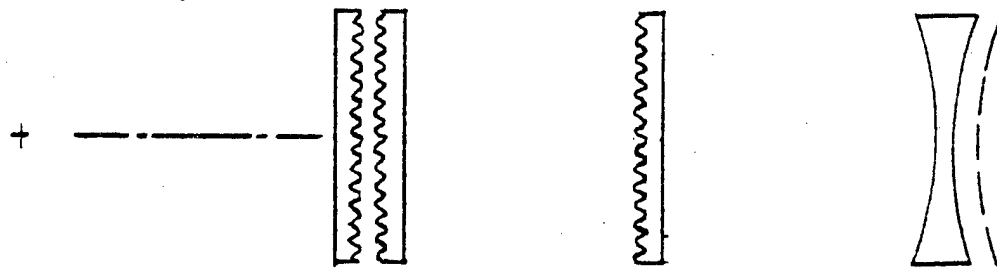
FILE NO. 109 Figure 11



FILE NO. 110 Figure 12



FILE NO. 111 Figure 13



THE SAME CONSTRUCTION IS USED ON FILE NO.'S 112 AND 113

File No. 113

This is of the same form as File No. 111.

File No. 114

(Figure 14)

This is of the same form as File No. 111 with all the paraxial power in the first pair of identical Fresnel elements. The separation has been reduced from 18.00 to 16.00 inches, and the rear separation reduced to 6.50 inches.

File No. 120

(Figure 15)

This is of the same form as File No. 111 with a re-distribution of paraxial power.

File No. 121

(Figure 16)

The introduction of the field flattener did not seem to have been of help in improving the standards of performance. It was therefore omitted in this form, which constituted a reversion to the form of File No. 108. Paraxial power was re-distributed among elements 1, 2, and 3.

File No. 122

Same as file No. 111 with a further redistribution of paraxial power.

File No. 123

This was a continuation of File No. 121 with the central air-space increased to 20.00 inches.

File No. 124

(Figure 17)

At this point a step was taken which substantially improved the standard of performance, namely to turn element 3 around so that the Fresnel surface faced the CRT.

Design Conclusions

As a result of this contract effort, the following has been concluded:

1) A standard of performance which comes close to that specified, in monochromatic light, may be achieved with 3 Fresnel elements, grouped into a close pair and a widely separated single element. In the preferred form this element has its Fresnel surface facing the C.R.T.

2) Power must be distributed between these three elements. All attempts to concentrate the power of the system on the front closely spaced pair, with the third element acting as a zero paraxial power correcting element did

not give satisfactory results.

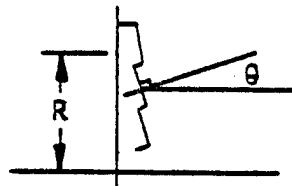
- 3) The spherical and aspheric terms on the front two elements are not identical for the optimum solution. A good deal of time was spent on efforts to use identical front elements but the results were not satisfactory.
- 4) The Seidel spherical aberration must be left slightly over-corrected. This is in sharp contrast to classical eyepiece design where the Seidel spherical aberration is left somewhat undercorrected.
- 5) The prevalence of higher order aberrations makes it unnecessary to use a negative field flattening lens.
- 6) Distortion is primarily controlled by the aspheric term \bar{b} in the formula for the single Fresnel element. Dipvergence and divergence at the point E in the field (the corner of the field) are largely controlled by the higher order terms.

Design Results (Monochromatic)

The final monochromatic form has these parameters (all elements are acrylic with $N_D = 1.4917$, and have a thickness of .475 inches nominally) (Figure 18)

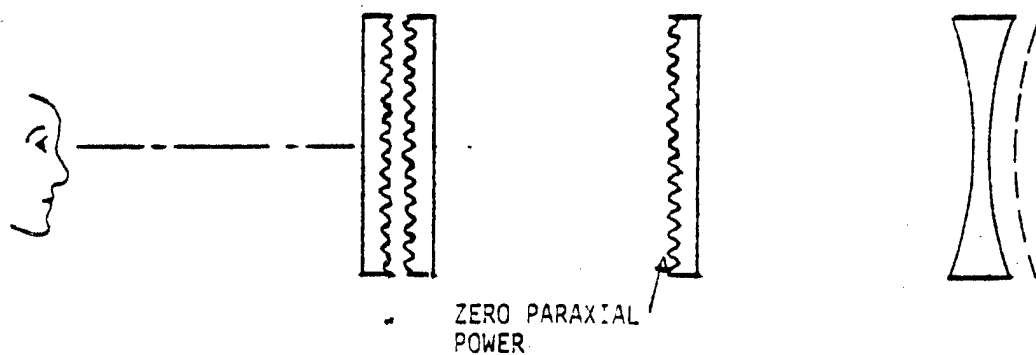
(All radial dimensions are in inches)

$$\sin \theta = aR + bR^3 + cR^5 + dR^7$$

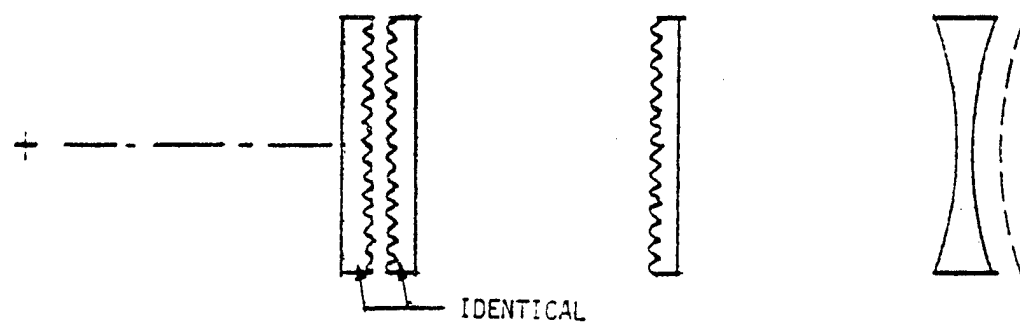


Element 1.	$a = -3.49 \times 10^{-2}$
	$b = 4.90 \times 10^{-5}$
	$c = -2.03 \times 10^{-7}$
	$d = 2.907 \times 10^{-10}$
Element 2.	$a = 3.99 \times 10^{-2}$
	$b = -6.808 \times 10^{-5}$
	$c = 2.519 \times 10^{-7}$
	$d = -3.714 \times 10^{-10}$
Element 3	$a = -3.97 \times 10^{-2}$
	$b = 5.00 \times 10^{-5}$
	$c = 4.50 \times 10^{-7}$
	$d = -4.121 \times 10^{-10}$

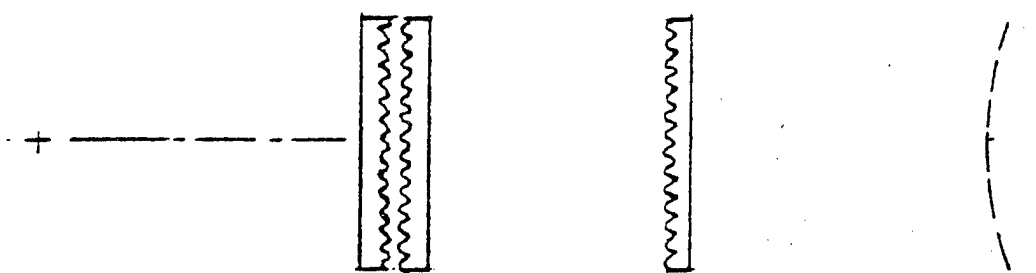
FILE NO. 114 Figure 14



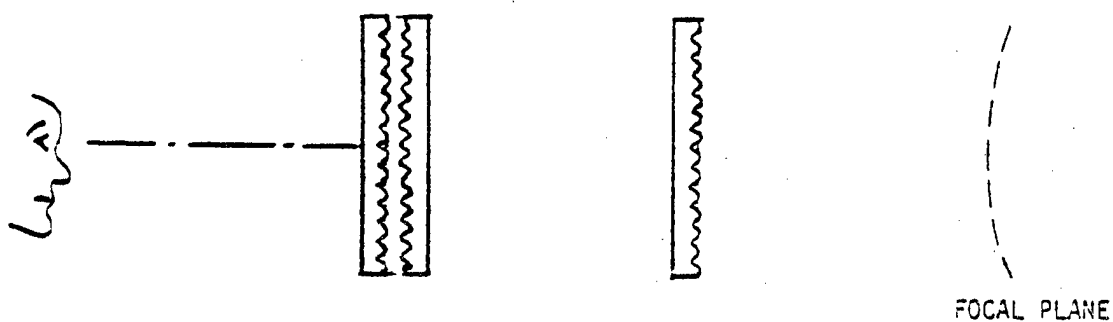
FILE NO. 120 Figure 15



FILE NO. 121 Figure 16



FILE NO. 124 Figure 17



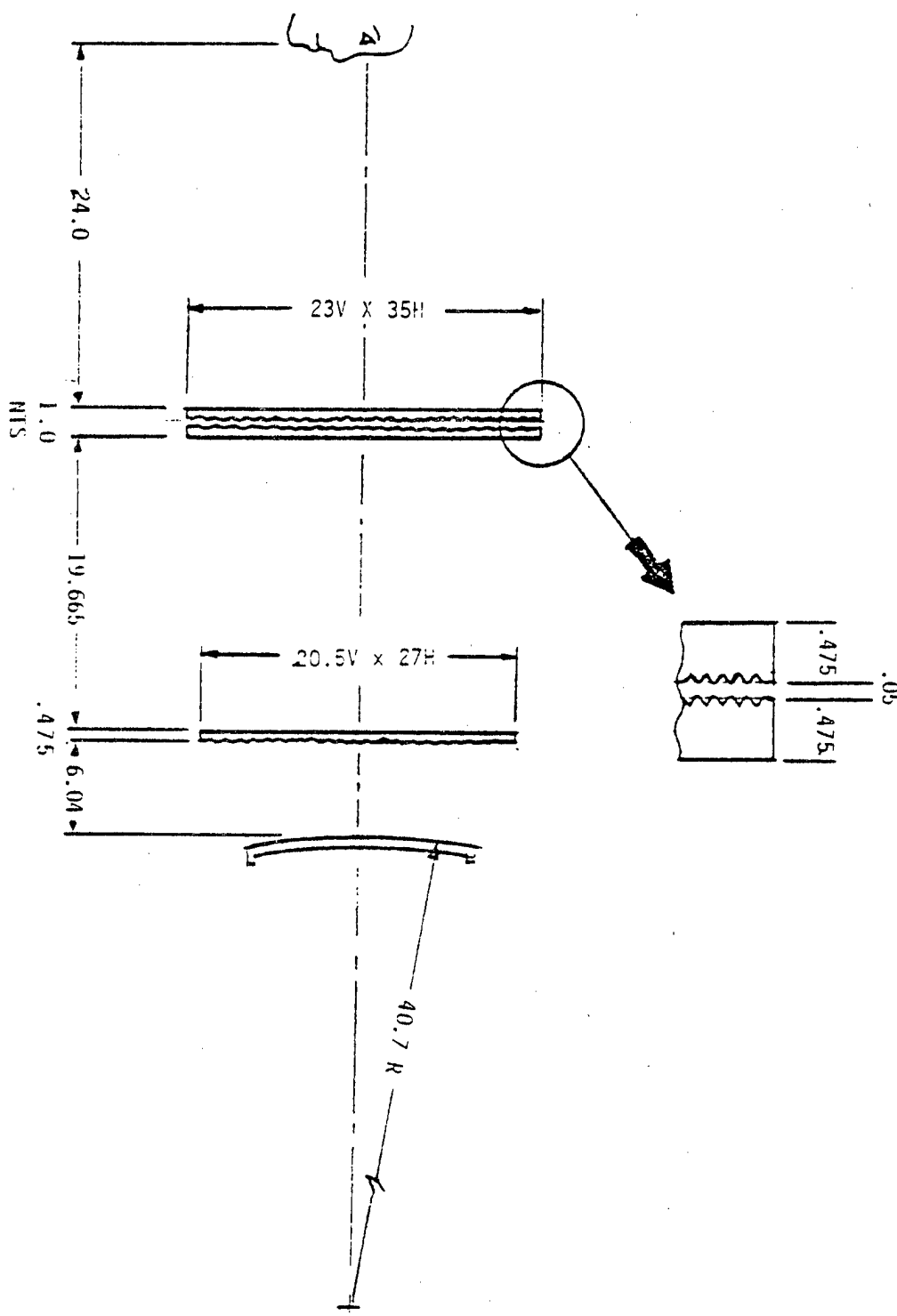


FIG. 18

The separation between Element 1 and Element 2 is .05 inches.

The separation between Element 2 and Element 3 is 19.665 inches.

The focal length of the system is 24.00 inches.

The back focal length of the system, to the front surface of the CRT faceplate is 6.04 inches.

The distortion at point B is - 1.51 %

The distortion at point A is - 2.38%

The distortion at point E is - 3.68%

The eye clearance with this system is 24.00 inches.

Calculated results for this design are given in table 2.

Results are given for 5 field positions, C, B, A, D and E in accordance with the terminology of the specification. For each of these field positions the dipvergence and convergence are given for 10 groups of points 1-10 in accordance with the terminology of the specification. A positive value indicates convergence for which the tolerance is 30 minutes of arc in Area A, and 40 minutes of arc in Area B. A negative value indicates divergence. The upper value in each pair is the dipvergence; the lower value is the convergence or divergence.

The field and pupil points at which we have not been able to meet the specification requirements are marked with an asterisk. For example at field point B and pupil position 3, there is a divergence of 3.61 minutes of arc where none is allowed. At pupil positions 2,3, 4 for field position A the convergence is greater than the allowed value of 30 minutes of arc in the best seeing area.

In some instances the transgression of the specification limits we believe to be minor, and will not significantly impact the performance of the system. The most serious offenders are the pupil positions 6, 7, 8 and 9 for field position E.

This system also has been calculated for an eye clearance of 24.0 inches rather than the specified 25.0 inches. It has also been calculated for a paraxial focal length of 24.00 inches. When this is combined with the distortion at points B, C, and E we get an angular field of 35.2 x 46.2 degrees, with a diagonal of 56.45 degrees in place of the 36 x 48 degrees, with a diagonal field of 57.72 degrees.

TABLE 2. DES. 124.019B Non-Achromatized Design

Results are in minutes of arc.

AREA A

<u>GROUP</u>	<u>FPC</u>	<u>FPB</u>	<u>FPA</u>	<u>FPD</u>	<u>FPE</u>	
1	0.0 .84	3.73 1.17	0.0 27.26	10.66 23.75	9.42 4.56	Dipvergence Div(-)/Convergence } Typ.
2	0.0 .84	3.73 1.17	0.0 31.16*	9.70 5.14	19.58* 15.67	"
3	0.0 .45	0.0 -3.61*	3.86 33.16*	7.08 14.37	16.71* 17.85	"
4	0.0 .45	0.0 6.30	3.86 33.16*	13.09 17.54	11.00 7.56	"

AREA B

5	0.0 3.35	7.79 -4.62	0.0 -7.92	6.03 16.00	15.55 5.12	"
6	0.0 3.35	7.79 -4.62	0.0 -1.05	5.22 -22.62*	26.38* -2.60	"
7	.89 2.75	3.95 .11	5.94 -3.49	1.83 12.64	31.91* 39.55	"
8	.89 2.75	3.95 .11	16.88 8.01	14.45 -7.50	23.95* -1.09	"
9	.89 2.75	12.80 -12.54*	5.94 -3.49	6.27 21.75	13.34 -12.13*	"
10	.89 2.75	12.80 -12.54*	16.88 8.01	3.64 -23.67*	19.24 3.10	"

This is the best compromise, in our opinion, that we have been able to obtain. The problem with which we are faced is that when under correct astigmatism and spherical aberration are introduced to correct the excessive dipvergence and convergence at pupil pairs 6, 7, and 8 of field position E, then we get excessive divergence at pupil point 9 for field position E, and pupil pairs 9 and 10 for field point B.

We should also point out that there is a very rapid onset of the deficiencies at pupil points 6, 7, and 8 for a slight increase in the radial distance off axis for field point E, due to seventh order over correct aberration. Trade-off's in performance may be obtained if the position of field point E is moved in towards the center of the field by about 1 inch.

Also trade-off's can be made if the distortion requirement is relaxed to, say, 8%. These two factors are closely related. The problem is caused by higher order aberrations which come from the rear distortion correcting unit. In the case of movement of point E towards the center of the field there is a reduction of the incidence heights of rays which encounter this surface, so that the effect of high order terms is reduced. In the case of a relaxation of distortion requirements the co-efficients in the higher order terms are reduced and this in turn reduces their effects.

Achromatization

The angular disparity $\delta\theta$, introduced because of chromatic effects, for an ingoing ray with nominal direction cosines (l, m, n) is given by

$$(\delta\theta)^2 = \frac{1}{n^2} [\delta_l^2 (l^2+n^2) + \delta_m^2 (m^2+n^2) + 2 l m \delta_l \delta_m] \quad (15)$$

where, as before,

$$\delta_l = \frac{n}{F} [\delta X (1-l^2) - \delta Y \cdot l m]$$

$$\delta_m = \frac{n}{F} [\delta Y (1-m^2) - \delta X \cdot l m]$$

Hence

$$\delta\theta = \frac{n}{F} [\delta X^2 (1-l^2) + \delta Y^2 (1-m^2) - 2 l m \delta X \delta Y]^{1/2} \quad (16)$$

For the relevant field positions we have

	<u>n</u>	<u>1-l²</u>	<u>1-m²</u>	<u>2_lm</u>
Position C	1.0	1.0	1.0	0.0
Position B	.9545	.9110	1.0	0.0
Position A	.9231	1.0	.8521	0.0
Position D	.9677	.9771	.9594	.0305
Position E	.8869	.9232	.8634	.1024

Calculations have been made for angular disparity for all 5 field positions for all points in the point pairs 1-10, rather than for the points listed in Figure 4 of the specification because data for these points was available from the extensive ray-tracing carried out using the specially developed program and it was believed that this did not result in any significant loss of information. Data for a non-achromatized system is given in Table 3. The points and their system of labelling is shown in Figure 19.

These results show that a non-achromatized system will not meet specification requirements, and the need to achromatize the system was therefore confirmed quantitatively.

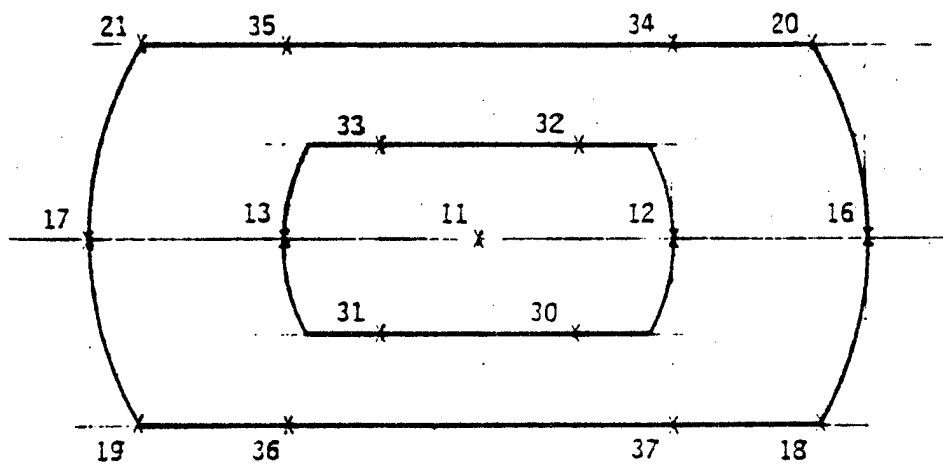


FIGURE 19. POINTS IN THE VIEWING AREA FOR CHECKING CHROMATIC DISPARITIES

TABLE 3. COLOR DISPARITY - (NON-ACHROMATIZED) Figure No. 18

Disparity is between C & F lines. Results are in minutes of arc.

<u>POINT</u>	<u>FPC</u>	<u>FPB</u>	<u>FPA</u>	<u>FPD</u>	<u>FPE</u>	*Note: All values are out of specification
11	0.0	17.78	22.93	15.64	31.77	
12	7.24	19.00	29.89	21.19	38.70	
13	7.24	19.00	17.10	11.28	26.62	
30	5.10	15.15	26.49	17.93	32.71	
31	5.10	15.15	20.19	11.17	26.77	
32	5.10	21.14	26.49	20.19	37.68	
33	5.10	21.14	20.19	15.76	31.62	
- - - - -						
16	14.92	22.63	39.74	28.15	48.15	
17	14.92	22.63	11.46	9.73	22.67	
18	14.93	16.66	38.23	24.40	41.07	
19	14.93	16.66	14.46	2.84	19.07	
20	14.93	27.61	38.05	30.01	51.68	
21	14.93	27.61	14.46	16.48	29.40	
34	9.04	24.81	28.96	23.72	42.68	
35	9.04	24.81	19.67	17.88	33.52	
36	9.04	12.75	19.67	8.26	23.67	
37	9.04	12.75	28.96	17.47	32.50	

Design Results (Achromatized Design)

Two main possibilities are open to us for the color-correcting doublet. The first is to use positive Fresnel elements of low dispersive power and a liquid of high dispersive power. The second is to use negative power Fresnel elements made of high dispersion material with a liquid of low dispersion.

A list of possible liquids for either situation was provided by Dr. Gottfried Rosendahl. A literature search was also made but did not uncover any further significant candidates.

The first approach was to use negative Fresnel elements of styrene or polycarbonate. This gives a wide choice of non-corrosive liquids to fill the space between the Fresnel elements. After discussions with representatives from Optical Sciences Group, Inc. this approach was set aside because of their concern over fabrication problems. They have had extensive experience in the diamond turning of acrylic elements, but have not yet developed a parallel expertise in the fabrication of turned styrene or polycarbonate. The tools tend to tear chips out of these materials, and the recommended approach, if these materials were to be used, would involve the fabrication of molds.

A further search for high dispersion liquids was therefore made and an immersion liquid made by Cargille Laboratories (on a proprietary basis) was found with suitable dispersion characteristics. Relevant data are as follows:

Acrylic N_C 1.48920

N_D 1.49170

N_F 1.49780

$V = 57.4$

Cargille Liquid N_C 1.52869

N_D 1.53326

N_F 1.54487

$V = 32.46$

There was some concern that this liquid might attack the polished surfaces of acrylic Fresnel elements. Sample elements were therefore obtained from Optical Sciences Group and forwarded to Cargille Laboratories for testing with this liquid. Up to the time of writing this report no signs of attack upon the acrylic surfaces have been observed.

While these tests were in progress, a design was completed using this liquid as the dispersive medium between the acrylic Fresnel lenses.

The design parameters of this system are as follows:

Fresnel #1. $a = -3.868 \times 10^{-2}$
 $b = 5.275 \times 10^{-5}$
 $c = -2.030 \times 10^{-7}$
 $d = 2.907 \times 10^{-10}$

Fresnel #2. $a = 4.375 \times 10^{-2}$
 $b = -7.247 \times 10^{-5}$
 $c = 2.509 \times 10^{-7}$
 $d = -3.714 \times 10^{-10}$

Fresnels #3 & #4

$a = -5.00 \times 10^{-2}$
 $b = 5.00 \times 10^{-5}$
 $c = 0.0$
 $d = 0.0$

Fresnel #5 $a = -4.098 \times 10^{-2}$
 $b = 5.00 \times 10^{-5}$
 $c = 4.500 \times 10^{-7}$
 $d = -4.120 \times 10^{-10}$

All Fresnel elements are .475" thick.

The separation between #1 and #2, and between #3 and #4 is .050 inches.

The separation between #2 and #3 is .50 inches.

The separation between #4 and #5 is 18.465 inches.

The equivalent focal length is 24.01 inches.

The back focus measured to the front surface of the CRT faceplate is 5.907 inches. (Figure 20)

The distortion at field point A is -2.47%, at field point E is -3.76%.

Results for dipvergence and convergence/divergence are given in Table 4.

These results are very comparable with the results already quoted for the non-achromatized system, and the comments made about the earlier system are applicable here also.

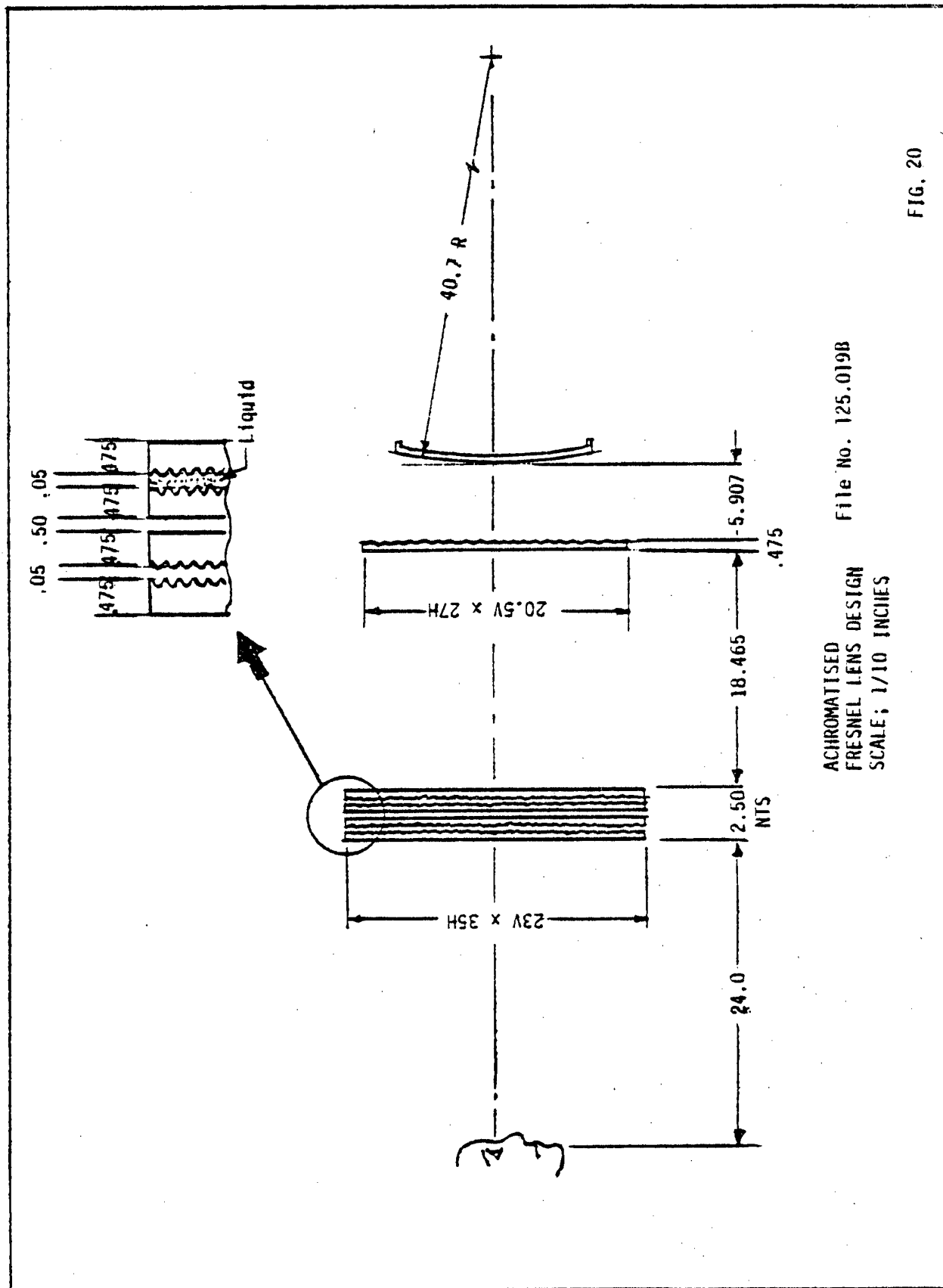


TABLE 4. DES. 125.019B Figure No. 20

Results are given in minutes of arc.

AREA A

<u>GROUP</u>	<u>FPC</u>	<u>FPB</u>	<u>FPA</u>	<u>FPD</u>	<u>FPE</u>	
1	0.0 .84	3.84 1.08	0.0 27.86	10.74 23.92	8.99 3.57	Dipvergence Div(-)/Convergence } Typ
2	0.0 .84	3.84 1.08	0.0 31.39*	9.65 4.89	19.87* 15.78	"
3	0.0 .44	0.0 -5.08*	4.01 33.80*	7.01 14.17	17.00 18.18	"
4	0.0 .44	0.0 5.28	4.01 33.80*	13.20 17.51	10.56 6.81	"

AREA B

5	0.0 3.52	9.54 -4.09	0.0 -7.20	6.17 17.02	13.85 1.00	"
6	0.0 3.52	9.54 -4.09	0.0 -1.48	5.21 22.74*	26.59* -2.71	"
7	.97 2.89	3.50 .69	6.13 -4.98	2.14 13.36	29.66* 35.24	"
8	.97 2.89	3.50 .69	17.00 7.86	14.39 -7.53	23.66* -1.24	"
9	.97 2.89	12.77 -12.48*	6.13 -4.98	6.06 22.62	12.75 -13.59*	"
10	.97 2.89	12.77 -12.48	17.00 7.86	3.63 -23.84	19.45 2.92	"

The angular disparities introduced by chromatic effects have also been evaluated for the C and F lines. Results are given in Table 5.

These show a marked improvement over the results previously quoted and fall within the specification limits, namely an angular spread not to exceed 4 minutes of arc in the best seeing area and not to exceed 6 minutes of arc in the good seeing area.

Fresnel Shading

An aspect of performance to which particular attention must be paid is the loss of transmission resulting from the finite groove structure of the Fresnel surface. The situations which create this loss are shown in figures 21, 22 and 23. x is the slope of the light ray and is positive as shown in figure 21. θ is the draft angle of the high rise part of the Fresnel groove, and θ is the slope of the refracting surface.

In figure 21, where x is greater than θ the light loss is equal to $DE + gE$. In terms of the relevant angles it is given by

$$L(1) = \frac{\sin \theta}{\cos x} \left[\frac{\sin (x - \theta)}{\cos (\theta - \theta)} + \frac{\sin (i - r)}{\cos r} \right]$$

$$i = \theta - x \text{ and } \mu \sin r = \mu^1 \sin i$$

As the ray angle x decreases and becomes negative we have the condition shown in figure 22. The loss in this case is given by

$$L(2) = \frac{\sin \theta}{\cos x} \frac{\sin (i - r)}{\cos r}$$

The transition from L(1) to L(2) takes place when $x = \theta$. As before $i = \theta - x$ and $\mu \sin r = \mu^1 \sin i$.

As the angle x decreases, or becomes more negative, we encounter the situation shown in figure 23, where the refracted ray does not encounter the corner C. In this case the loss L(3) is given by

$$L(3) = \frac{\sin \theta}{\cos x} \frac{\sin (\theta - x)}{\cos (\theta - \theta)}$$

The transition from L(2) to L(3) occurs when $r = \theta - \theta$, and x derived from this has the value x_0 where

$$x_0 = \theta - \text{arc Sin} \left[\frac{\mu}{\mu^1} \sin (\theta - \theta) \right]$$

A short computer program was written to evaluate the loss L for the three categories of loss. For a turned Fresnel lens of the type that we are proposing to use a reasonable value for θ is 3 degrees.

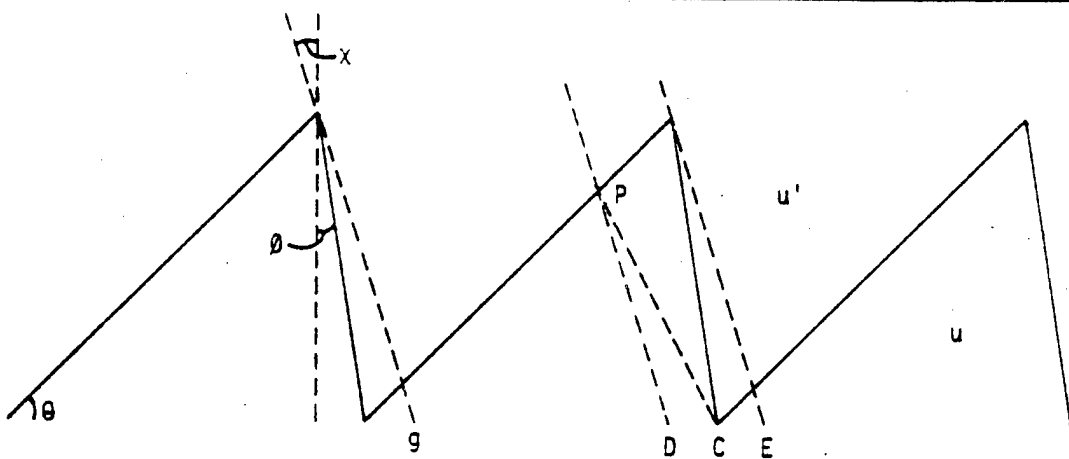
These formulae show that there is no one figure which specifies the transmission of a Fresnel lens because of the dependence upon θ and x .

TABLE 5. COLOR DISPARITY - (ACHROMATIZED)

Figure No. 20
File No. 125.019B

Disparity is between C & F lines. Results are in minutes of arc.

<u>POINT</u>	<u>FPC</u>	<u>FPB</u>	<u>FPA</u>	<u>FPD</u>	<u>FPE</u>
11	0.0	.69	.49	.97	2.62
12	.24	.62	1.75	.30	3.08
13	.24	.62	.79	1.26	1.35
30	.20	1.05	1.24	.85	2.76
31	.20	1.05	.24	1.27	1.43
32	.20	.22	1.24	.39	3.14
33	.20	.22	.24	.97	2.56
- - - - -					
16	.01	.84	1.61	.88	1.65
17	.01	.84	1.52	1.24	.46
18	.01	1.09	1.81	.75	2.74
19	.01	1.09	1.28	1.19	.75
20	.01	1.09	1.81	.95	.90
21	.01	1.09	1.28	1.03	2.03
34	.24	.56	1.63	.20	2.81
35	.24	.56	.91	.80	2.82
36	.24	1.27	.91	1.31	1.55
37	.24	1.27	1.63	.82	2.70



RAY REFRACTED AT POINT P GOES TO C.

FIGURE 21

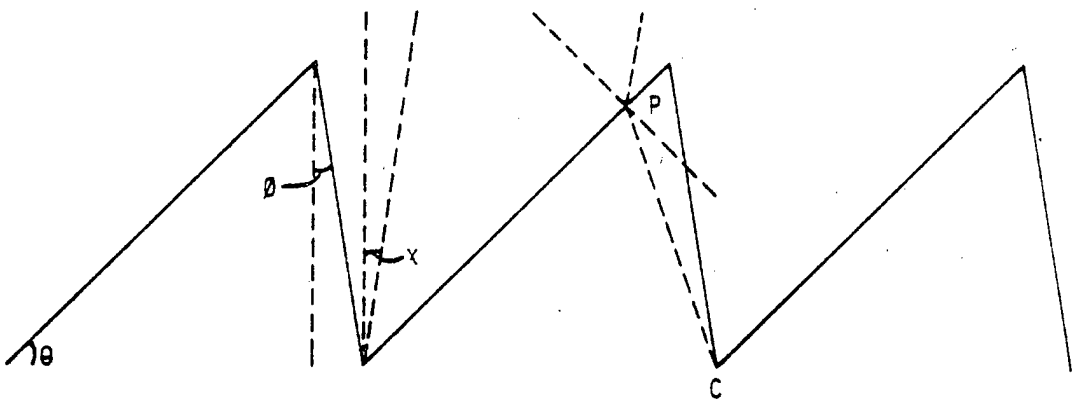
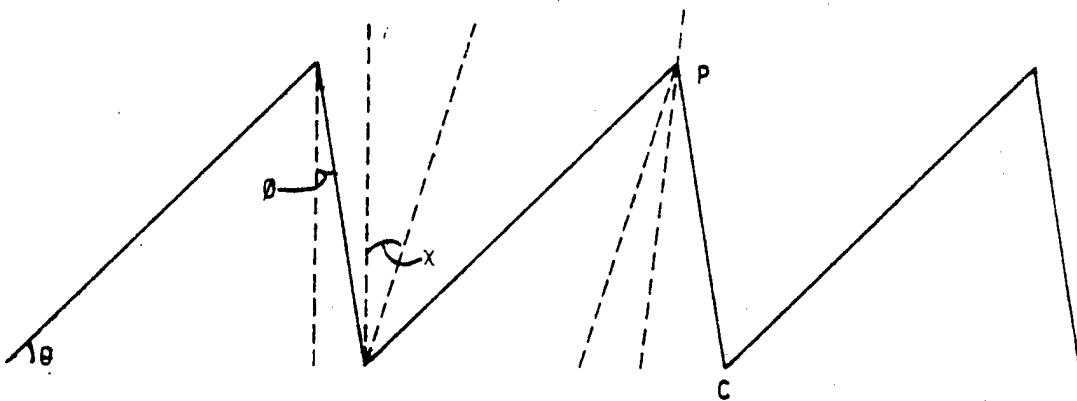


FIGURE 22



RAY REFRACTED AT P DOES NOT REACH C.

FIGURE 23

For the achromatized system for which specific data has been given above we have the following values of θ in Table 6 for a range of radial distances R from the center of each element (in inches).

TABLE 6 Achromatized Design-Figure No. 20-File No. 125.0198

<u>ELEMENT</u>	#1		#2		#3/#4		#5	
	<u>R (in.)</u>	<u>$\sin \theta$</u>	<u>θ Deg</u>	<u>$\sin \theta$</u>	<u>θ Deg</u>	<u>$\sin \theta$</u>	<u>θ Deg</u>	<u>$\sin \theta$</u>
1.0	.0386	2.21	.0437	2.50	.0500	2.86	.0409	2.35
2.0	.0769	4.41	.0869	4.99	.0996	5.72	.0815	4.68
3.0	.1146	6.58	.1294	7.43	.1487	8.55	.1215	6.98
4.0	.1515	8.72	.1706	9.82	.1968	11.35	.1603	9.22
5.0	.1874	10.80	.2104	12.15	.2438	14.11	.1973	11.38
6.0	.2222	12.84	.2487	14.40	.2892	16.81	.2317	13.40
7.0	.2558	14.82	.2853	16.58	.3329	19.44	.2625	15.22
8.0	.2845	16.77	.3203	18.68	.3744	21.99	.2884	16.76
9.0	.3203	18.68	.3540	20.73	.4136	24.43	.3078	17.92
10.0	.3514	20.58	.3864	22.73	.4500	26.74	.3189	18.60
11.0	.3423	22.48	.4180	24.71	.4835	28.91	.3198	18.65
12.0	.4131	24.40	.4490	26.67	.5136	30.90	.3081	17.95
13.0	.4441	26.36	.4794	28.65	.5401	32.69	.2817	16.36
14.0	.4753	28.38	.5094	30.63	.5628	34.25	.2379	13.76
15.0	.5067	30.44	.5387	32.60	.5813	35.54	.1746	10.06
16.0	.5376	32.52	.5666	34.51	.5952	36.53	-.0896	5.14
17.0	.5673	34.57	.5915	36.27	.6044	37.18	-.0189	-1.08
18.0	.5942	36.46	.6116	37.70	.6084	37.47	--	--
19.0	.6159	38.02	.6234	38.57	.6071	37.38		
20.0	.6291	38.98	.6227	38.52	.6000	36.87		
21.0	.6293	39.00	.6034	37.11	.5870	35.94		
22.0	.6104	37.61	.5575	33.88	.5676	34.58		

In order to calculate the light loss involved in the system, the following rays were traced:

- 1) On axis - Rays at pupil radius 3.00 inches and 6.00 inches.
- 2) Field Zone - Gaussian image height 8.75 inches.
Upper and lower rim rays for a 3 inch radius pupil.
Upper and lower rim rays for a 6 inch radius pupil.
- 3) Field Corner
Upper and lower rim rays for a 3 inch radius pupil.
Upper and lower rim rays for a 6 inch radius pupil.

Intercept heights and the values of x are given for the two pairs of elements and for the single element. For the pairs of elements the intercept height is taken as being the same on each element and the value of θ is obtained by interpolation from the tables given above. The value of x which is used is that of the ray between the elements, with a change in sign from one element to the other.

(H is the intercept height,
 T is the transmission,
 u denotes upper rim ray,
 L denotes lower rim ray.)

In making the analysis we have used a "worst-case" method of computation. The losses at each surface have been added. This does not take into account that rays which are taken as being lost at a particular Fresnel surface may already have been lost at an earlier surface. It gives a lower limit to the transmission.

On the other hand an approach which uses the product of transmissions at each surface will give an optimistic value for the overall transmission. We recommend that future plans be based upon the first, more pessimistic, value for the transmission.

An examination of the results obtained from this detailed analysis shows that the major drop in transmission occurs at the corner of the field for the full un-vignetted pupil. When this situation occurs then the light which comes to one eye is much more attenuated than the light coming to the other eye. We believe that this will not significantly affect the overall performance of the system.

<u>RAY</u>	<u>6" PUPIL RADIUS</u>			<u>3" PUPIL RADIUS</u>		
	<u>H</u>	<u>X</u>	<u>TRANS. %</u>	<u>H</u>	<u>X</u>	<u>TRANS. %</u>
<u>AXIAL</u>						
Pair 1 & 2	6.00	-.11353	93.54	3.00	-.05695	98.37
Pair 3 & 4	5.72	-.22382	87.03	2.86	-.11456	96.73
Single 5	1.56	-.24465	<u>98.06</u>	.765	-.12421	<u>99.51</u>
PRODUCT			79.82			94.69
ADDED LOSSES			(78.63)			(94.61)
<u>FIELD ZONE (u)</u>						
Pair 1 & 2	14.86	.07816	77.20	11.86	.13586	82.16
Pair 3 & 4	14.60	-.19160	74.41	11.74	-.08546	91.00
Single 5	11.41	-.34626	<u>86.25</u>	10.55	-.23753	<u>90.17</u>
PRODUCT			49.55			67.42
ADDED LOSSES			(37.86)			(63.33)
<u>FIELD ZONE (L)</u>						
Pair 1 & 2	2.86	.28802	93.62	5.86	.23552	88.66
Pair 3 & 4	3.13	.22980	92.62	5.99	.11807	93.08
Pair 5	7.79	.09548	<u>96.92</u>	8.52	-.02157	<u>96.57</u>
PRODUCT			84.04			79.78
ADDED LOSSES			(83.16)			(78.41)
<u>FIELD CORNER (u)</u>						
Pair 1 & 2	18.65	.13353	61.24	15.65	.19097	66.29
Pair 3 & 4	18.37	-.20991	69.31	15.49	-.11415	84.99
Pair 5	14.85	-.27883	<u>93.64</u>	13.85	-.21507	<u>93.22</u>
PRODUCT			39.75			52.52
ADDED LOSSES			(24.19)			(44.50)
<u>FIELD CORNER (L)</u>						
Pair 1 & 2	6.65	.34130	81.56	12.65	.24465	71.89
Pair 3 & 4	6.88	.20183	86.09	12.62	-.00477	93.66
Single 5	11.14	.05649	<u>96.98</u>	13.03	-.12494	<u>94.87</u>
PRODUCT			68.09			63.88
ADDED LOSSES			(64.63)			(60.42)

TABLE 7
ACHROMATIZED DESIGN

Astigmatism

There is no conventional equivalent to the astigmatism requirement imposed by the specification. In standard optical treatises the question of astigmatism is considered in terms of the behavior of rays surrounding a principal ray, i.e. one which goes through the center of the entrance pupil of the system. When this is the case we have two well defined azimuths, namely tangential and sagittal in which ray behavior may be examined. We lose this natural choice of azimuths when ray behavior is to be examined for small off-axis areas.

The procedure which was therefore adopted comprised the tracing of rays through the pupil points shown in the diagram. The other half of the pupil area gives symmetrical results. Other networks of pupil points could equally well be used, but this particular form was the most convenient to implement in computer program changes. These rays were traced for an axial field point, and for field points at 4.375, 6.00, 8.75 and 12.50 inches from the center of the field.

For each ray the ΔX and ΔY intercept values in the focal plane, relative to the intercept point of the principal ray were calculated. These values are listed in Table 8 to 12 and are plotted in Figures 24 to 28. No figure is given for the axial case since these values are too small to appear on the plot. See table 7 for values. In the tables, θ is the orientation of the radius vector. When $\theta = 0^\circ$ we have the upper rim ray. When $\theta = 180^\circ$ we have the lower rim ray. The value listed as position is the radial distance of the pupil point measured as a fraction of a 6 inch pupil radius. In the tables also the first figure given in each pair is the ΔX coordinate of the intersection of the ray with the image plane, and the second is the ΔY coordinate referred to the intersection point of the principal rays. In the graphs the plot is of a conventional form in which negative values of the abscissa represents the lower rim rays.

The specification calls for not more than .75 diopters of astigmatism for any 5 mm pupil. This can be interpreted as meaning that if the angular spread of a pair of rays from the top and bottom of the pupil

is α , and if the corresponding spread from a ray pair at the right and left sides of the pupil is β , then $(\alpha - \beta)$ must be numerically less than K where

$$K = \frac{.2}{39.37} \times .75 \text{ radians} \quad (.2'' = 5 \text{ nm})$$

$$= \frac{.2}{39.37} \times .75 \times 57.3 \times 60 \text{ minutes of arc}$$

Alternatively, to a sufficient approximation, we can convert these angular spreads into ΔX and ΔY displacements in the image plane.

$$\Delta Y = \alpha \times 24.0, \quad \Delta X = \beta \times 24.0$$

where the focal length of the system is 24.0 inches.

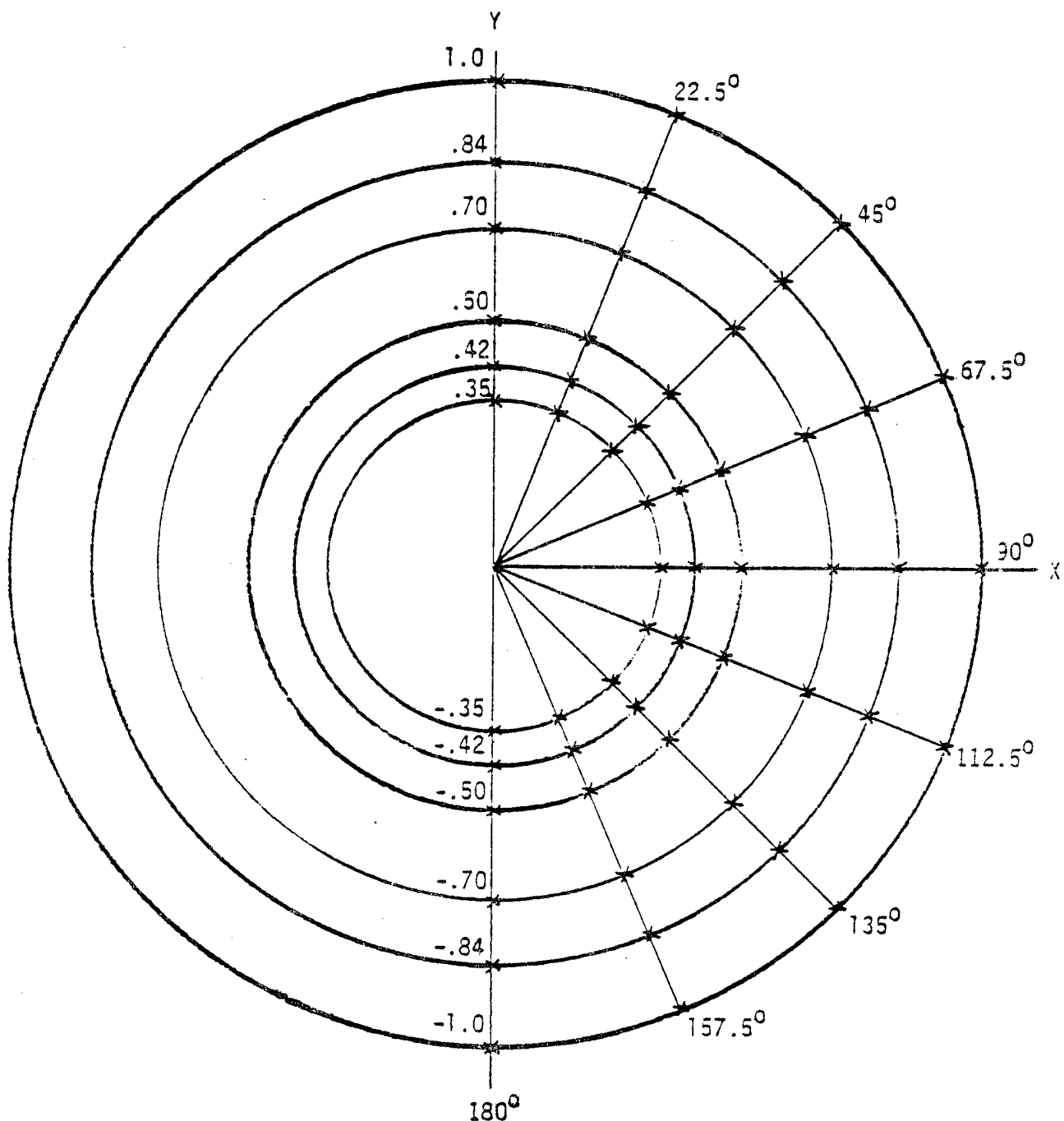
Hence the condition becomes

$$|\Delta Y - \Delta X| < \frac{.2}{39.37} \times .75 \times 24.0$$

To a sufficient approximation this can be made equal to .09 inches.

In other words we have to examine the graphs of ΔX and ΔY to ascertain that $|\Delta Y - \Delta X| < .09$ for any abscissa value of .033. (The pupil radius is 6 inches for the system, and the eye area to be selected is $.2''$ diameter).

An examination of the graphs shows that this condition is satisfied, and that the only time that we come near to exceeding it is for the upper rim rays at the edge of the pupil for the 12.5" off-axis image point.



PUPIL POINTS FOR ASTIGMATISM CALCULATIONS.

FIGURE 24

TABLE 8 - Axial Point

*POSITION	$\theta = 0^\circ$	22.5°	45°	67.5°	90°	112.5°	135°	157.5°	180°
1.00 ΔX	0.0	.01165	.02152	.02811	.03043	.02811	.02152	.01165	0.0
ΔY	.03043	.02811	.02152	.01165	0.0	-.01165	-.02152	-.02811	-.03043
.84 ΔX	0.0	.00843	.01557	.02034	.02202	.02034	.01557	.00843	0.0
ΔY	.02202	.02034	.01557	.00843	0.0	-.00843	-.01557	-.02034	-.02202
.70 ΔX	0.0	.00561	.01036	.01353	.01465	.01353	.01036	.00561	0.0
ΔY	.01465	.01353	.01036	.00561	0.0	-.00561	-.01036	-.01353	-.01465
.50 ΔX	0.0	.00224	.00414	.00541	.00586	.00541	.00414	.00224	0.0
ΔY	.00586	.00541	.00414	.00224	0.0	-.00224	-.00414	-.00541	-.00586
.42 ΔX	0.0	.00137	.00253	.00331	.00358	.00331	.00253	.00137	0.0
ΔY	.00358	.00331	.00253	.00137	0.0	-.00137	-.00253	-.00331	-.00358
.35 ΔX	0.0	.00083	.00153	.00201	.00217	.00201	.00153	.00083	0.0
ΔY	.00217	.00201	.00153	.00083	0.0	-.00083	.00153	-.00201	-.00217

* As a fraction of 6 inch pupil radius.

TABLE 9. 4.375" Off-Axis Field Point

<u>*POSITION</u>	<u>$\theta = 0^\circ$</u>	<u>22.5°</u>	<u>45°</u>	<u>67.5°</u>	<u>90°</u>	<u>112.5°</u>	<u>135°</u>	<u>157.5°</u>	<u>180°</u>
1.00 ΔX	0.0	.06235	.08795	.08507	.02071	-.06453	-.11469	-.08881	0.0
ΔY	.35031	.32588	.25788	.16570	.08472	.05265	.07972	.13289	.15910
.84 ΔX	0.0	.05318	.08246	.07121	.02040	-.04395	-.08076	-.06254	0.0
ΔY	.30875	.28554	.22210	.13812	.06396	.02815	.03716	.06756	.08336
.70 ΔX	0.0	.04225	.06491	.05568	.01708	-.05026	-.05672	-.04388	0.0
ΔY	.25863	.23838	.18355	.11161	.04719	.01173	.00982	.02540	.03436
.50 ΔX	0.0	.02447	.03721	.03175	.01070	-.01413	-.02768	-.02146	0.0
ΔY	.17130	.15741	.11998	.07077	.02492	-.00527	-.01668	-.01620	-.01439
.42 ΔX	0.0	.01817	.02758	.02360	.00840	-.00934	-.01899	-.01478	0.0
ΔY	.13746	.12625	.09696	.05598	.01784	-.00902	-.02182	-.02478	-.02470
.35 ΔX	0.0	.01341	.02036	.01754	.00666	-.00597	-.01289	-.01011	0.0
ΔY	.11016	.01017	.07683	.04436	.01272	-.01086	-.02385	-.02866	-.02958

* As a fraction of 6 inch pupil radius.

TABLE 10. 6.25" Off-Axis Field Point

<u>*POSITION</u>	<u>$\theta = 0^\circ$</u>	<u>22.5°</u>	<u>45°</u>	<u>67.5°</u>	<u>90°</u>	<u>112.5°</u>	<u>135°</u>	<u>157.5°</u>	<u>180°</u>
1.00 ΔX	0.0	.04940	.08052	.06968	.00172	-.09892	-.16198	-.12492	0.0
ΔY	.30832	.35004	.29306	.19997	.09611	.02869	.02814	.07020	.09471
.84 ΔX	0.0	.04838	.07687	.06648	.01095	-.06561	-.11158	-.08607	0.0
ΔY	.35874	.33698	.27306	.17664	.07380	.00190	-.01924	-.00455	.00699
.70 ΔX	0.0	.04159	.06507	.05607	.01295	-.04363	-.07660	-.05911	0.0
ΔY	.32198	.30044	.23887	.14922	.05504	-.01514	-.04607	-.04746	-.04377
.50 ΔX	0.0	.02636	.04061	.03503	.01094	-.01889	-.03575	-.02776	0.0
ΔY	.23445	.21732	.16933	.10120	.02941	-.02885	-.06416	-.07899	-.08233
.42 ΔX	0.0	.02016	.03049	.02689	.00939	-.01196	-.02399	-.01877	0.0
ΔY	.19505	.18049	.13984	.08228	.02112	-.03017	-.06387	-.08048	-.08507
.35 ΔX	0.0	.01525	.02343	.02053	.00795	-.00727	-.01591	-.01260	0.0
ΔY	.16123	.14902	.11501	.06680	.01509	-.02957	-.06053	-.07725	-.08229

* As a fraction of 6 inch pupil radius.

TABLE 11. 8.75" Off-Axis Field Point

<u>*POSITION</u>	<u>$\theta = 0^\circ$</u>	<u>22.5°</u>	<u>45°</u>	<u>67.5°</u>	<u>90°</u>	<u>112.5°</u>	<u>135°</u>	<u>157.5°</u>	<u>180°</u>
1.00 Δ	0.0	-.00010	.00210	-.00630	-.05482	-.14495	-.20793	-.15838	0.0
Δ	.23933	.23684	.22338	.17570	.07784	-.03627	-.10637	-.11801	-.11253
.84 Δ	0.0	.01524	.02582	.01794	-.02545	-.09559	-.14087	-.10693	0.0
Δ	.29395	.28448	.24989	.17626	.06305	-.05746	-.14137	-.17561	-.18181
.70 Δ	0.0	.01983	.03193	.02462	-.01102	-.06349	-.09544	-.07220	0.0
Δ	.30294	.28911	.24388	.16148	.04856	-.06722	-.15320	-.19718	-.20909
.50 Δ	0.0	.01680	.02599	.02078	-.00026	-.02834	-.04407	-.03319	0.0
Δ	.25930	.24376	.19695	.12130	.02684	-.06758	-.14240	-.18725	-.20168
.42 Δ	0.0	.01372	.02103	.01695	.00120	-.01873	-.02972	-.02238	0.0
Δ	.22760	.21303	.16997	.10225	.01945	-.06299	-.12951	-.17082	-.18452
.35 Δ	0.0	.01082	.01648	.01341	.00189	-.01228	-.01998	-.01507	0.0
Δ	.19633	.18319	.14483	.08552	.01398	-.05715	-.11528	-.15221	-.16468

* As a fraction of 6 inch pupil radius.

TABLE 12. 12.5" Off-Axis Field Point

<u>*POSITION</u>	<u>$\theta = 0^\circ$</u>	<u>22.5°</u>	<u>45°</u>	<u>67.5°</u>	<u>90°</u>	<u>112.5°</u>	<u>135°</u>	<u>157.5°</u>	<u>180°</u>
1.00 ΔX	0.0	-.06575	-.16953	-.24379	-.25519	-.26158	-.27522	-.18458	0.0
ΔY	.48632	.32628	.05923	-.03728	-.02894	-.10341	-.26410	-.40070	-.44915
.84 ΔX	0.0	-.06220	-.12750	-.16717	-.17667	-.18541	-.18488	-.12560	0.0
ΔY	.18426	.12510	.03215	.00375	-.01229	-.10536	-.25748	-.38521	-.43248
.70 ΔX	0.0	-.04926	-.09287	-.11808	-.12736	-.13503	-.13139	-.08696	0.0
ΔY	.09727	.07579	.04320	.02895	-.00440	-.09988	-.23488	-.34669	-.38868
.50 ΔX	0.0	-.02833	-.05135	-.06573	-.07350	-.07729	-.07102	-.04463	0.0
ΔY	.07949	.07533	.06544	.04610	.00046	-.08028	-.17749	-.25558	-.28510
.42 ΔX	0.0	-.02171	-.03944	-.05113	-.05775	-.06000	-.05360	-.03287	0.0
ΔY	.08147	.07824	.06816	.04591	.00090	-.06959	-.15000	-.21355	-.23752
.35 ΔX	0.0	-.01698	-.03104	-.04070	-.04619	-.04733	-.04120	-.02473	0.0
ΔY	.08095	.07765	.06658	.04311	.00093	-.05957	-.12561	-.17696	-.19625

* As a fraction of 6 inch pupil radius.

4.375" Axial Field Position

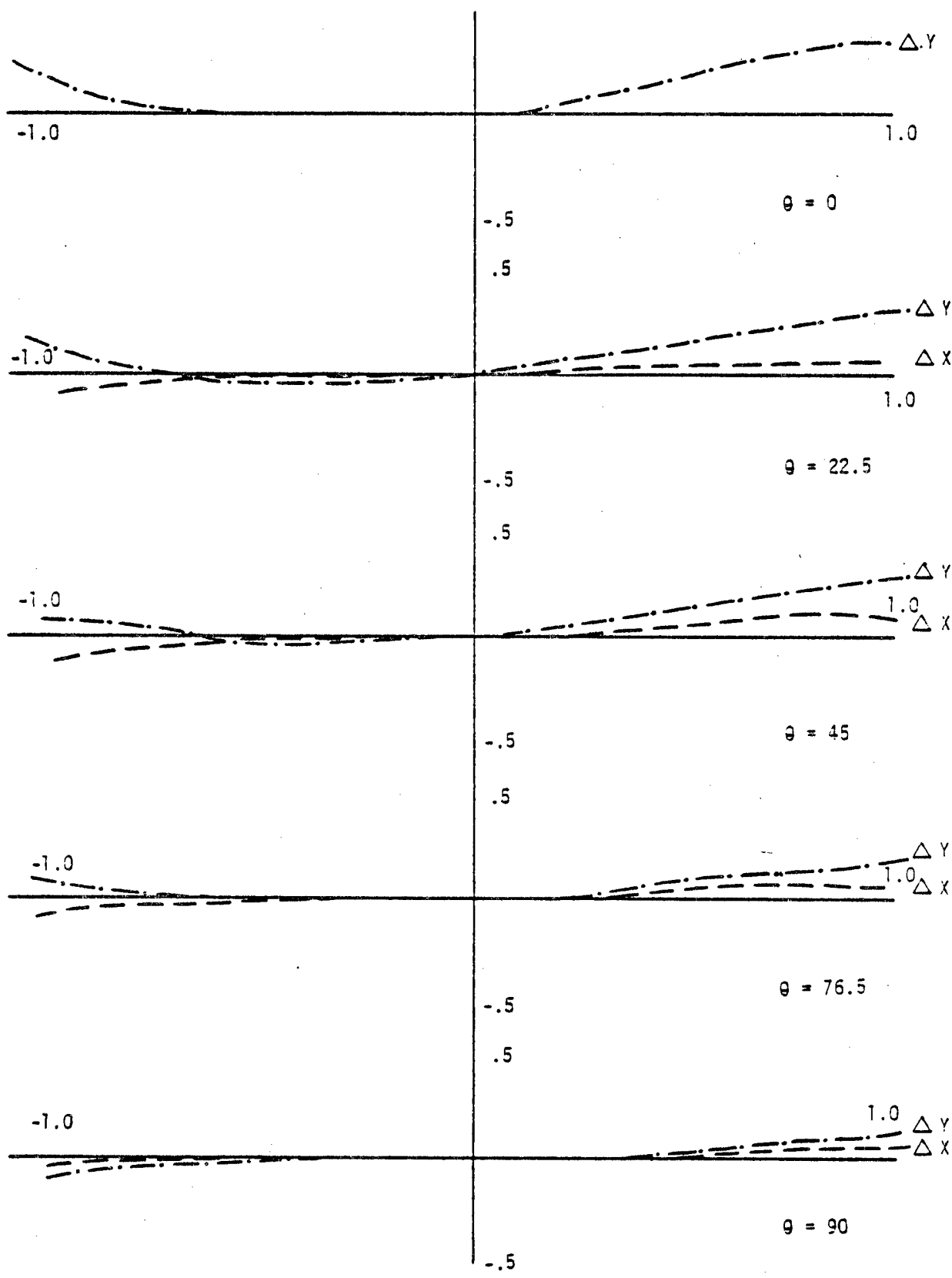


FIG. 25

6.25" Axial Field Position

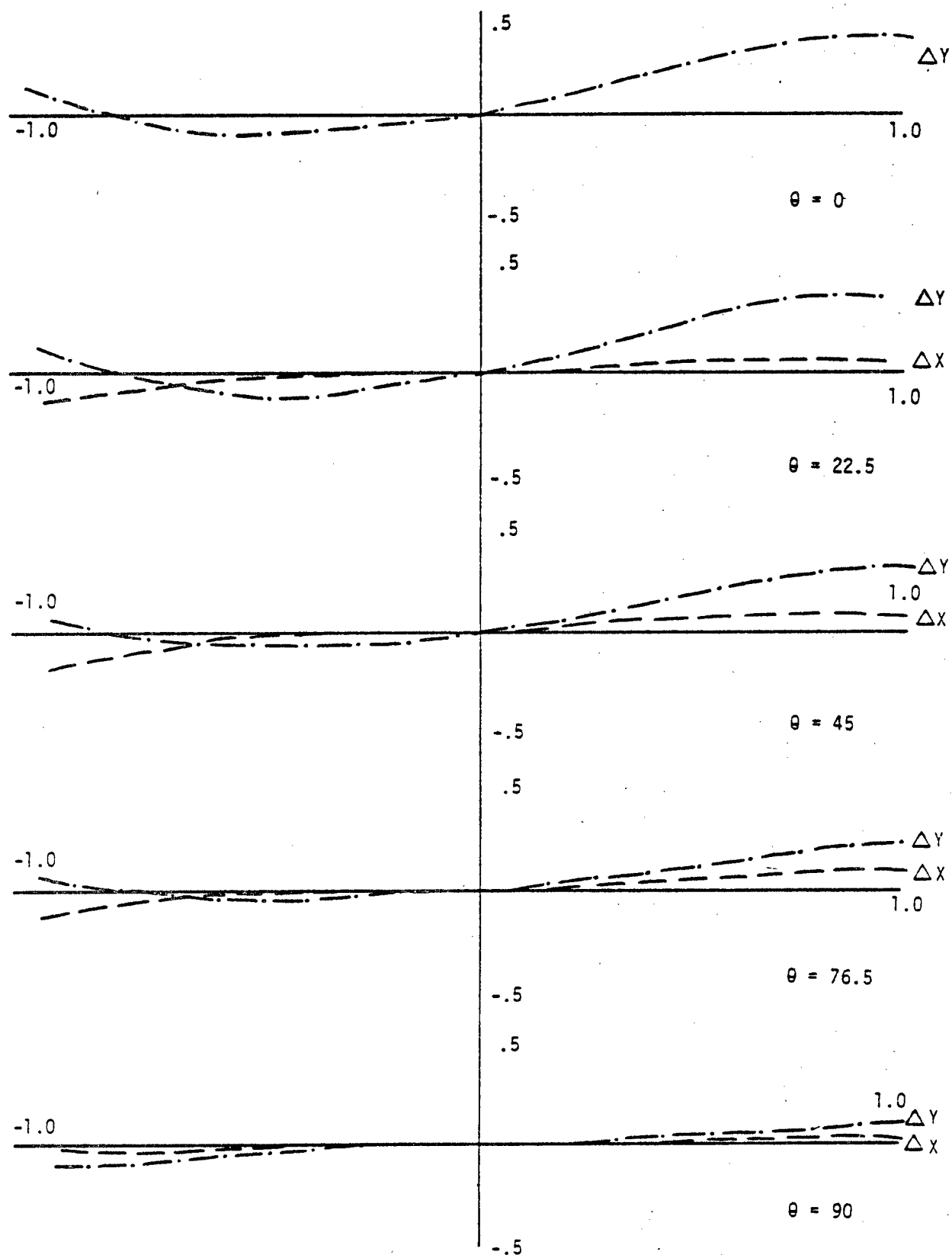


FIG. 26

8.75" OFF-AXIS FIELD POINT

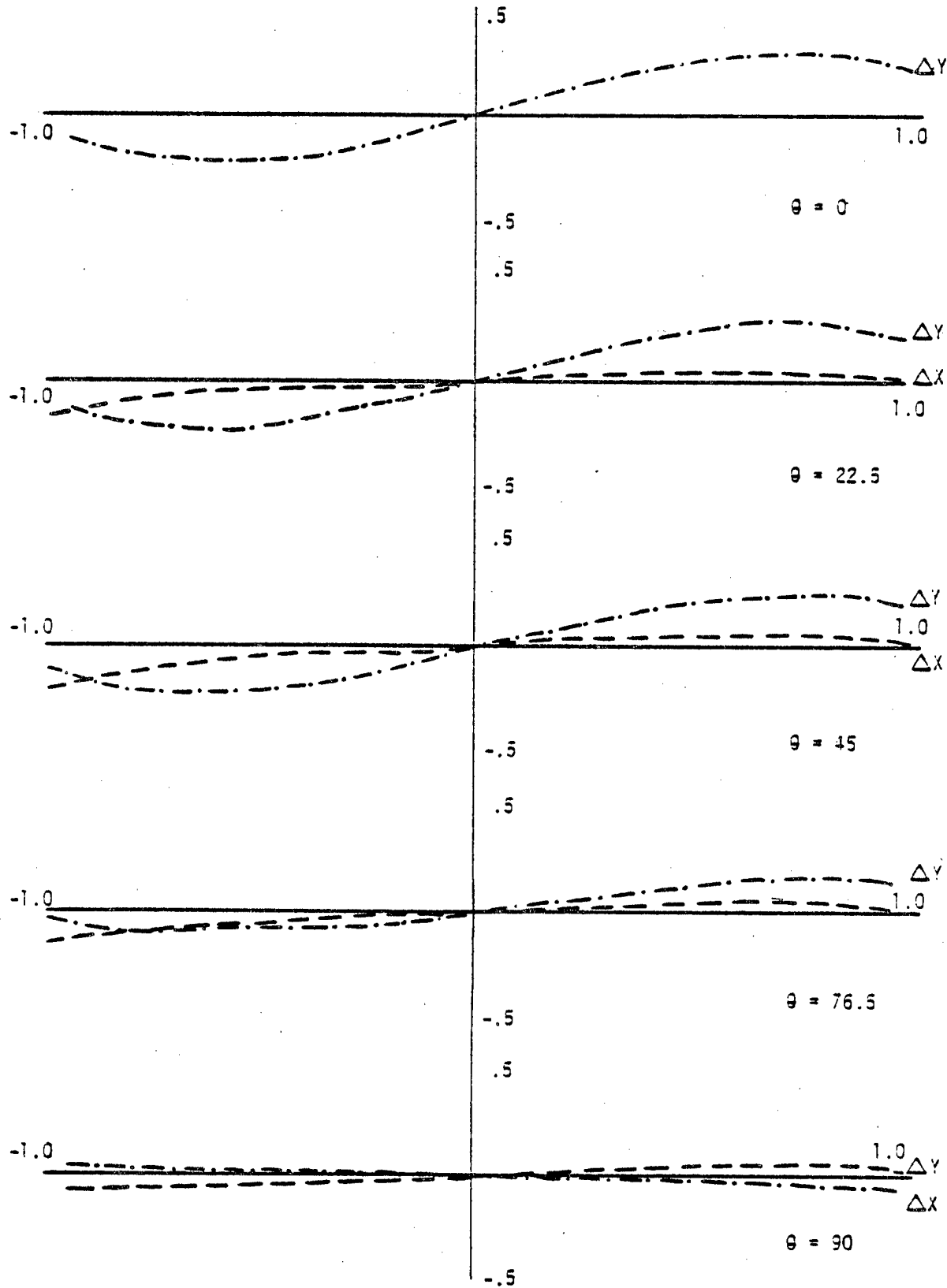


FIG. 27

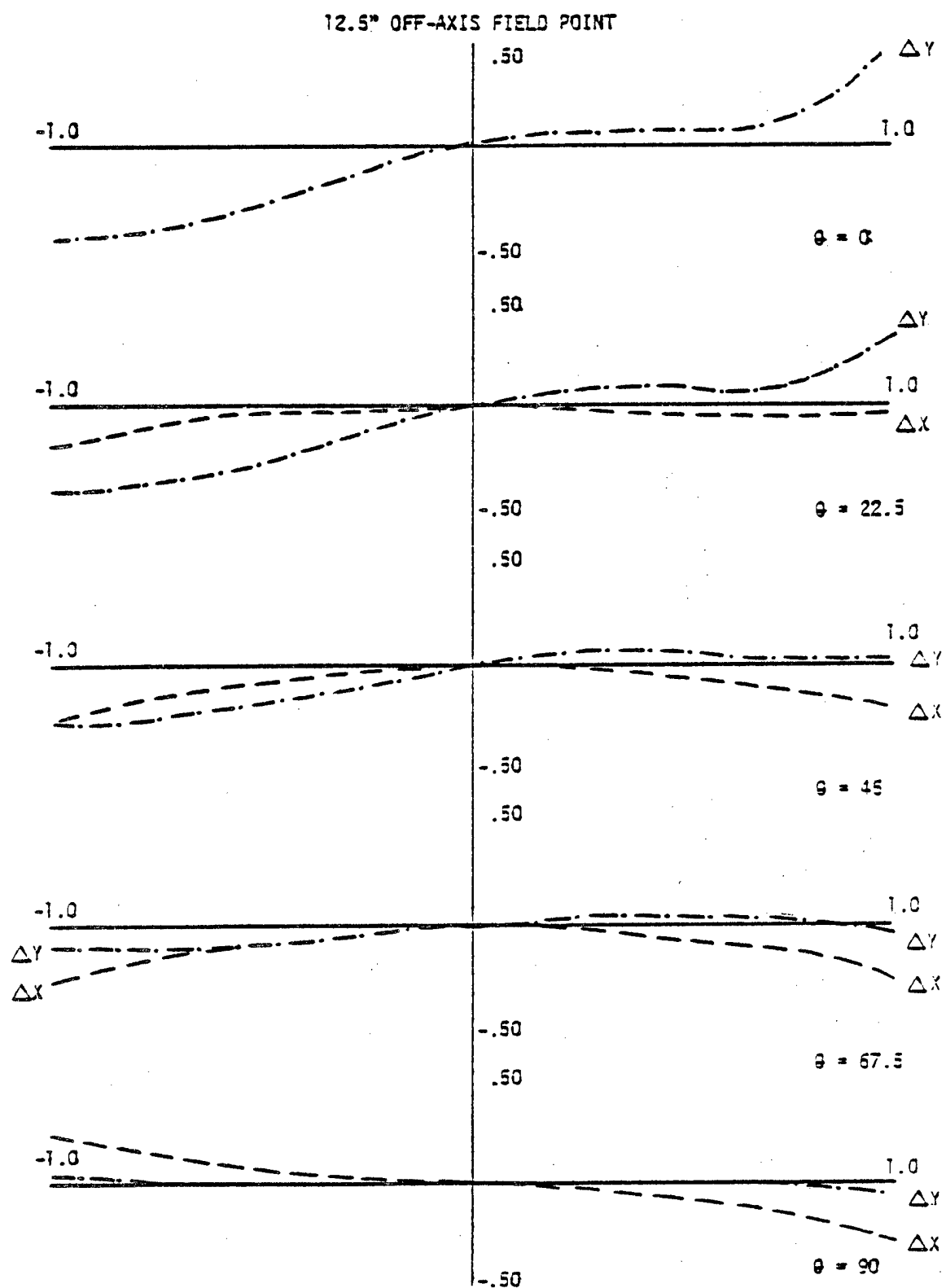


FIG. 23

MECHANICAL DESIGN

Mechanical Design Parameters

The mechanical tolerances necessitated by the Fresnel lens design require individual axial lens adjustments in the X, Y, and Z planes to eliminate Fresnel lens decentration. The Z axis axial motion range for each assembly has been determined as $\pm .06$ inches to be maintained within an accuracy of $\pm .03$ inches. The cross-axes X and Y motions of the design require corrections to 2nd order precision. These measurements must be controlled over their travel of $\pm .032$ inches with a vernier scale to $\pm .001$ inches.

The liquid-tight Fresnel assembly requires a positive seal to contain the fluid between elements without introducing distortion of the lenses. The movement of the assembly's individual Fresnel elements is limited to one plane, either X or Y, whereas the entire unit is adjustable in the X, Y, and Z planes.

Adjustable Fresnel Mounts

The X and Y adjustable motions will use two fine pitch screw actuators on each frame. These Fresnel frames slide on two guide rods parallel to each axis. Adjustable stops will lock the frames.

The Z travel motion for each Fresnel mount will be guided on three precision rods which track parallel to the optical axis. The mounts slide on linear bearings and may be locked in position by adjustable stops.

The positive seal for the liquid-tight assembly uses the O-ring controlled principle where the groove confines the elastomer. This leak-proof principle is similar to that used in hydraulic applications to effectively retain the hydraulic fluid in a closed loop at pressures in excess of 1000 psi. In this Fresnel package, the static head of the liquid requires compression at the frames less than 20 psi to maintain the seal.

Mechanical Provisions

The Virtual Image Display (VID) System will be mounted to a portable structural base. Four adjustable legs with rollers and a manual lockable brake will accommodate the system's placement to any table surface.

A removable enclosure will set over and around the Fresnel optics eliminating dust as well as ambient light. Quick release hardware on the cowling will provide easy access for inspection of the interior. The front and rear panels will be bezeled to fit closely with the Fresnel front pair and the rear CRT faceplate (see figure 29).

The structural base design will be a thin wall, light weight, aluminum or magnesium casting featuring skirt and rib gussets. The design calculations for this casting will consider the minimum deflection and maximum stiffness for the least weight of material.

Opto-Mechanical Adjustment & Alignment Design - Achromatized Design

The mechanical mounting design of the VID will provide adjustment and alignment of Fresnel lens components and the CRT faceplate.

The air spaced front pair of Fresnels will be adjustable in X and Y with respect to each other (see figure 30). Each Fresnel lens will have one degree of freedom, in either X or Y, to achieve lateral alignment to a resolution of $\pm .001$ inch. The criteria for adjustment will be the visual elimination of moire patterns as viewed through the Fresnel lens pair. Air spacing of the pair is not critical and will have a looser built in tolerance.

A second independent mount will contain the liquid filled Fresnel lens sandwich (see figures 31 & 32). This mount will feature a leakproof design which allows X and Y adjustment of one Fresnel lens with respect to the other. This doublet will be separately adjusted in X and Y using moire viewing and then placed in the full lens mount, behind the air spaced Fresnel lens pair. The liquid doublet mounting will now provide for a combination of X and Y adjustments to eliminate moire patterns as viewed through all four Fresnel lenses.

The final Fresnel lens singlet will be inserted for final X, Y and Z adjustment.

The CRT faceplate will be adjustable in the X, Y and Z direction. Three horizontal guide rods running from the front to the rear plates of the assembly will provide stiffness to the Fresnel lens sub-assemblies eliminating tilt between them and retaining critical lateral alignment.

The non-achromatized Fresnel lens mechanical design would encompass the same features as the achromatized design.

Fresnel Doublet Leakproof Design

The Liquid Doublet design package will be a fluid-tight, leakproof frame assembly, wherein the Fresnels are able to move independently in predetermined X or Y directions. A fluid will fill the designed separation between elements. Two top ports with cap seals will be used to fill and vent the void with the liquid (see figure 32.)

The positive sealing between Fresnel elements will be accomplished with a controlled confinement principle using a gasket O-ring seal. The molded elastomer O-ring seats in the groove voids where controlled confinement is obtained (see figure 31.)

An alternate design approach for the leakproof Fresnel package may be considered utilizing a teflon seal. The teflon resists absorption, elongates under low compressive pressure, and has a low coefficient of friction. A teflon tape applied to the inner abutting faces of the Fresnel channel frames will provide positive sealing.

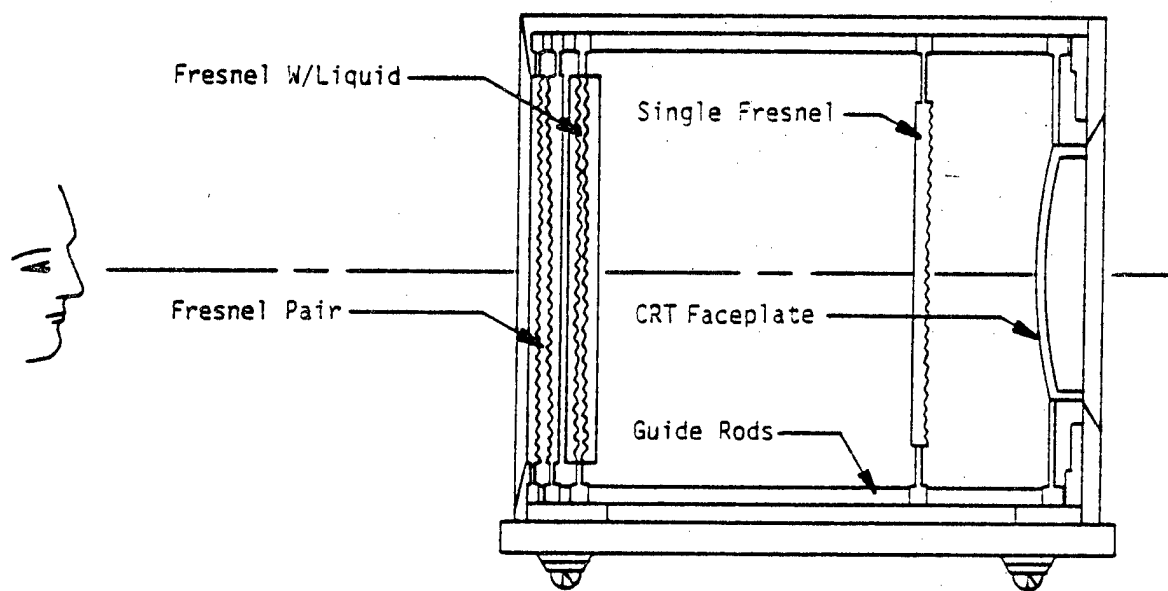
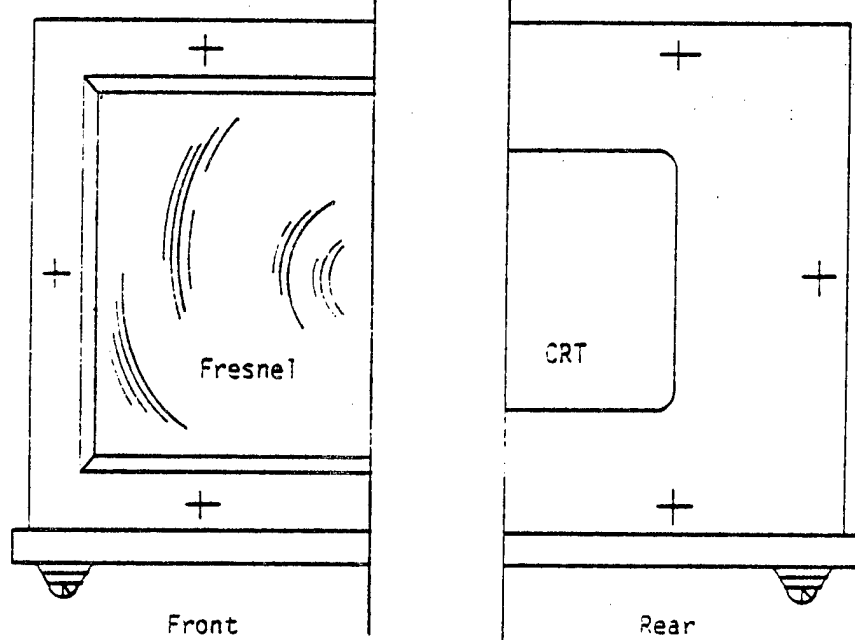


FIG. 29. MECHANICAL ARRANGEMENT

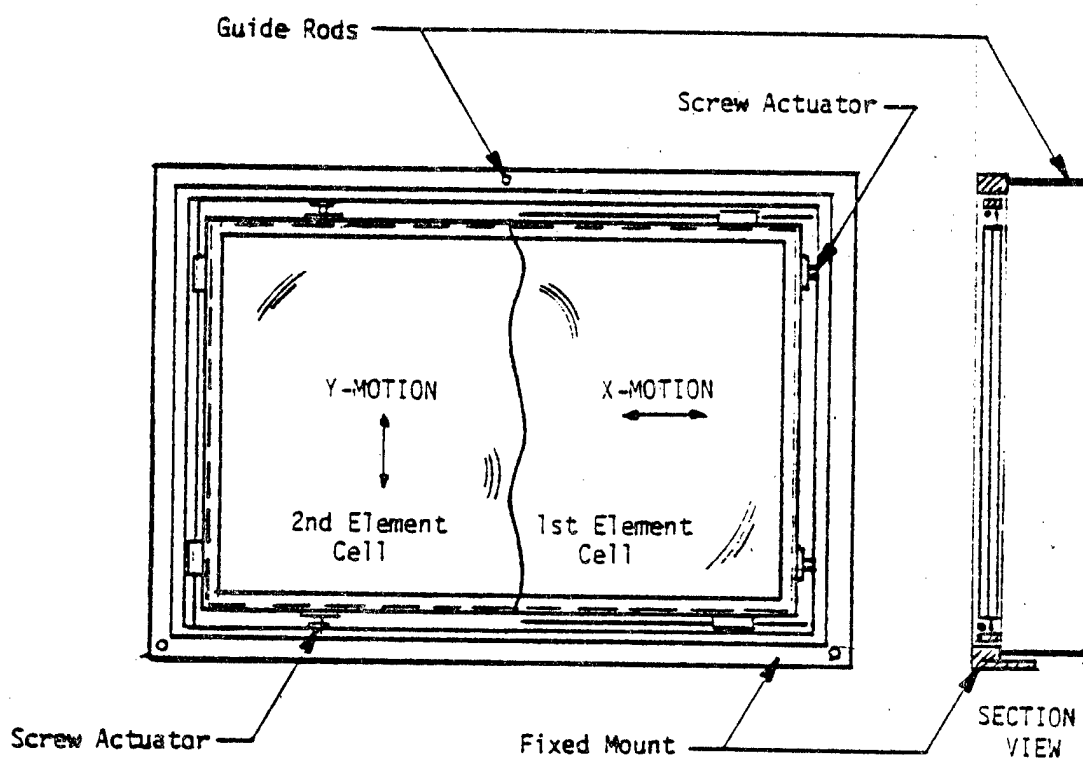
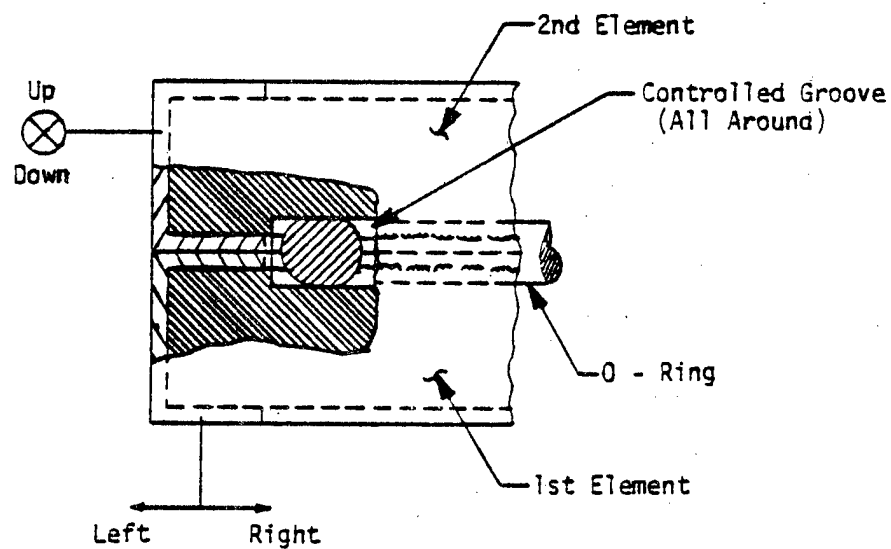


FIG. 30. FRESNEL CELLS & MOUNT



ENLARGED VIEW A

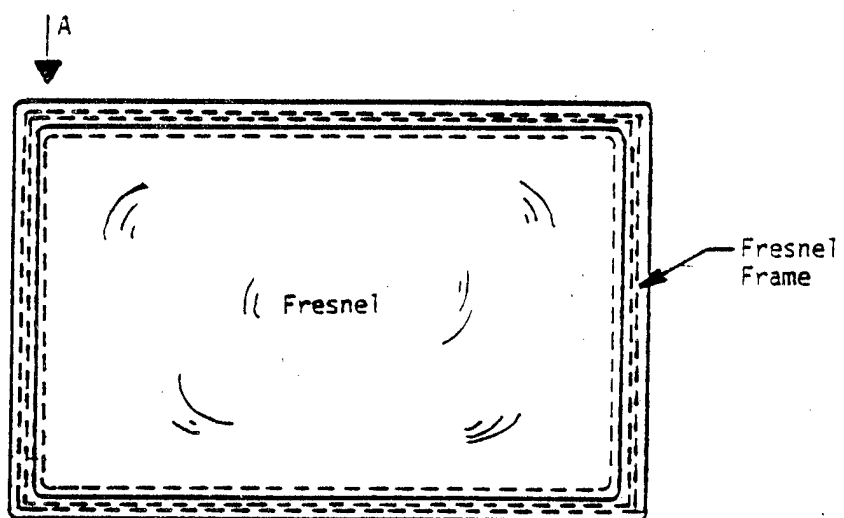


FIG. 31. LIQUID-TIGHT ASSEMBLY

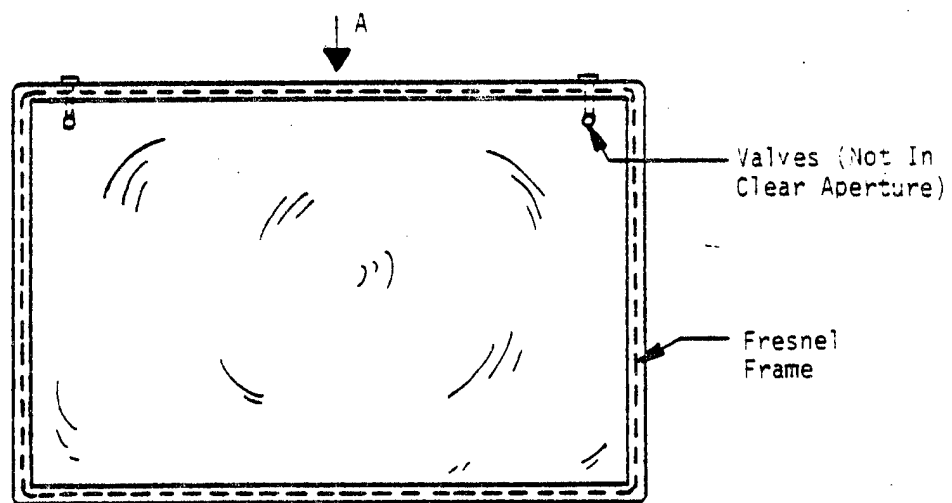
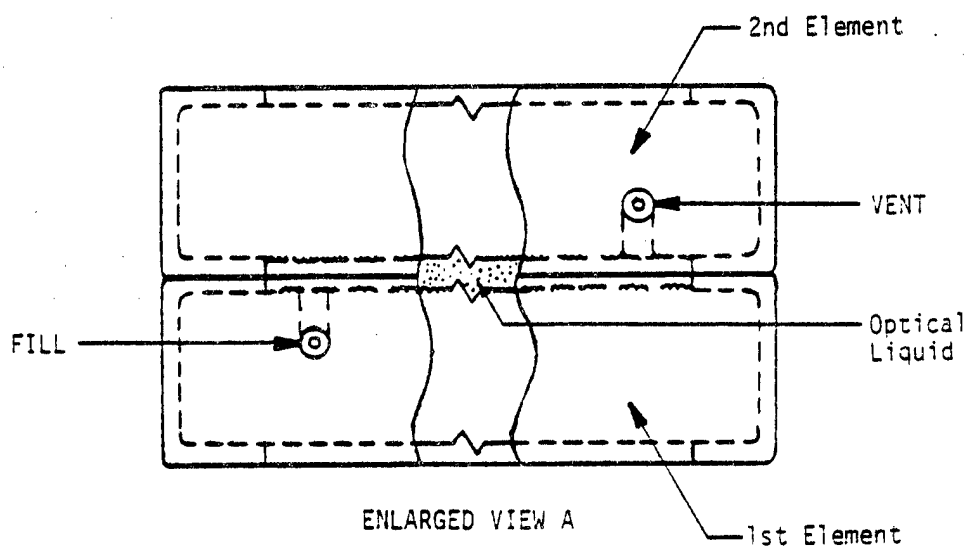


FIG. 32. FRESNEL & LIQUID

CONCLUSIONS

In view of the much improved performance obtained with the achromatized system, we recommend that this system be fabricated.

At the same time, we believe that consideration should be given to the possibility of using the non-achromatized system, with its cost advantages, in conjunction with a CRT display where the blue picture is made approximately one percent smaller than the red picture in order to compensate for lateral color in the non-achromatized system. We believe that the lateral color defects, which may be corrected in this way, are more harmful to the system performance than axial color defects, for which no like correction can be made. The non-achromatized system will show a ray disparity in the best seeing area of 7.5 minutes of arc, reaching a maximum value of 15 minutes of arc at the edge of the 12" diameter pupil. The use of this non-achromatized system may be considered as a cost effective trade-off. However our preference, as stated above, is still for the use of the achromatized system and we recommend that this one be fabricated in order to assess the system performance on a practical basis.

SECTION V

IMPROVED VIDS DESIGN

DISCUSSION

It was the intention of Advanced Technology Systems, Contractor for the VIDS, to obtain finished polished slabs of nominally half inch thick optical grade acrylic as blanks for the Fresnel elements. A subcontractor would cut a Fresnel groove frequency of 70 per inch for the facets and return them to ATS for anti-reflection coatings and assembly. During the diamond turning (cutting) process the unused portion of the Fresnel lenses were to be painted black to reduce stray light and improve contrast. Neither the "groove blackening" nor the application of anti-reflection coatings was accomplished. The anti-reflections were not applied because of the danger of damage to the element that may have occurred during the evaporative coating process and the fact that the effects of this process are predictable. The "groove-blackening" process would not be necessary after a discovery was made during the study contract, N61339-79-M-1950, in November 1979. Under this contract Dr. Cox found that by changing the Fresnel lens design developed under contract N61339-77-C-0113, to incorporate curved facets and undercut grooves the following advantages could be realized:

1. Transmission increases dramatically. For example, it increases at the edge of the field-of-view from approximately 24% to approximately 75%.
2. Because the grooves appear more on edge, they tend to be less obtrusive, mollifying the visual subjective effect.
3. The increased pitch of the facets (from .015 in. to .150 in.) decreases the required mechanical alignment accuracy.
4. The increased pitch of the facets improves the diffraction limitation on resolution.
5. The increased pitch facets tend to lessen any moire' effect interaction with a television raster.
6. The increased pitch of the facets also enhances producibility by eliminating the need to blacken the grooves because the total groove area decreases.

Improved VIDS Design Report As a deliverable under contract N61339-79-N-1950, Dr. Cox prepared a paper entitled, "An Improved Virtual Image System" which was published by Arthur Cox Associates in November 1979. The remainder of this section is taken directly from Dr. Cox's paper.

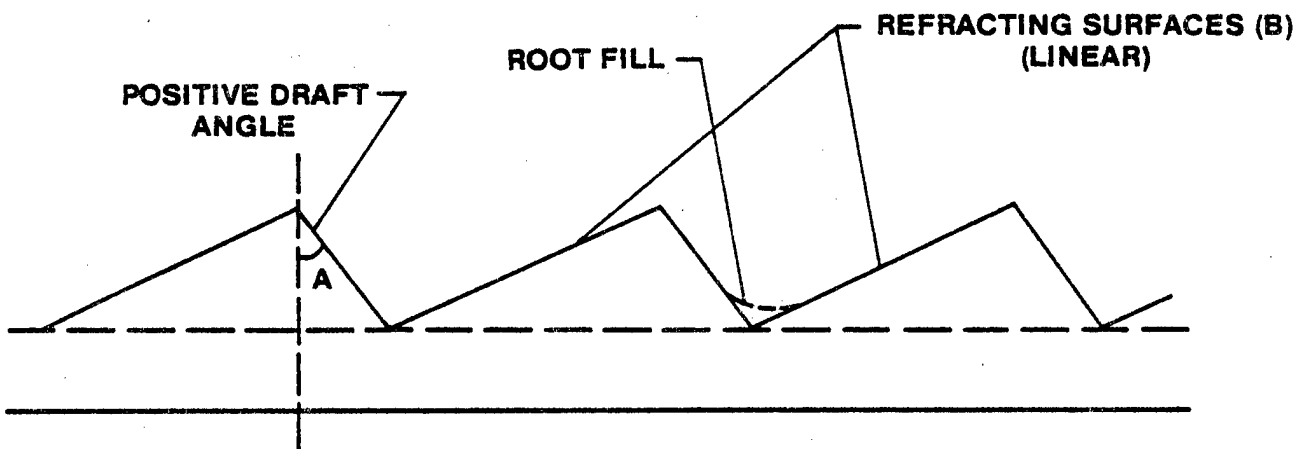
Improved Virtual Image System

Introduction

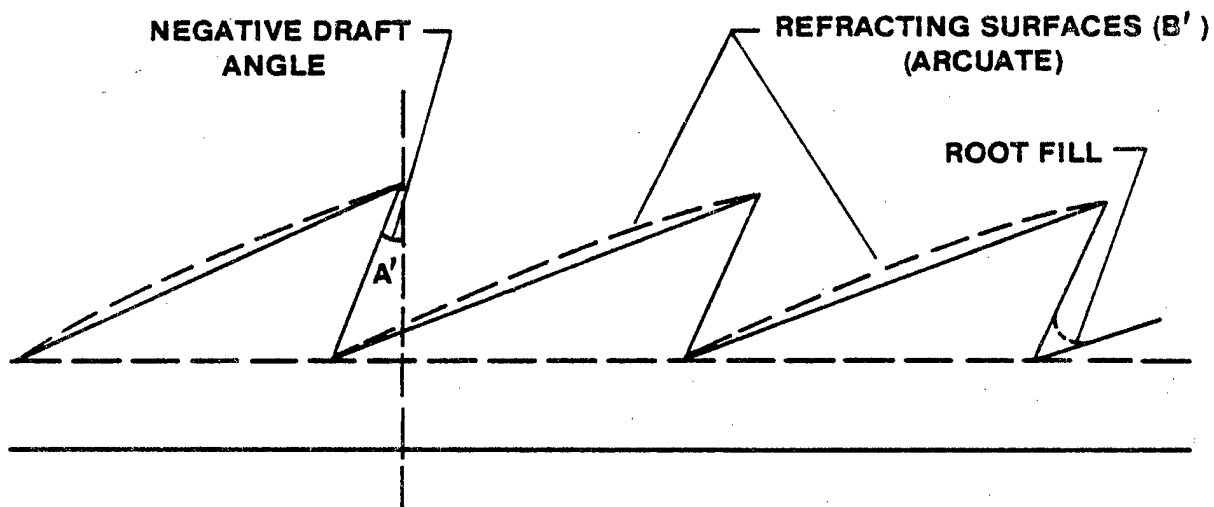
Under an earlier contract for N.T.E.C. (No. N61339-77-C-0113) which was reported on in March, 1978, a Fresnel lens optical system was designed for use in a Virtual Image Display. Two versions of the system were, in fact, designed. The first comprised 3 Fresnel lens elements and was not achromatised. The second comprised 5 Fresnel lens elements and was achromatised in order to remove chromatic disparity. Both versions came quite close to meeting the specification requirements of the contract in monochromatic light, with a distinct advantage adhering to the 5 element version because of its color correction.

The aberrational correction of the system was established by assuming that at any point where a light ray encountered the nominal plane of a Fresnel surface, it met a surface element with a prescribed slope. The grooves on the Fresnel surface were to be made with a sufficiently fine pitch so that no significant errors would be introduced because of their finite structure.

In this earlier work it was assumed that only the classical type of Fresnel structure was possible, as shown in Fig. 1a. This uses a positive draft angle A , and linear contours on the refracting faces B . Recent developments in diamond turning of plastic elements on numerically controlled machine tools of extreme precision make it feasible to contemplate the use of Fresnel elements such as those shown in Fig. 1b, where the draft angle A^1 may be negative (as shown) and where the refracting surfaces B^1 have an arcuate contour. This leads to the possibility of using Fresnel surfaces with a coarser pitch, and this in turn leads to a minimisation of diffraction effects and to a significant reduction in manufacturing difficulties. For example, it eases the drastic requirements otherwise imposed on the radius of the diamond tool which is used to machine the surfaces, since we can now tolerate a larger fill-in at the bottom of the Fresnel grooves, as shown by the dotted line in Fig. 1b.



a). STANDARD FRESNEL SURFACE



b). NEW (LIVERMORE) FRESNEL SURFACE

FIG. V-1

In view of this it seems to be highly desirable to examine in detail the potential gain afforded by the use of non-classical Fresnel contours.

Fresnel Obscuration

The first step in this analysis is to examine the circumstances in which the Fresnel surface structure gives rise to obscuration. Four cases have to be considered, as shown in Figs. 2a, b, c and d. (For the present we may neglect the arcuate form of the refracting surfaces, and consider them as having a linear contour).

At each point on a Fresnel surface we may consider the incident light to be composed of parallel pencils of rays making a variety of angles $u(1)$ with the system axis. This family of ray pencils is generated by rays which come from different points in the entrance pupil of the system and which are directed to different points in the image plane. Only meridional rays need to be considered. These incident angles $u(1)$ fall between limits described as $T_1(\text{MAX})$ and $T_1(\text{MIN})$, where the signs of the angles are taken into account. After refraction at the Fresnel facet the angles $u(2)$ of the ray pencils lie between $T_2(\text{MAX})$ and $T_2(\text{MIN})$. All angles are considered as positive when the rays are sloping up from left to right. The angles which the non-refractive surfaces, associated with each Fresnel facet, make with the system axis is denoted by H . H is positive in Figs. 2a, 2d, and negative in Figs. 2b, 2c.

In what follows we consider light as travelling from the observer's eye to the image plane.

Consider first the case shown in Fig. 2a where both $u(1)$ and H are positive. When $u(1)$ is greater than H then all ingoing light which crosses the face PR meets the refracting face PQ, and the Fresnel structure of the surface does not lead to any light loss as far as ingoing rays are concerned. When $u(1)$ is less than H then light which crosses the entrance face PR in the region RX is lost because it encounters the non-refracting face RQ.

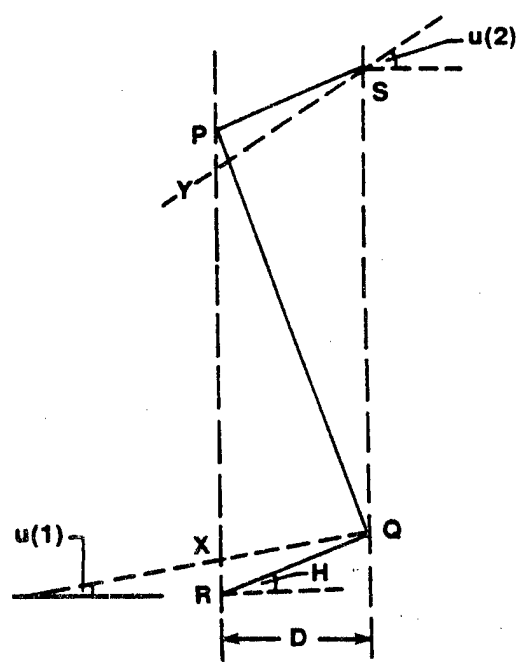


FIG. V-2a

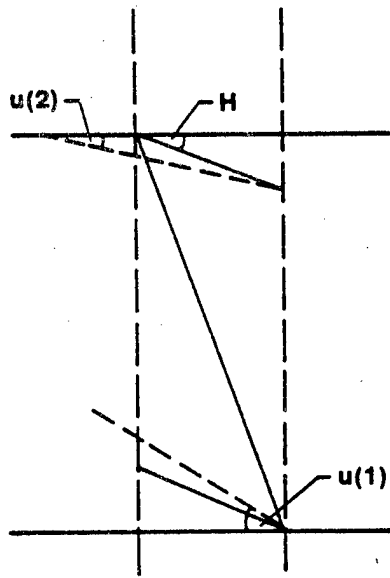


FIG. V-2b

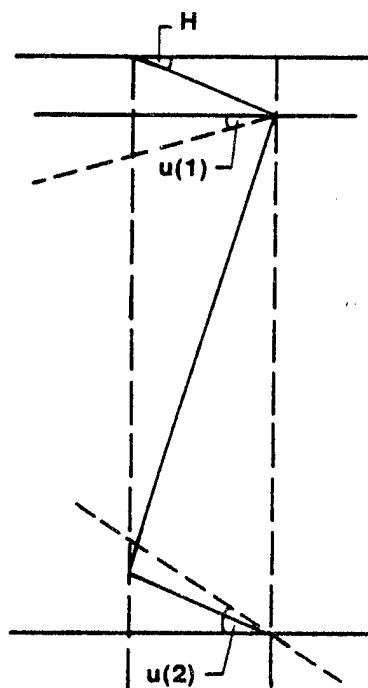


FIG. V-2c

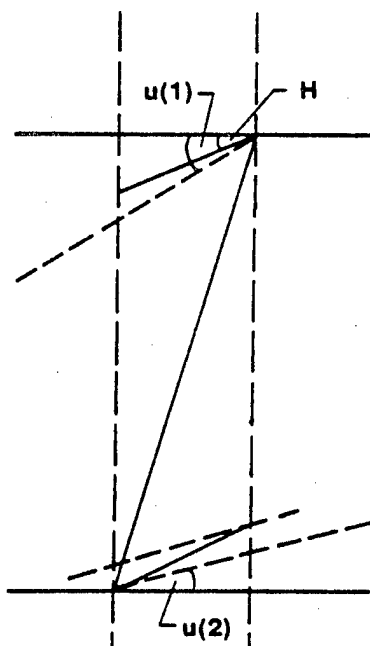


FIG. V-2d

If the depth of the Fresnel structure is D , as shown in the diagram, then $RX = D$. ($\tan H - \tan u(1)$). The maximum value is RX is reached when $u(1) = T1(\text{MIN})$. When RX is negative, according to this formula, then it is set equal to zero, and there is no light loss of the ingoing rays. No dark area is perceived by the observer.

If $u(2)$ for the refracted pencils is less than H , then all the light refracted at the point P will encounter the exit face QS , and no light will be lost in the pencil of rays which proceeds from the observer's eye to the image plane (the face of a CRT). If $u(2)$ is greater than H then to a good approximation light from the area PY will not be transmitted to the image plane. (An exact formula for PY is given in Appendix B, and an estimate is made of the error introduced by using the approximation now employed). The value of PY is given by $PY = D$. ($\tan u(2) - \tan H$) and has its maximum value when $u(2) = T2(\text{MAX})$.

The optimum value of H may be taken as that which makes the maximum values of RX and PY equal. We then have

$$\tan H = .5(\tan T1(\text{MIN}) + \tan T2(\text{MAX})) \quad (1)$$

$$\text{and } RX = PY = .5(\tan T2(\text{MAX}) - \tan T1(\text{MIN})) \times D \quad (2)$$

The same type of approach shows that Equations (1) and (2) also hold for the case shown in Fig. 2b.

For the situations shown in Figs. 2c, 2d, we have

$$\tan H = .5(\tan T1(\text{MAX}) + \tan T2(\text{MIN})) \quad (3)$$

$$RX = PY = .5(\tan T1(\text{MAX}) - \tan T2(\text{MIN})) \times D \quad (4)$$

If either RX or PY as given by Equations (2) and (4) is negative, then their actual values are to be set equal to zero, corresponding to the fact that there is no obscuration. The slope of the Fresnel facet, measured in degrees is denoted by F . In Figs. 2a, 2b, F is negative: in Figs. 2c, 2d, F is positive.

A special computer program was written, and is given in Appendix B, in order to obtain the relevant values of $T1(\text{MAX})$, $T1(\text{MIN})$, $T2(\text{MAX})$ and $T2(\text{MIN})$. This program requires that 451 rays be traced through the system. These rays correspond to an image

point on the axis of the system and to 10 equally spaced off-axis field points. For each of these eleven points a ray is traced through the center of the entrance pupil and 20 lower and 20 upper rim rays are also traced through the pupil.

The procedure which is followed in the computer program consists in selecting a particular off-axis field point and tracing all 41 rays through the entrance pupil. The values of the intersection points of these rays with each Fresnel surface, as well as the ray slopes before and after refraction at each surface are stored in the computer. From this data the values of the rays slopes at a fixed set of points on each surface are obtained by linear interpolation. This process is repeated for all eleven field positions. The required maximum and minimum values are obtained, for the fixed surface positions, from these sets of values.

Forty-four equally spaced points, chosen to cover the free aperture of each Fresnel surface, are used.

These are for the 5 element Fresnel lens system referred to in the Introduction. Typical results for 11 points on the Fresnel surfaces are given in Tables 1 and 2.

If the size of the Fresnel pitch, i.e. the distance PR in Fig. 1 is equal to $\frac{z}{k}$, then to a good approximation $D = \frac{z}{k} \times F$, so that we have from Equations (2) and (4), with the definition of k given above,

$$\begin{aligned} RX = PY &= D \times k \\ &= k \times \frac{z}{k} \times \tan F \end{aligned} \quad (5)$$

$$\text{so that } RX = PY = \frac{z}{k} \tan F \quad (6)$$

This gives a rapid method of determining RX or PY given $\frac{z}{k}$. In the computer program as finally written, we calculate $RP = 1 \div F$, and in place of the angle H , we calculate the draft angle according to the usual convention. In Figs. 2a, 2c the draft angle is positive: in Figs. 2b, 2d the draft angle is negative.

We also calculate the clearance angle CLRA, shown in Fig. 1. The significance of this angle is that the angle of the diamond

TABLE V-1

Fresnel Surface #1

<u>Height</u>	<u>T1(MAX)</u>	<u>T1(MIN)</u>	<u>T2(MAX)</u>	<u>T2(MIN)</u>	<u>SLOPE</u>
19.00	0.0	0.0	0.0	0.0	-38.018
17.10	18.037	16.529	9.340	6.939	-34.764
15.20	18.037	14.940	11.528	6.709	-30.857
13.30	18.037	11.533	13.580	3.579	-26.964
11.40	18.037	9.725	15.465	2.837	-23.242
9.50	18.037	5.939	17.255	-1.043	-19.628
7.60	18.037	3.982	19.043	-2.092	-15.994
5.70	16.529	1.998	18.649	-6.192	-12.232
3.80	13.273	-1.998	15.733	-7.163	-8.294
1.90	11.533	-5.939	15.179	-11.022	-4.194
0.0	7.857	-7.857	11.767	-11.767	0.0

Fresnel Surface #2

19.00	0.0	0.0	0.0	0.0	38.568
17.10	9.349	6.946	-7.715	-9.016	36.428
15.20	11.539	6.716	-4.946	-7.631	32.987
13.30	13.593	3.583	-2.126	-7.932	29.239
11.40	15.478	2.839	.582	-6.942	25.493
9.50	17.269	-1.044	3.221	-8.034	21.735
7.60	19.059	-2.094	5.891	-7.361	17.849
5.70	18.666	-6.198	7.318	-8.690	13.733
3.80	15.748	-7.170	7.170	-7.889	9.350
1.90	15.194	-11.033	8.472	-8.954	4.740
0.0	8.261	-8.261	8.035	-8.035	0.0

TABLE V-1 (Continued)

Fresnel Surface #3

<u>Height</u>	<u>T1(MAX)</u>	<u>T1(MIN)</u>	<u>T2(MAX)</u>	<u>T2(MIN)</u>	<u>SLOPE</u>
19.00	0.0	0.0	0.0	0.0	-37.377
17.10	-8.035	-9.397	-6.489	-7.777	-37.228
15.20	-5.178	-7.994	-3.844	-6.525	-35.761
13.30	-2.222	-8.300	-1.125	-6.941	-33.187
11.40	.607	-7.246	1.469	-6.085	-29.731
9.50	3.359	-8.381	3.993	-7.341	-25.603
7.60	6.154	-7.683	6.565	-6.838	-20.981
5.70	7.661	-9.091	7.889	-8.365	-16.006
3.80	7.518	-8.266	7.607	-7.730	-10.793
1.90	8.899	-9.402	8.804	-8.991	-5.432
0.0	8.261	-8.261	8.035	-8.035	0.0

Fresnel Surface #4

19.00	0.0	0.0	0.0	0.0	37.377
17.10	-6.496	-7.786	-5.542	-6.881	37.228
15.20	-3.849	-6.533	-2.849	-5.636	35.761
13.30	-1.126	-6.949	-.121	-6.160	33.187
11.40	1.471	-6.092	2.443	-5.397	29.731
9.50	3.998	-7.349	4.909	-6.822	25.603
7.60	6.573	-6.846	7.409	-6.443	20.981
5.70	7.899	-8.376	8.609	-8.162	16.006
3.80	7.617	-7.740	8.149	-7.655	10.793
1.90	8.817	-6.967	9.222	-7.009	5.432
0.0	8.046	-8.046	8.272	-8.272	0.0

TABLE V-1 (Continued)

Fresnel Surface #5

<u>Height</u>	<u>T1(MAX)</u>	<u>T1(MIN)</u>	<u>T2(MAX)</u>	<u>T2(MIN)</u>	<u>SLOPE</u>
15.00	0.0	0.0	0.0	0.0	-10.057
13.50	-1.367	-6.296	-9.969	-17.930	-15.195
12.00	4.750	-3.617	-1.963	-15.301	-17.948
10.50	6.508	-2.158	.332	-13.387	-18.710
9.00	8.575	-1.509	3.900	-11.832	-17.925
7.50	3.994	-6.405	-2.093	-18.670	-16.029
6.00	5.002	-6.593	.818	-17.264	-13.397
4.50	6.138	-6.990	4.078	-16.026	-10.314
3.00	7.202	-7.455	7.312	-14.849	-6.978
1.50	7.879	-7.860	10.034	-13.595	-3.514
0.0	8.059	-8.059	12.071	-12.071	0.0

Note: A value of zero in all four columns means that no rays go through this point.

Equations 1) and 2) are applicable to surfaces #1, 3 and 5.

Equations 3) and 4) are applicable to surfaces #2 and 4.

Hence by applying the relevant equations we can determine the values of H for a series of points on each surface, and also the values of k, the coefficient of D in the expressions for RX or PY. A value is also given for a term P whose significance will be discussed later. P is equal to the reciprocal of k multiplied by the absolute value of the tangent of the SLOPE angle given in Table 1.

$$P = 1.0 \div (k \times \tan (\text{SLOPE}))$$

TABLE V-2

<u>Fresnel #1</u>						
Height	19.00	17.10	15.20	13.30	11.40	9.50
H	0	12.99	13.25	12.56	12.63	11.71
k	0	0	0	.0188	.0526	.1033
P				104.6	44.23	27.15

<u>Fresnel #2</u>						
Height	19.00	17.10	15.20	13.30	11.40	9.50
H	0	.170	2.00	2.93	4.44	4.85
k	0	.1616	.1691	.1906	.1993	.2260
P	8.38	9.11	9.37	10.52	11.10	13.09

<u>Fresnel #3</u>						
Height	19.00	17.10	15.20	13.30	11.40	9.50
H	0	-7.95	-5.93	-4.73	-2.91	-2.22
k	0	.0259	.0366	.0631	.0764	.1086
P	50.86	37.92	24.22	22.92	19.22	20.86

<u>Fresnel #4</u>						
Height	19.00	17.10	15.20	13.30	11.40	9.50
H	0.0	-6.69	-4.74	-3.65	-1.97	-1.42
k	0.0	.003	.016	.044	.060	.095
P	386.0	88.42	34.64	29.17	22.02	22.86

TABLE V-2 (Continued)

<u>Fresnel #5</u>		Height	15.00	13.50	12.00	10.50	9.00	7.50	6.00	4.50	3.00	1.50	0.0
H	0	-8.14	-2.79	-.91	1.20	-4.25	-2.90	-1.47	-.07	1.11	2.07		
K	0	.014	.022	.047	.038	.065	.097	.130	.157	.178			
P		213.4	135.8	65.4	91.9	64.7	56.7	63.0	109.6				

tool must be less than this angle, and practical experience shows that the included angle of the diamond tool should not be less than 45 degrees.

A further point to be noted, and one which was brought out in discussions with Jim Bryan at Livermore Lab., is that the machine in which the Fresnel elements will be cut does not have the capability of varying the tool angle during the course of a cut. It is desirable, therefore, that the value of $90 - \text{MAX SLOPE} + \text{DRAFT}$ should be greater than 45 degrees, taking into account the sign of the draft angle DRAFT. The values of SLOPE are plotted in Fig. 5. It will be seen from Figs. 3 and 5 that this condition is satisfied for Fresnel elements #1, 2, 4 and 5. For element #3, the value of the expression is 44 degrees, and the minimum clearance angle is also approximately 44 degrees. In view of the problems of making tools with an angle of less than 45 degrees, it is recommended that tools with an angle of say 43 degrees be used only on this Fresnel surface.

A further option is open to us, however, namely to exchange refractive power between surfaces #3 and #4, particularly as far as higher order terms are concerned. The main function of these two surfaces is to establish the chromatic correction, and on the face of it this should not be sensitive to a change of higher order power. (This analysis will be done for Advanced Technology Systems to facilitate the manufacture of the Fresnel system using diamond tools already procured).

There are two pupil areas to which a different degree of importance is assigned. There is an inner area of approximately 6 inches diameter for which the higher degree of optical performance is required. Because of this a complete set of calculations was run with a 6 inch diameter pupil in place of the 12 inch diameter pupil of the earlier set of calculations recorded in Figs. 3 and 4. The results for the 6 inch diameter pupil are given in Figs. 6 and 7.

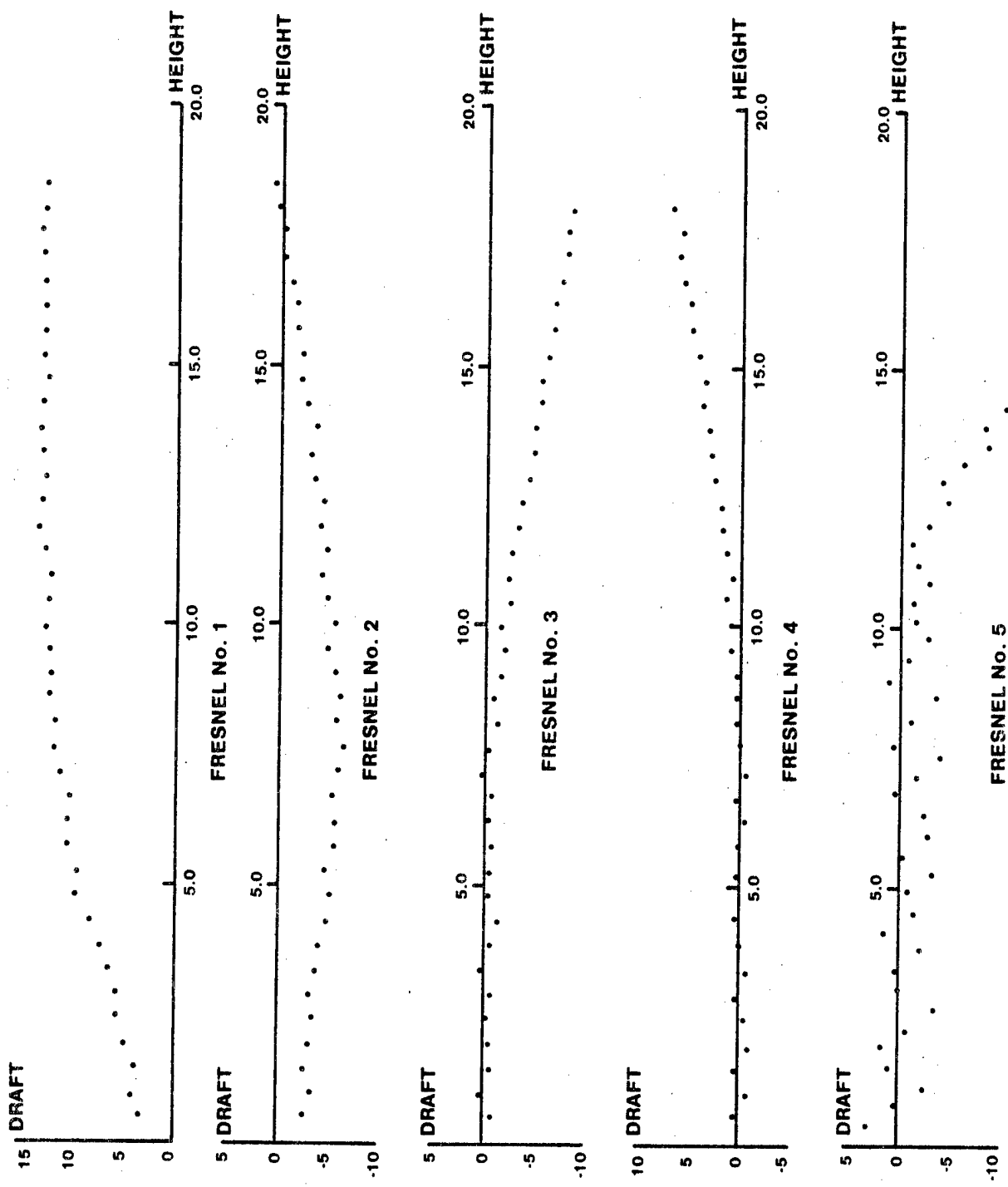


FIG. V-3 FRESNEL DRAFT ANGLES

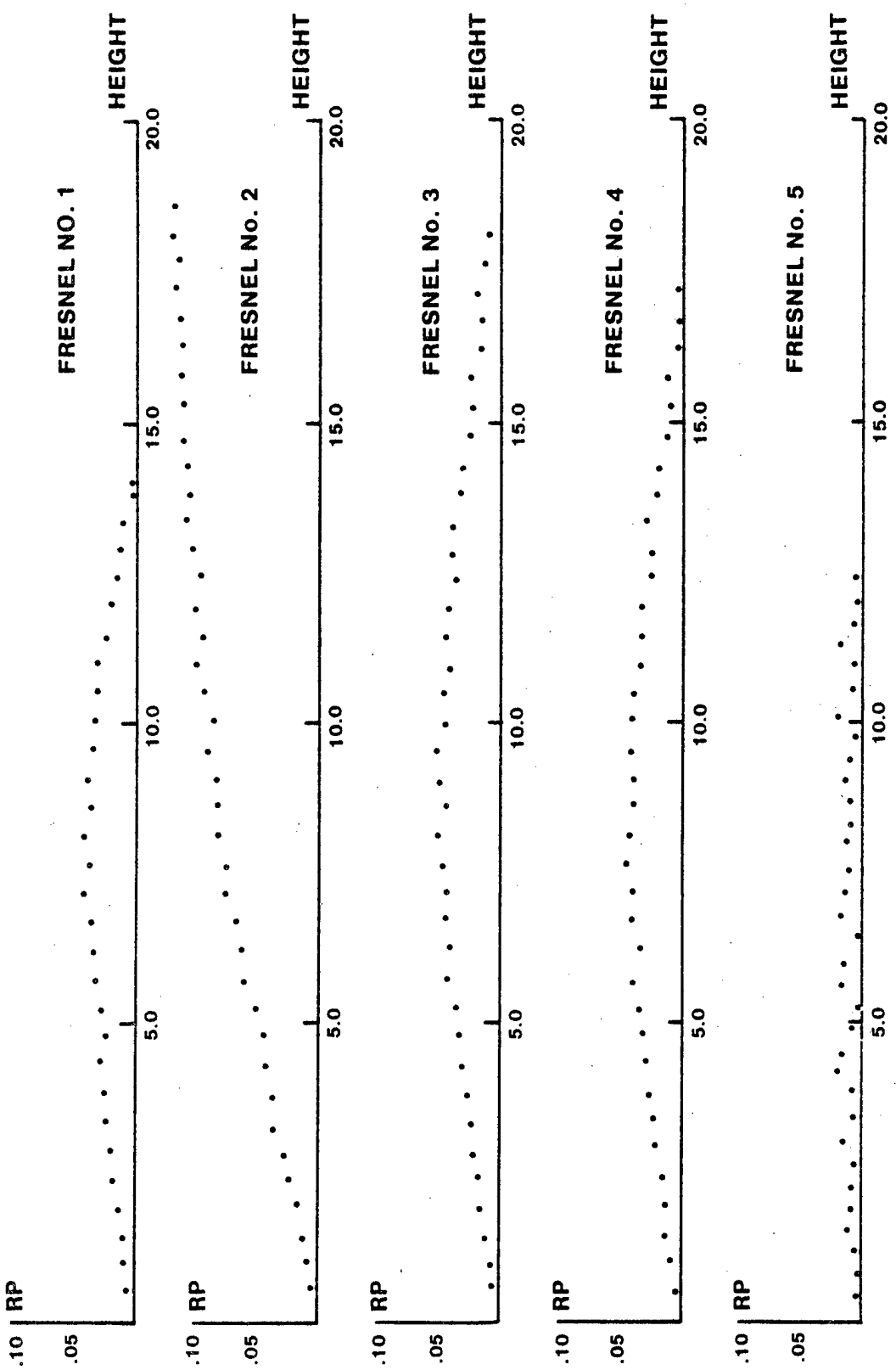


FIG. V-4 FRESNEL OBSCURATION (FULL PUPIL)

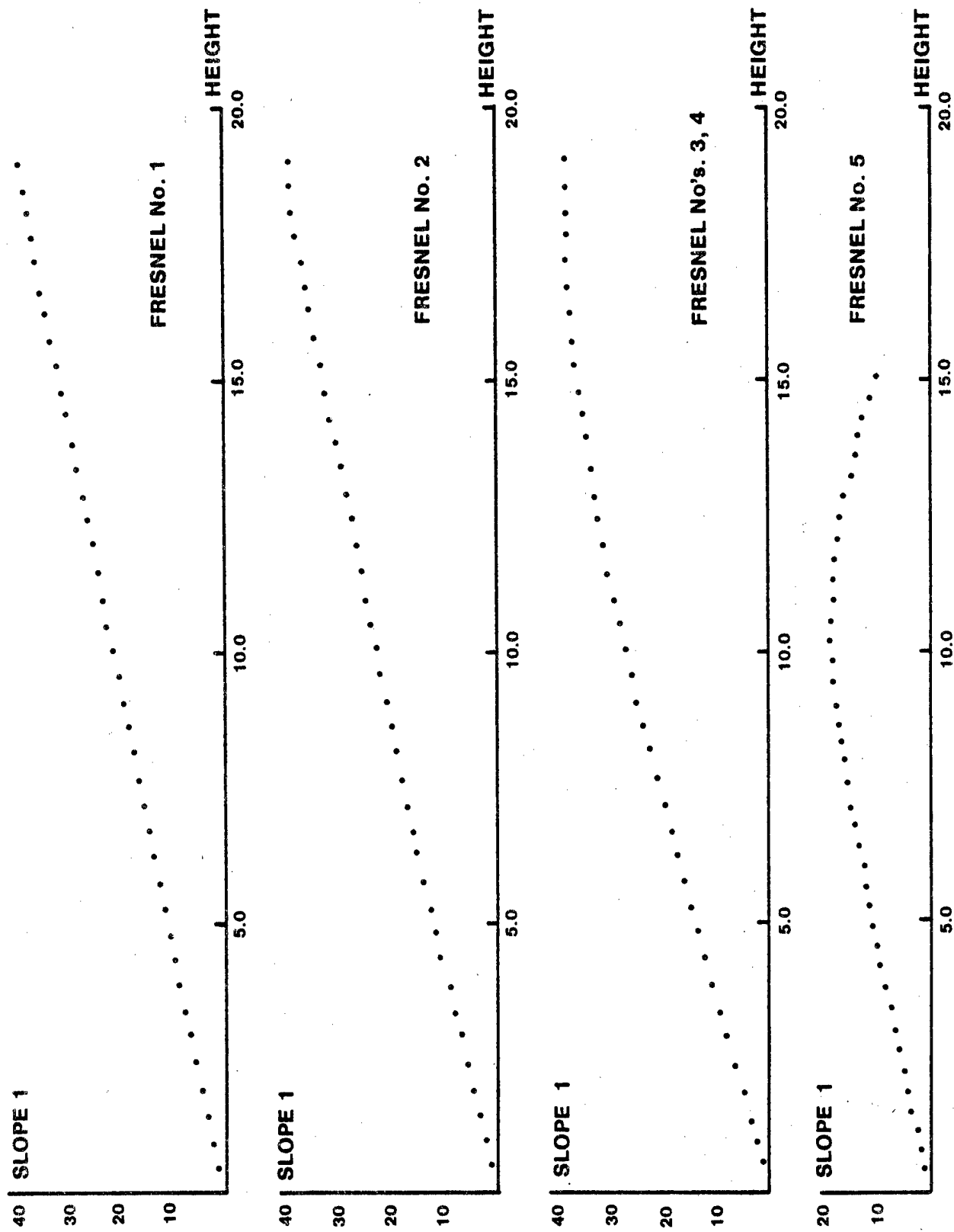


FIG. V-5 SLOPE VALUES

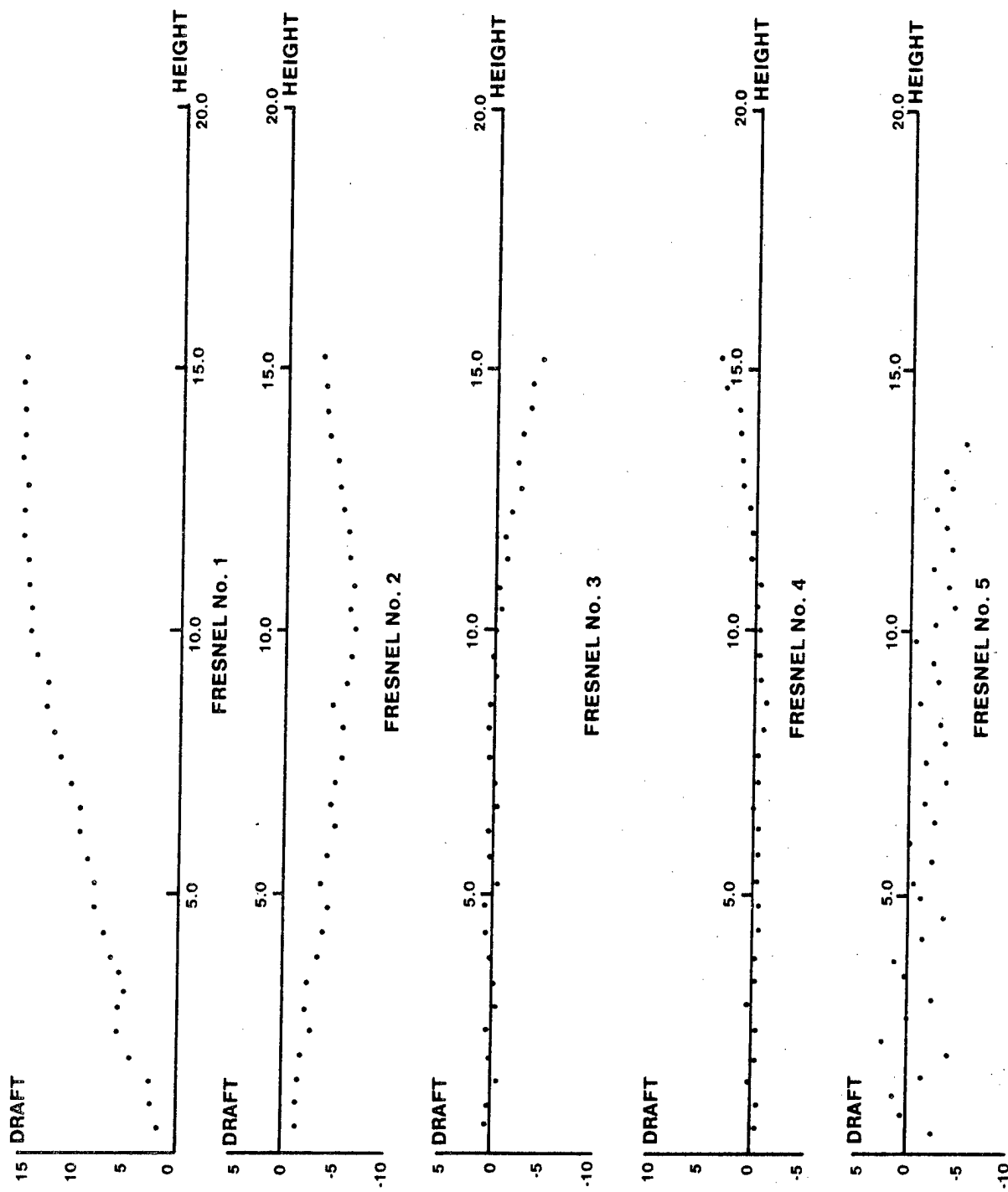


FIG. V-6 FRESNEL DRAFT ANGLES /6.0" DIA. PUPIL

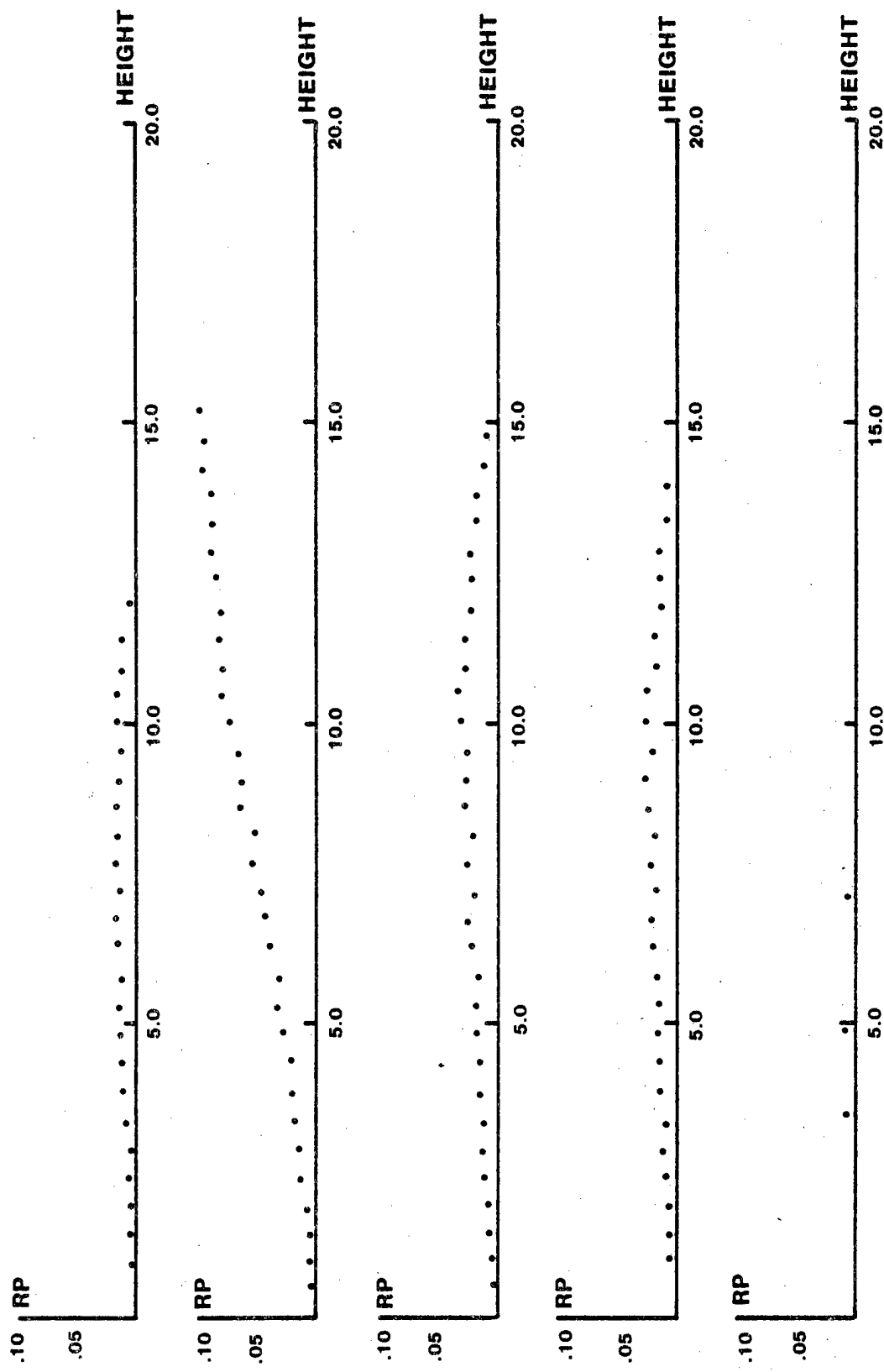


FIG. V-7 FRESNEL OBSCURATION / 6.0" DIA. PUPIL

Obscuration Values

The next point to consider is the permissible maximum values of RX or PY on the several surfaces. Two criteria may be used to establish these values. The first relates to the loss of light in a pencil of rays as it traverses the system. The second relates to the visual effects which arise because we have apparent obstructions created by areas such as RX or PY. (It should be noted that at any Fresnel surface we cannot have both RX and PY, since a maximum slope for an ingoing ray cannot correspond to a minimum value for a refracted ray).

In the worst case we can add the values for RP corresponding to the same value of HEIGHT for the first four elements, and the maximum value of RP for the fifth element. For the draft angles determined by the 12 inch diameter pupil, this approach gives a minimum transmission of 75%. For the draft angles associated with the 6 inch diameter pupil, the minimum transmission is approximately 88%.

If we consider light as travelling from the observer's eye to the CRT faceplate, then light which encounters areas such as RX and PY will be diverted from its proper path and will meet the CRT in a wrong area or it may hit the walls of an enclosure. In any event the resulting effect is that we will see superimposed upon the picture area an array of light or dark rings. These will not necessarily be complete circles because of the rectangular shape of the image on the CRT, and it may well happen that the obscuration will result in a ring being visible to one eye and not to the other.

If we consider first the group of four Fresnel surfaces closest to the eye, and take the Fresnel pitch as being equal to z , then the physical size of either RX or PY is equal to $z \times RP$, where RP has been previously defined. We can take the angular subtense of either RX or PY as being approximately $z \times RP \div 24$ radians.

If we take the values of RP from Fig. 4, and if we set $z = .150$ inches then we have:

Fresnel #1	Maximum subtense is equal to .9 minutes of arc.
Fresnel #2	Maximum subtense is equal to 2.8 minutes of arc.
Fresnel #3	Maximum subtense is equal to 1.0 minutes of arc.
Fresnel #4	Maximum subtense is equal to .9 minutes of arc.

The maximum values of subtense for #'s 1,3 and 4 occur at about the same value of the height so that in the worst case they could combine to give an obstruction with a 2.8 minute of arc subtense. At this point the subtense of the obscuration produced by surface #2 is 1.7 minutes of arc. We thus could conceivably have an apparent obscuration produced by the front group of Fresnel lenses which subtended an angle of 4.5 minutes of arc. The angular subtense of neighbouring rings is 21.5 minutes of arc.

As far as the visibility of obscuration rings due to the fifth Fresnel element is concerned, we may take it as lying within the focal distance of the front group. The separation between the Fresnel surface and the rear nodal point of the front group is 20.42 inches. The focal length of the front group is 27.355 inches. Thus if an obscuration on the fifth Fresnel has a width a it appears, when viewed through the front group of 4 elements to have a dimension $a \times 3.944$ inches at a distance of 80.55 inches. It thus appears to lie at a distance of 104.55 inches from the observer's eye, and to have an angular subtense of $a \div 26.5$ radians.

If we take the values of RP for this surface from Fig. 4, the maximum subtense of an obscuration is .4 minutes of arc.

The exact psychological effects of these obscuration rings are difficult to predict. Their physical appearance will depend to a considerable degree on the picture content and the way in which light may be directed to other than the correct picture areas. The attention paid to them will also depend strongly on the picture content.

The value of .150 inches for the Fresnel pitch has been chosen arbitrarily. If it is made larger then the obscurations subtend large angles. If it is made smaller then the relative size of root-fill due to the diamond turning process increases.

It should also be noted that with the coarser Fresnel structure now contemplated the effects of diffraction are reduced to negligible levels.

Alternative Systems

It was felt that in view of the somewhat different emphasis placed on the various factors governing the performance of the system it would be of value to re-examine the original design to see what trade-offs could be made between obscuration visibility and optical performance. The following changes were made and their consequences examined in detail:

a) #5 Fresnel Reversed

When this element was reversed and the aberrations re-balanced, it was found that the dipvergence and divergence correction was not quite as good as the original system, and the obscuration produced by the Fresnel pattern on this surface was increased by about 50%.

b) #2 Fresnel Reversed

The greatest obscuration comes from this element. By reversing it the obscuration was greatly reduced. However, it was not then possible to control the aberrations. In view of the improvement in obscuration which results from reversing this element a good deal of time was spent in trying to correct the aberrations, but this work only reinforced the conclusions of the earlier work, namely, that the best performance is achieved in the original configuration.

c) Interchange of Power #1,2

Refractive power and higher order terms were interchanged between Fresnels #1 and 2. Once again this led to a degradation of performance with no gain in obscuration effects.

d) Aspheric #5

Element #5 is primarily a distortion correcting component with comparatively weak power. It was therefore tempting to replace it with an element having an aspheric surface. This, of course, would eliminate any obscuration effects from this element.

If the same paraxial power and higher order correction terms provided by the Fresnel are retained in the aspheric element, then its center thickness is approximately 6 inches. In order to reduce this thickness it is necessary to readjust the paraxial power between this element and the front group of four elements. When this transfer of power is effected, it has not proven feasible to correct the aberrations. In particular the Petzval sum of a Fresnel surface depends upon its position in the system, whereas the Petzval sum of an aspheric surface is independent of its position. By replacing the Fresnel surface on element #5 by an aspheric surface, or by transferring power to the front group adversely affects the total Petzval sum of the system. In retrospect too much time was spent on the attempt to replace Fresnel #5 by an aspheric surface in view of the small obscuration effects produced on this surface.

Finite Depth Fresnels

In the classical type of Fresnel surfaces with a fine pitch no significant problems are created because the longitudinal position of a Fresnel facet, measured along the system axis, changes from top to bottom of the facet. With the coarser grooves now contemplated this change in position becomes significant and a special computer program, FRESNEL, was developed to deal with this.

In order to provide input for this program each Fresnel element is successively reduced in thickness and the following air space increased by the same amount, so that the overall length of the system remains unchanged. This variation in system parameters changes both the back focus and focal length of the system, as well as upsetting somewhat the aberrational correction. The same set of rays that were traced through the original system, with their identical entrance angles and pupil positions, are traced through the altered system and their intersection points with the image plane of the original system are determined. The Fresnel parameters are then varied until the ray distribution in the image plane is as close as possible to the original distribution. This gives an alternative set of Fresnel parameters for each surface when it is displaced through a distance Δ .

The procedure followed by the FRESNEL program is to calculate the slope of the Fresnel surface at the beginning of a facet cut. From this we derive the depth of the cut at the end of the cut as the facet. By linear interpolation, using the data prepared as described above, we obtain the Fresnel coefficients appropriate to the bottom of the groove. Using these coefficients we then calculate the appropriate slope at the end of the facet cut. The program prints out the radial coordinates of the start and end of each facet cut and the tangents of the slope angles at the beginning and end of each cut. The draft angle tangent is also printed out. Intermediate values of the slope angle are obtained by linear interpolation.

The output of this program gives a tabulation of numerical data which can be used for the control of a machine tool. As an alternative the basic input data may be used with segments of the program in order to effect the control.

In connection with this approach to the fabrication of Fresnel elements we may consider also replacing the central area of the Fresnel elements by spherical or aspheric refracting surfaces.

In the approach to Fresnel design which has been taken the slope θ of a Fresnel facet is given by

$$\sin \theta = aR + bR^3 + cR^5 + dR^7$$

$$\text{But } \tan \theta = \sin \theta (1 - \sin^2 \theta)^{-1/2}$$

Hence if we retain only terms up to the fifth order

$$\tan \theta = a'R + b'R^3 + c'R^5$$

$$\text{Where } a' = a; b' = b + 1/2a^3; c' = c + 3/2a^2b + 3/8a^5$$

If we put $dY/dR = \tan \theta$ for a smooth aspheric surface then we have

$$Y = 1/2a'R^2 + 1/4b'R^4 + 1/6c'R^6$$

For the system which has been designed we have the following results:

Fresnel #1

$$a = .38680 \times 10^{-1}; b = -.52750 \times 10^{-4}; c = .2030 \times 10^{-6}$$

$$\text{So that } a' = .38680 \times 10^{-1}; b' = -.23812 \times 10^{-4}; c' = .15660 \times 10^{-6}$$

$$\text{This gives } Y = .01934R^2 - .5953 \times 10^{-5}R^4 + .2610 \times 10^{-7}R^6$$

$$\text{When } R = 2.0 \quad Y = .0772$$

When $R = 1.0$ $Y = .0193$ and the sixth order terms may be neglected. The obscuration produced by this is negligible.

It is therefore recommended that for each Fresnel surface, the inner 2.0 inches of diameter be of aspheric form with the following equations:

Fresnel #1

$$Y = .1943 \times 10^{-1}R^2 - .5953 \times 10^{-5}R^4$$

Fresnel #2

$$Y = .2188 \times 10^{-1}R^2 - .7650 \times 10^{-5}R^4$$

Fresnel #3,4

$$Y = .2500 \times 10^{-1}R^2 - .3125 \times 10^{-5}R^4$$

Fresnel #5

$$Y = .2049 \times 10^{-1}R^2 - .3897 \times 10^{-5}R^4$$

In these equations Y is the depth of cut.

Meetings

A meeting was held with Mr. James Bryan at Lawrence Livermore Laboratory on October 23, 1979 to discuss practical aspects of fabricating Fresnel elements with negative draft and with curved Fresnel facets. Lawrence Livermore Laboratory is currently under contract with Advanced Technology Systems to fabricate the Fresnel elements for a Virtual Image display system. Work which they have carried out in the past few months has shown that a satisfactory technique for blackening the non-refracting surfaces of the Fresnel elements has not been developed. The variety of paints which have been used all result in significant damage to the diamond turning tool.

The present approach eliminates the need for such blackening and represents a major advance from the point of view of fabricating large elements. The general feeling emerging from this meeting was

that the blackening of the elements should be omitted, and that the Fresnel elements should be fabricated using the approach detailed in this report.

A meeting was also held at N.T.E.C. in Orlando on October 31, 1979 at which time a verbal report was made on the results of this investigation, and at which time the recommendation was also made that the system being made by Advanced Technology Systems be modified in accordance with the recommendations of this report and of Lawrence Livermore Laboratory. (Parts of this report have been re-written after the Orlando meeting to clarify points raised at that meeting).

Conclusion

Recent developments in diamond turning of plastic lens elements make it feasible to consider the use of Fresnel elements with either positive or negative draft angles on the non-refracting surfaces of the individual Fresnel facets, if gains in performance and reduction in cost result in particular from the use of negative draft angles.

A technique has been developed, and a computer program has been written in order to determine the optimum draft angles on each Fresnel element and to assess the effects of the Fresnel structure when the optimum draft angles are used. These effects are of two kinds. The first is a reduction in visible brightness. The second is the appearance of light or dark rings in the field of view. The technique and the program are of quite general application, but for the purposes of this project they have been applied to an analysis of the five element Fresnel Virtual Image system designed at an earlier time, and now being fabricated by Advanced Technology Systems. Both effects described above are very significantly reduced by using optimum draft angles.

The use of optimum draft angles permits the use of Fresnel elements of greater groove width. The effects of this are to reduce the relative proportions of manufacturing defects, such as root-fill at the bottom of the Fresnel grooves which is a consequence of the necessarily finite radius of the diamond tool.

With narrower Fresnel grooves these manufacturing defects can be of greater importance.

By using optimum draft angles, the light or dark circular rings in the field of view which result from the non-refracting surfaces of the individual Fresnel facets cover a much smaller fraction of the field of view, and it is therefore possible to dispense with the blackening of these surfaces. This eliminates what has been found to be a major (unexpected) manufacturing problem. It had been proposed to fabricate the Fresnel elements in two stages. In the first stage the precision diamond turning of the element is carried out. The whole element is then painted. In the second stage the precision turning of the first stage is repeated to remove the paint from the refracting faces. This would be quite a practical operation except for the fact that experiments have shown that every paint which has been tried ruins the diamond tool. We expect a significant reduction in cost, and a greater productivity from the machine tools, by eliminating the painting and second cut operations.

The use of broader Fresnel facets means that the profile of the refracting surface of each Fresnel facet is curved rather than being a straight line. A program has been developed to compute this curve. It presents no manufacturing problems.

It is recommended that this technique of designing and fabricating Fresnel elements be applied to the Virtual Image system now being produced by the Advanced Technology Systems Company under a separate contract.

Recommendations

The work which has been done up to the present shows that optical systems can be designed using Fresnel elements which have a standard of performance equal to that provided by systems using spherical or aspheric elements. A simple method has been developed for achromatising such systems. It has also been shown that by using appropriate draft angles the effects which result from the

finite structure of the Fresnel surface may be significantly reduced. It is meaningful, therefore, to consider types of optical systems in which Fresnel lenses may be of significant value.

The most obvious application is in comparatively large systems, such as those used for visual simulation, where the weight and bulk of normal refracting systems is prohibitive. The Virtual Image system previously referenced is only one example of a family of such systems. Other systems, with different angular coverage and pupil conditions, may be used, for example, in a pattern of abutting elements to cover a hemisphere or more. It is recommended that the specifications of systems of this type be drawn up and paper studies made to determine the total individual standards of performance that can be attained with Fresnel elements.

A second application is in heads up display systems, or binocular systems. These are essentially lenses of very high aperture (low F/number) with elements of moderate diameter. The problem which arises with such systems is that there is hardly enough room for the rather thick optical elements which are needed, and the correction of aberrations is therefore difficult. The fact that Fresnel elements can provide considerable power without requiring bulk makes them prime candidates for use in such systems.

Finally, a possible application of Fresnel elements is in the eyepieces of night vision goggles. Here, weight is of prime importance and projects are already under way to use standard plastic elements in order to reduce weight.

A Fresnel element may be regarded as a highly degenerate form of a holographic lens and may find practical applications where the use of holographic lens elements has been considered.

SECTION VI

OPTICAL TESTING

GENERAL

Optical testing of the Virtual Image Display System was accomplished by ATS personnel at the contractor's plant and witnessed by a NTEC representative. Testing was completed to show compliance with the contract specifications in the areas of Ray Disparity, Chromatic Correction, Collimation, Astigmatism, Distortion, Transmission and Resolution.

Testing was conducted in accordance with a contractor furnished, government approved, Test Plan which had been submitted as part of contract N61339-77-C-0113, Data Item A004.⁸ The test plan and test results are available but only the test results will be discussed in this report.

TEST DATA:

1. Ray Disparity tests provided data for each of the five object points through the ten point pairs. The two rays were measured in both the vertical and horizontal directions. Twelve rays out of the 100 tested were out of specification (seven in the vertical direction and five in the horizontal direction). Many of the "out of specification" points were associated with field point "E" which is located at the greatest distance from the center of the field (See Figure 3, Section III). ATS believes that minor misalignment of the optics, slightly incorrect index and dispersion of the acrylic, small errors in the slope of the Fresnel facets and thickness and curvature tolerances on the CRT faceplate all could have contributed to the points being out of specification.

2. Chromatic correction tests were accomplished by measuring angles for three colors (green-5300A, blue-4900A and red-6200A). Test results indicated the difference between the three colors in minutes of arc. Eleven points were defined in the exit pupil and tested for chromatic disparities (See Figure 4). Nine out of the 55 angles determined were found to be out of specification. Again, as in the Ray Disparity Test, the majority of the out of specification points were associated with field point "E". And again, the contractor feels minor misalignment of the optics, index and dispersion variation of the acrylic, small errors in the slope of the Fresnel facets, and thickness and curvature tolerances on the CRT faceplate could all combine to force the test

8. Test Plan for Virtual Image Display System, N61339-77-C-0113, Item A004, ATS. Fairlawn, NJ, 10 March 1981

points out of specification. The contractor suggests adding an additional 20% to the Vergence Angle Tolerances for the extreme points to allow for imperfections in lens fabrication, optical alignment and small errors in measurements.

3. Collimation was checked with a diopter scope located on the optical axis in the exit pupil, while viewing an image in the faceplate location. The test reading was "0". Thus, the image did appear to originate at infinity as it should have.

4. Astigmatism was measured with a diopter scope, except that this time it was fitted with a 5mm entrance pupil. The diopter scope was focused first on the vertical member of a crosshair, then on the horizontal member in the object plane (TV faceplate location) from all 19 points in the exit pupil (See Figure 2). The astigmatism was determined as the difference between these readings. The readings did not exceed .2 diopters, well below the .75 diopters tolerance.

5. Distortion for an image seen from the center of the exit pupil did not exceed the 4% allowed in the specification.

6. Transmission was read with a Pritchard photometer and a regulated tungsten light source. Transmission through the VIDS was measured at object points on the horizontal axis at 0 degrees, 10 degrees, 20 degrees and 24 degrees. In addition, measurements were made for three horizontal positions in the exit pupil for each field point. The on-axis transmission was 68% with uncoated elements. There are five Fresnel lenses used in this design which equal eight airglass surfaces (the liquid doublet has only two air glass surfaces). With reasonable expectations from anti-reflection coatings, the loss could be reduced to approximately 1 1/2% or less per surface. Thus, 85 to 90% transmission might be expected.

7. Resolution was checked with Air Force resolution targets located in the object plane and viewed with a 3X diopter scope stopped down to a 5mm entrance pupil. The limiting resolution was better than one minute of arc across the field-of-view. Although not required in testing, a 7x50 binocular was used to view the object field and the visual resolution was described as "excellent" with no Fresnel grooves visible. Also (not part of the contract), when ATS substituted either a 525 or a 1025 TV line monitor in the focal plane of the VIDS, no disturbing moire effects were visible with either static or dynamic scenes or test patterns.

Upon delivery of the VIDS to NTEC, further testing continued until the "breadboard" device was found to have excessive spherical aberration resulting in an undesirable image movement with head motion. ATS was notified that the VIDS was "unacceptable" until the excessive spherical aberration was eliminated or drastically reduced. ATS tried but, no easy fix could be found without recomputing the design and recutting the elements; a fix which was

out of the question. As "Consideration" for not meeting specification, ATS offered to assist with subjective evaluations and provide a 1025 line color TV monitor. NTEC and PM TRADE accepted the ATS offer.

SECTION VII

SUBJECTIVE EVALUATION

In October 1981, personnel from NTEC, Code N-731 conducted a subjective evaluation of the Virtual Image Display System, at Fort Rucker, AL. The prototype device was evaluated by students transitioning into CH-47 helicopters and their instructors. First, both were asked to answer a questionnaire comparing the new VIDS with the visual display of the CH-47 trainer (Device 2B31). The second part of the questionnaire dealt with optical properties of the VIDS and its potential as a "trainer visual." The questionnaire was completed by 25 experienced helicopter pilots having between 800 and 8000 flight hours each. After each participant had an opportunity to view both visual devices for a reasonable length of time, he was asked to complete the questionnaire. The following results were obtained:

a. "How would you compare the overall picture quality of the VIDS with the visual display of the CH-47 simulator?"

3 indicated VIDS was "much better"

17 indicated VIDS was "slightly better"

3 indicated both were the "same"

2 indicated the CH-47 simulator "slightly better"

0 indicated CH-47 simulator was "much better"

b. "How would you compare your perception of seeing depth in pictures?"

8 indicated VIDS was "much better"

13 indicated VIDS was "slightly better"

4 indicated both were "the same"

0 indicated CH-47 simulator was "slightly better"

0 indicated CH-47 simulator was "much better"

c. "How would you compare image brightness?"

9 indicated VIDS was "much better"

12 indicated VIDS was "slightly brighter"

3 indicated "both the same"

1 indicated CH-47 simulator was "slightly brighter"

0 indicated CH-47 simulator was "much brighter"

Note: The CH-47 simulator's visual display was viewed in darkness with a red lighted instrument panel. The 2B31 simulator light level was 7.3 foot lamberts. The VIDS was evaluated in normal classroom light (would not need night instruments). The VIDS, even without anti-reflection coatings, has 22 foot lamberts of light.

To the second part of the questionnaire, questions and answers were as follows:

(1) "As you concentrate on the picture, are the grooves (circles on the VIDS) bothersome?"

4 indicated "not bothersome"

15 indicated "slightly bothersome"

6 indicated "very bothersome"

(2) "Are all portions of the picture equally in focus?"

13 indicated "about equal in focus"

12 indicated "better at center"

0 indicated "better at edges"

(3) "Do you notice any lines in the picture which should appear straight but appear to be curved?"

15 indicated "none"

10 indicated "few"

0 indicated "many"

(4) "Do black objects appear black and white objects white?"

22 indicated "yes"

3 indicated "almost"

0 indicated "very noticeable"

(5) "Do dust or scratches on lens or TV face plate bother you?"

11 indicated "no bother"

12 indicated "slightly bothersome"

2 indicated "very bothersome"

(6) "Is viewing "window" (exit pupil) adequate for helicopter flight training?"

13 indicated "about right"

9 indicated "slightly too small"

0 indicated "much too small"

(7) "If more than one VIDS could be placed side by side, what angular coverage would be adequate for helicopter training using forward as the 12 o'clock position?"

4 indicated "10 to 1"

13 indicated "9 to 3"

7 indicated "8 to 4"

0 indicated "any other areas"

(8) "If your choice of horizontal angle (see 7 above) was made, could the VIDS be used for training in any of the following areas? (You may check more than one.)"

For:

Routine helicopter flight - 24 "checks"

Nap-of-the-earth - 21 "checks"

Takeoffs and landings - 24 "checks"

Night and poor visibility - 20 "checks"

None of the above - 0 "checks"

(9) "If the VIDS' windows could be stacked vertically, what angular average do you feel would be adequate for helicopter training using straight up as 12 o'clock?"

2 indicated "2 to 6"

2 indicated "2 to 5"

5 indicated "2 to 4"

4 indicated "1 to 4"

5 indicated "12 to 6"

5 indicated "12 to 5"

1 indicated "12 to 1"

Note: Many commented that a "chin window" or "look down" video capability was needed for more effective training.

(10) "If your choice of "vertical angular coverage" (see question 9 above) was made, would the VIDS be used for training in any of the following areas? (You may check more than one.)"

Routine helicopter flight - 24 "checks"

Nap-of-the-Earth - 20 "checks"

Takeoffs and landings - 24 "checks"

Night or poor visibility - 20 "checks"

None of the above - 0 "checks"

SECTION VIII

RECOMMENDATIONS

After several years of research and development by NTEC, a contract that experienced a number of design changes, an earthquake that knocked out the diamond turning equipment for a period of time, and some financial problems, the VIDS was delivered and tested. From an optical standpoint, the VIDS program was a success even though it did not meet the entire design specification. Its subjective evalution by Army helicopter pilots at Fort Rucker, AL also gives the VIDS a ring of success. These are only part of the story. A production cost estimate for the VIDS of \$20K-30K as compared to \$70K-100K for the mirror beam splitter or the pancake window makes it even more interesting. Because of the high optical transmission, the VIDS with off-the-shelf TV color monitors can yield about 20-30 foot lamberts of brightness. Its low weight and multi-window stocking capabilities make it ideal for use by motion simulators needing a wide angle visual display. VIDS can also take advantage of Government patent rights and design data which make competitive procurements possible to keep the price down.

The VIDS approach for visual simulation has many advantages over other existing virtual imaging devices. However, the "breadboard" device as designed and produced has several optical imperfections, the most noticeable of which is caused by excessive spherical aberration causing an undesirable image movement with head motion. An Optical Improvements Program is needed to perform an optical analysis to eliminate or drastically reduce this imperfection to a point that no undesirable movements would be observable. A second area of concern found in the VIDS was Fresnel groove discernibility. This quality needs to be analyzed and corrections made. A third area of concern in the present VIDS is light "cross talk" through the optical elements or system. This problem should be investigated and actions taken to correct this imperfection. Lastly, action should be accomplished during the Systems Improvement Program to apply anti-reflection coatings to a Fresnel element with "undercut" grooves such as in the VIDS. How evenly and how effectively the coatings can be applied is questionable.

The use of the VIDS Fresnel lens approach is the most logical answer for use in the visual displays on motion platforms because weight is minimal as compared to conventional lens counterparts. However, the VIDS as designed and constructed has only a 24 inch eye clearance and a 48 H x 36 V field-of-view. If similar VIDS were used for wrap-around viewing, such as for a helicopter simulator, there would be little room for the trainer's cab or cockpit. Also, the required number of optical systems would be high if the size of each was not increased. A development effort should be initiated to provide the optical design and manufacture of a large window VIDS which takes advantage of the Fresnel lens while keeping the exit pupil as large as possible. The eye clearance of such a system would need to be increased and the means for "input" considered. Another effort is needed to study the requirements for

mosaicking VIDS units to form wide angle displays. Several units could be abutted with each other to provide large continuous fields for simulation. This effort should study the best multi-window geometry, resolution requirements, mechanical structure arrangements, and image overlap and collimation considerations. Other uses for the VIDS approach might be for "head up" displays in special vision goggles where space or weight requirements need to be considered.

DISTRIBUTION LIST

Defense Technical Information Center
Cameron Station
Alexandria, VA 22314 12 copies

Technical Information Center
NAVTRAEEQUIPCEN
Orlando, FL 32813 2 copies

NAVTRAEEQUIPCEN
Orlando, FL 32813 25 copies

PM TRADE
NAVTRAEEQUIPCEN
Orlando, FL 32813 5 copies

Defense Advanced Research Project Agency
ATTN: SSD (Major Jack Thorpe)
1400 Wilson Blvd.
Arlington, VA 22209 1 copy

HQDA
ATTN: DAMO-TR
The Pentagon
Washington, D. C. 20310 1 copy

Commander
U. S. Army Materiel Development & Readiness Command
ATTN: DRCLD (Dr. Odom)
5001 Eisenhower Avenue
Alexandria, VA 22333 1 copy

Commander
U. S. Army Training Support Center
ATTN: ATIC-DST
Ft. Eustis, VA 23604 1 copy

Commandant
USA Infantry School
ATTN: ATSH-I-V
Ft. Benning, GA 31905 1 copy

Commandant
USA Armor School
ATTN: ATZK-TD
Ft. Knox, KY 40121 1 copy

Commander
USA Aviation Center & Ft. Rucker
ATTN: ATZQ-TD
Ft. Rucker, AL 36362 1 copy

Chief
ARI Field Unit
P. O. Box 476
Ft. Rucker, AL 36362 1 copy

Director
USA Human Engineering Laboratory
ATTN: DRXHE-D
Aberdeen Proving Ground, MD 21005 1 copy

Program Manager
USA Research & Rotocraft Systems Integration
ATTN: DAVDL-D (Aeromechanics Lab)
Ames Research Center
Moffett Field, CA 94035 1 copy

Director
Night Vision & Electro-Optics Laboratory
ATTN: DELNV-D
Ft. Belvoir, VA 22060 1 copy

Commander
Aeronautical Systems Division (AFSC)
ATTN: ASD/YWB (Bob Swab)
Wright-Patterson Air Force Base, OH 45433 1 copy